INFORMATION TO USERS

This manuscript has been reproduced from the microfilm master. UMI films the text directly from the original or copy submitted. Thus, some thesis and dissertation copies are in typewriter face, while others may be from any type of computer printer.

The quality of this reproduction is dependent upon the quality of the copy submitted. Broken or indistinct print, colored or poor quality illustrations and photographs, print bleedthrough, substandard margins, and improper alignment can adversely affect reproduction.

In the unlikely event that the author did not send UMI a complete manuscript and there are missing pages, these will be noted. Also, if unauthorized copyright material had to be removed, a note will indicate the deletion.

Oversize materials (e.g., maps, drawings, charts) are reproduced by sectioning the original, beginning at the upper left-hand corner and continuing from left to right in equal sections with small overlaps.

Photographs included in the original manuscript have been reproduced xerographically in this copy. Higher quality 6" x 9" black and white photographic prints are available for any photographs or illustrations appearing in this copy for an additional charge. Contact UMI directly to order.

Bell & Howell Information and Learning
300 North Zeeb Road, Ann Arbor, MI 48106-1346 USA
800-521-0600

UMI®

Dissertation

A METHOD TO IDENTIFY THE PARAMETRIC DYNAMIC MODEL OF A SINGLE-SHAFT GAS TURBINE ENGINE

Submitted by

Troy V. Nguyen

Department of Mechanical Engineering

In partial fulfillment of requirements

For the Degree of Doctor of Philosophy

Colorado State University

Fort Collins, Colorado 80523

Summer 2000

COLORADO STATE UNIVERSITY

July 6th, 2000

WE HEREBY RECOMMEND THAT THE DISSERTATION PREPARED UNDER OUR SUPERVISION BY TROY V. NGUYEN ENTITLED A METHOD TO IDENTIFY THE PARAMETRIC DYNAMIC MODEL OF A SINGLE-SHAFT GAS TURBINE ENGINE BE ACCEPTED AS FULFILLING IN PART REQUIREMENTS FOR THE DEGREE OF DOCTOR OF PHILOSOPHY

Committee on Graduate Work

Advisor

Co-Advisor

Department Head

ABSTRACT OF DISSERTATION

A METHOD TO IDENTIFY THE PARAMETRIC DYNAMIC MODEL OF A SINGLE-SHAFT GAS TURBINE ENGINE

This dissertation presents the development of a method to identify the dynamic model of a single-shaft industrial gas turbine engine operating in closed loop control. Besides providing a safe and robust identification procedure for a fully operational turbine system, the method alleviates the difficult issues of data identifiability and model accuracy that exist when estimating the open-loop dynamics from closed-loop experimental data.

A majority of previous work on gas turbine dynamics identification focuses primarily on open-loop estimation where the control feedback is disconnected. All of the work assumes a certain amount of knowledge about the turbine dynamics in the formulation of the excitation signal and the turbine model structure. The method presented here does not assume *a priori* knowledge about the turbine design, but relies on data from a step response to estimate the turbine characteristics. The on-line step response provides the necessary system parameters to design the appropriate excitation signal and to aid in formulating the model structure.

The ultimate objective is to arrive at an accurate turbine model that is easy to use for control synthesis and at the same time does not require excessive computational effort to obtain. It will be shown that this objective is well met using the linear discrete models, ARX and ARMAX, in conjunction with the multi-sine excitation signal and the prediction error estimation algorithm. The multi-sine excitation signal is selected based

on the fact that it can reduce the risk of upsetting the turbine operation, and at the same time, contribute to maximizing the accuracy of identification test results. The prediction error algorithm is chosen for its computational robustness and applicability to the problem of estimating the open-loop dynamic parameters using closed-loop data.

The contribution of this research is a robust method that can be applied effectively to characterize the dynamics of the single-shaft gas turbine engine operating in a full-production mode. With minor improvements, the method can be utilized for identification of other turbine dynamic processes as well as other physical systems operating in closed loop control.

Troy V. Nguyen
Department of Mechanical Engineering
Colorado State University
Fort Collins, Colorado 80523
Summer 2000

ACKNOWLEDMENTS

I thank Jack Schade of the Woodward Governor Company for being a great friend and for all those valuable advice and encouragement. My personal appreciation goes to my graduate committee members, especially Dr. Wade Troxell and Dr. Bryan Willson who have made it possible for me to continue on this path.

DEDICATION

To my wife, Kim Tien, and my daughters, Victoria Linh-Chi and Julia Thien-Ly.

TABLE OF CONTENTS

LIST OF FIGURES

LIST OF TABLES

CHAPTER 1: INTRODUCTION

1.1 Background

It is advantageous for control system vendors to have good knowledge of the dynamics of the systems on which their equipment operates. Having this knowledge enhances their ability to design and tune the control system to achieve optimum system performance, even when there are some unknowns in system operating conditions. The ability to readily obtain and update the system dynamics for optimizing control parameters offers distinct technical advantages over business competitors and can contribute to the long-term cost savings due to equipment servicing.

1.2 The Problem

The goal of this dissertation is to develop an effective method to characterize (identify) the dynamics of a single-shaft industrial gas turbine during the commissioning of the control system and during normal system operation. The intention is to be able to apply the method to obtain the turbine dynamic parameters that lead to useful mathematical models for control design and analysis purposes. These mathematical models can then be utilized for either designing control strategies off-line or for adjusting a controller's parameters on-line to meet turbine performance requirements. The main focus of the research is to develop a procedure to obtain turbine parametric data and to formulate accurate models that can closely represent the turbine dynamic characteristics. To ensure the robustness of the models, it will be necessary to include model validation and

implementation approaches in the turbine dynamics identification procedure. A suggested extension of this research project will be to provide a unified framework for developing procedures to characterize the dynamics of similar turbo-machinery equipment such as steam turbines and rotating compressors.

A majority of the technical literature and industrial applications deals with identification of systems operating in the open-loop mode. For most cases, open-loop operations can only be carried out in a controlled test cell environment where the risk of damaging the equipment is small. It is obvious that for a large piece of machinery, such as a gas turbine in full operation, the open-loop experiment is not practical or advisable from safety and production perspectives. The approach taken in this research is to allow the turbine to operate in closed-loop mode and utilize the turbine speed loop reference signal as the excitation signal (input) to the system. In this situation, the turbine controller is in total control of the equipment, hence mitigating the risk of injury and equipment damage.

A key issue in the ability to obtain good estimates of the turbine dynamics is the selection of an appropriate excitation signal. When the gas turbine is in operating, the applied excitation signal should not generate excessive speed oscillation above the normal rated speed of the turbine. At the same time, the excitation signal has to contain sufficient power and proper frequency components to excite all possible dynamic modes of the turbine so as to produce a rich set of output data for estimation. During this study, it has been found that the multi-sine signal has all the characteristics that meet both of the above requirements. The multi-sine is a band-limited signal consisting of a finite sum of

harmonically related sinusoids. The multi-sine signal design has become increasingly popular in system identification due to advances in signal processing algorithms and the availability of the computational power required for its design and implementation. Existing literature and applications of gas turbine system dynamics identification generally assume *a priori* knowledge of the necessary frequency components in the excitation signal. For most cases, the assumed *a priori* knowledge of frequency components is reasonable when the turbine design data is available for examination. However, in many cases, the data is not available to a turbine control vendor or the end users, so other means are necessary to determine this frequency range for the excitation signal. The approach taken in this research is to estimate the necessary frequency components in the excitation signal from a step response characteristic induced by a change in the turbine speed setpoint.

1.3 Approach

The proposed approach to the gas turbine dynamics identification problem includes the following steps:

a) Experiment Design

This step involves the determination of what turbine parameters to measure and when to measure them. This step necessitates a thorough review of the turbine instrumentation and operational procedures to determine the appropriate system parameters to be measured. Furthermore, to obtain meaningful and informative data from the measurements, possible input excitation signals have to be analyzed for appropriate signal

forms and amplitude. These excitation signals are also designed to ensure that the turbine remains within normal range of operating conditions. Other issues such as existence of noise signals, data sampling and pre-filtering, will have significant effects on the "goodness" of the measured data and by necessity have to be taken into account at the experiment design phase.

b) Development of Class of Models

This step involves the determination of a set of parametric mathematical models that can suitably represent the single-shaft gas turbine system. This step necessitates a thorough understanding of the governing physical principles of the gas turbine dynamics combined with turbine control systems design and application experience. Several non-parametric and parametric modeling techniques in both time domain and frequency domain were investigated to determine applicability to the single-shaft gas turbines. In this section, different model types and model orders are reviewed for optimal. Desirable characteristics of the candidate mathematical models are the ease of use and low complexity and computational effort required for implementation.

c) Identification Method Development

This is the development of the rules that determine the best model parameters (best-estimated model coefficients) given the system operating condition (closed loop) and the set of recorded data. Several identification methods will be reviewed for applicability and robustness for use in the closed-loop operation mode. Similar to the selection of a candidate model, examination of the complexity and computational effort of the

identification rule is necessary to ensure that the algorithm is ultimately implementable in a turbine control system.

d) Model Validation

This step involves comparing the output of the selected model against the observed data. Model stability and data convergence are analyzed using the MATLAB system identification software analysis and simulation tools. A mathematical model of a General Electric single-shaft gas turbine in a power generation application will be used as a test bed for simulating the results of the identification methods. This simulation model will be described in a subsequent section.

e) Implementation Guidelines

This step describes the experimental procedure and the application of the identification algorithm to obtain the turbine dynamic models. Issues in design implementation and software development are reviewed to ensure that there will be no difficulty of applying the identification method.

CHAPTER 2: LITERATURE SURVEY

In its most basic definition, the science of system identification involves using experimental input/output data to model dynamic systems. Most of the practical methods in system identification are for linear stochastic dynamic systems where the system behavior is assumed to be linear and influenced by externally generated noises. The experimental data can be used to generate graphs or curves that describe the input/output dynamic relationship or it can be fitted to a variety of mathematical models whose structures are defined using *a priori* knowledge of the system's characteristics. System identification methods are categorized into two distinct classes: parametric identification and non-parametric identification. Parametric methods use experimental data to determine the parameters of mathematical models such as the coefficients of continuous differential equations or coefficients of linear difference equations. These parametric methods typically entail searching for a solution to a cost function, which minimizes the error between the predicted and actual system outputs. Non-parametric methods, on the hand, are techniques that determine functions, which best describe the relationship between the system inputs and outputs. The non-parametric methods do not require selecting a set of possible system models. The survey below consists of the non-parametric and parametric methods and their application to the problem of open loop and closed loop identification and various approaches to using these methods for gas turbine dynamics identification.

2.1 Parametric Modeling and Identification Methods

The parametric methods require selection of a set of candidate models that are parameterized as model structures, using a parameter vector θ. The determination of an acceptable model within the set of candidate models then becomes the problem of estimating θ. This procedure typically involves searching for an optimal vector θ that minimizes some error criteria.

The candidate models evaluated for parametric identification are transfer functions, linear ordinary differential equations and linear difference equations. General mathematical techniques for modeling the dynamics of continuous and discrete systems can be found in [6] (Beltrami) and [61] (Smith). Different types of model used in system identification are discussed in standard textbooks such as [35] (Ljung), [62] (Soderstrom and Stoica), [60] (Sinha and Kuszta), [18] (Eykhoff], and covered in greater details in [37] (Ljung and Glad) and [48] (Richalet). These different types of model are summarized below:

Physics-Based Models: These are models based on first principles such as the law of physics, chemistry, etc. The parameters associated with these types of models are generally the physical parameters of the system. An example of the physical model would be that of a second-order differential equation describing the motion of a pendulum. The model is derived using Newton's Law of motion and the equation coefficients are directly related to the physical characteristics of the system such as mass, spring constant and friction.

Black Box Models: These models are standard linear models whose parameters do not reflect physical characteristics of the system in question. The parameters are basically viewed as vehicles for adjusting the fit to the data without reference to the physical attributes of the system. The models can be represented by either linear difference equations or s-domain transfer functions whose coefficients are adjusted to achieve certain desirable input/output relationship and frequency response behavior. Some examples of black box models are the popular Butterworth and Chebyshev linear filters [43] (Oppenheim et al.).

Grey Box Models: These models are hybrid between the physics-based and black box models where the model structure is a standard linear representation whose coefficients are adjustable and may have some physical interpretation.

For practical application of parametric identification using a digital computer, black box models are usually preferred. There are standard model structures such as Box-Jenkins, ARX (Autoregressive Exogeneous), ARMA (Autoregressive Moving Average), and ARMAX (Autoregressive Moving Average Exogeneous). These model structures are studied in [23] (Goodwin and Sin), [34] (Landau), [35] (Ljung), and [62] (Soderstrom and Stoica).

Prediction Error Methods: The Prediction Error Method (PEM) is a generalized parametric identification method that is also referred by other names such as the least-squares (LS) and maximum-likelihood (ML) methods. The particular name reference

depends on the choice of model structure, choice of model predictor, and choice of cost function criteria. The basic goal of the PEM is to minimize the difference between the actual system output and the predicted output. This difference is expressed mathematically as the error $e(t, \theta)$

$$e(t,\theta) = y(t) - y^*(t \mid t-1;\theta)$$

Where $y(t)$ is the actual system output and $y^*(t|t-1, \theta)$ is the predicted output at time t based on data measured up to and including time $(t-1)$.

The least squares (LS) methods determine the parameter vector θ that makes the sum of squared prediction error as small as possible. These methods have wide application in both technical and non-technical fields and are discussed extensively in system identification and statistics literature on optimization problems. The least squares methods are covered in details in typical texts on systems identification such as [35] (Ljung), [37] (Ljung and Glad) and [62] (Soderstrom and Stoica). The maximum likelihood (ML) method differs from the LS method in the choice of cost function criteria. In this method a function of the data and the unknown parameters is constructed reflecting the "likelihood" that an observed event should take place. A reasonable estimate of the parameter θ is such that it maximizes the likelihood that the observed event becomes "as likely as possible" [62] (Soderstrom and Stoica). The ML method is also discussed extensively in [35] (Ljung), [37] (Ljung and Glad) and [62] (Soderstrom and Stoica). The theory and applications of the Maximum Likelihood method and its relation to the prediction error methods is presented in details in Astrom [5].

The different prediction error methods discussed above can be applied to both open loop and closed loop systems. Other parametric methods, generally referred to as correlation methods, are restricted to systems that operate in open loop. These methods contain the instrumental-variable (IV) and rational transfer function procedures and are studied in [35] (Ljung) and [62] (Soderstrom and Stoica).

The parametric identification can be implemented using recursive techniques which compute the parameters recursively in time. This means that if there is an estimate of the parameter vector $\theta(t-1)$ based on data up to time $(t-1)$, then $\theta(t)$ is computed by some adjustment of $\theta(t-1)$. The recursive methods are typically called on-line methods because they can be implemented in real time. The counterpart to on-line methods are the so-called off-line or batch methods, in which all of the recorded data are used simultaneously to find the parameter estimates [62] (Soderstrom and Stoica). The recursive methods are standard topics in system identification textbooks referred to previously. References [36] (Ljung and Soderstrom] and [34] (Landau) provide exclusive focus on the theory and practice of recursive identification methods.

2.2 Non-Parametric Modeling and Identification Methods

Non-parametric identification methods are characterized by the property that the resulting system representations are curves or functions where the curves and functions are not necessarily parameterized by a finite-dimensional vector. Typical non-parametric identification methods are transient analysis, frequency analysis, correlation analysis, and spectral analysis.

Transient Analysis: The input to the system is either a step or an impulse and the recorded output is the system dynamic representation. The step response can be used to provide low-order, i.e. first and second order systems where approximation of system time delay, system gain, and dominant time constants can be derived from the step response data. The impulse response provides a method to derive the system transfer function. The impulse response function in the time domain can be calculated from the Convolution Integral using the impulse input and recorded output data. The frequency domain transfer function can then be calculated from the impulse response function. A tutorial in the methods utilizing the step response, frequency response and other non-periodic test signals is presented in [46] (Rake). The procedure for calculating the frequency domain transfer function from the impulse response function is detailed in [13] (Davies).

Frequency Analysis: This analysis employs periodic signals as input to the system. The signals commonly used are simple sinusoidal or multi-frequency signals which contain significant amplitudes at more than one frequency. In each case the output data for the frequency bands are recorded and a frequency response plot is approximated from the input/output data. This frequency analysis method is discussed extensively in system identification literature and is presented in details in [13] (Davies) and in [55] (Schoukens and Pintelon).

Correlation Analysis: This method employs white noise as the input signal. The resulting input/output data are used to estimate the cross covariance function (between input and output). The impulse response of the system can then be calculated from the cross covariance function since it is proportional to this function. This method is discussed widely in the system identification literature and is given particular attention in [21] (Godfrey).

Spectral Analysis: This is the most common method used for estimating frequency functions of linear systems. The basic assumption here is that the input signal and the noise signal are not correlated. The method requires computation of the cross spectrum of the input and output from the sampled data using the Fourier transform procedure. The frequency function $G_N(i\omega)$ is computed as

$$G_N(i\omega) = \frac{\left|\Phi^N_{yu}(\omega)\right|^2}{\Phi^N_u(\omega)}$$

where $\Phi^N_u(\omega)$ is the spectrum of the input signal u and $\Phi^N_{yu}(\omega)$ is the cross spectrum between the input signal u and the output signal y over the data record length N. The spectral analysis method is a standard subject discussed in many textbooks on time series and is discussed in detail in [18] (Eykhoff) and [35] (Ljung).

2.3 Open-Loop and Closed-Loop Identification

Some of the identification methods discussed above are applicable only to open loop operation. The assumption that the input signal is not correlated with the system noise or disturbance is invalidated when there is feedback in the system. There is general

agreement in the current literature on system identification that non-parametric methods are geared toward open loop operation whereas parametric methods are more suitable for closed loop operation where system response is effected by a controller.

The textbook by Ljung [35], published in 1999, discusses the problems and possibilities with identification data from closed loop operation. There are three basic approaches to closed loop identification presented in this textbook: the Direct approach, the Indirect approach, and the Joint Input-Output approach. In the Direct approach the prediction error method is applied in a straightforward manner: use the output of the process and the input in the same way as for open loop operation, ignoring any possible feedback. The Indirect approach identifies the closed loop system from the loop reference input to the process output. Assuming complete knowledge of the controller, the open loop dynamics can then be derives from the closed loop system. The Joint Input-Output approach considers the input and output of the open loop system as outputs of a system driven by the reference and noise and recovers knowledge of the system and the controller from this joint model. It was concluded that the Direct approach using the prediction error method and a flexible noise model is the best method. Forssell and Ljung [69] revisited the closed loop identification issues with respect to the three approaches described above. This paper shows that these methods are basically special parameterizations of the general prediction error method. It again emphasizes the direct approach as the best method that provides consistency and optimal accuracy, regardless of feedback. For approximation of the open loop dynamics in the case of a nonlinear regulator, it presents

the projection method which allows an user-chosen frequency domain norm regardless of feedback.

References [25] (Gustavsson et al.) and [26] (Gustavsson et al.) present identifiability and accuracy issues for system identification methods for systems under closed loop operation. Kurz and Isermann [33] developed methods for on-line process identification in noisy closed loops using correlation and least squares estimation algorithms. Ljung and Forssell [68] discusses possible biased results (error) in the Direct prediction error identification due to correlation between the input and the output noise. The Indirect approach with specially formulated noise model was presented as an alternative to the Direct method to avoid the bias. However, it was concluded that the alternative approach requires perfect knowledge of the regulator and provides sub-optimal accuracy. In another paper, Ljung and Forssell [78] study the statistical properties of the Direct and the Indirect methods and their parameterizations. The asymptotic variance (error) expressions were derived for these two methods. The conclusion was the Indirect method failed to give better accuracy than the Direct method. Van den Hof [76] reviewed and compared the characteristic properties of the classical prediction error identification methods (Direct and Indirect methods) and the Two-Step (TS) method. The Two-Step method consists of two consecutive open-loop identification steps, in which a Prediction Error Method (PEM) is used to obtain estimates of the loop sensitivity function and the plant, respectively. This paper also discussed the role in which closed loop identification can play in the identification of optimal models for model-based control design. Landau and Rolland [72] addressed the problem of unbiased parameter estimation in closed loop

operation when the plant output is corrupted by stochastic disturbances. The authors derived a closed loop parameter estimation algorithm using the pole placement control design approach. They also examined the convergence properties of the algorithm in a stochastic environment. Ditmar et al. [81] examined the application of the Pseudo Random Gaussian Noise (PRGN) perturbation in closed loop frequency response estimation. The PRGN is a periodic multi-level, multi-frequency perturbation signal which is modeled on the spectral properties of a band-limited Gaussian noise signal. They concluded that the closed loop bias can be avoided by making the estimation procedures coherent only with the external excitation signal which is orthogonal to other signal within the feedback loop.

Klauw et al. [80] focused on the closed loop identification of a distillation column for control design purpose. The models of the distillation column are obtained using two different approaches: the Direct identification (DI) method and the Two-Step (TS) method. These methods have been discussed in previous paragraphs of this literature survey. It was shown in both frequency domain and time domain that the TS model provides better prediction than the DI model. The TS model was subsequently used to redesign the control loop for the distillation column. Pasadyn et al. [75] benchmarked eight different identification algorithms on an industrial wastewater reactor operating under both closed loop and closed loop conditions. The system under consideration is a multi-input multi-output dynamic system. The algorithms included both non-parametric and parametric methods. The experimental results indicated that closed-loop operational data can not be used for model identification regardless of the identification method

(parametric or non-parametric) when the system is in normal operating conditions, i.e. without additional excitation. Baars and Bongers [73] presented the identification experimental results for an industrial wind turbine operating with four single-loop PI controllers. The experiment was conducted using Pseudo Random Binary Sequence (PRBS) test signals and data sampling rate of 100 Hz. The data was fitted to a 7^{th}-order ARX model. The identification model compared fairly well against the linear physical model of the wind turbine system except at the very low frequencies.

2.4 Gas Turbine Dynamics Identification

Cottington and Pease [12] presented the results of aero and marine gas turbine dynamics identification using Pseudo Random Binary Signal (PRBS) as input excitation. The experimental inputs included fuel flow to the engine and the output is primarily the engine rotor speed. The experiment was carried out with the engines operating in open loop, i.e. the turbine speed control system was disabled. The frequency response of the system was obtained by applying the cross-spectra analysis method to the measured data. The identification results showed good agreement in the frequency response characteristics of the system with the input being either the conventional sine wave technique or the Pseudo Random Binary Signal.

Hill [30] described various problems encountered in attempting to estimate linear models of gas turbine engine dynamics using standard time-domain identification technique, specifically the Extended Least Square (ELS) method. The problems include bias in the estimates of the model parameters and incorrect estimation of the time delay in the

system. Bias can be introduced on the estimates of the model parameters when the input to the system is not constant between sampling intervals. The latter problem is the result of the standard time-domain methods being able to estimate the time delay only to the nearest sample interval. It was shown that using a multiple-output form of the parameter estimation algorithm diminished these problems. The identification was performed on the open-loop data (no controller in the loop), i.e. using the fuel flow as the input and turbine speeds as the output. The input excitation signal used in this experiment was a PRBS with sample time of 35 ms.

Evans et al. [17] discussed frequency-domain techniques for estimating gas turbine dynamics. The gas turbine engine and the experiment setup are identical to those outlined in [30] (Hill). In this method a multi-sine input signal was used in which its power spectrum covers the bandwidth of the gas turbine system. The transfer function model obtained from the experiment was found in good agreement with the thermodynamic model except in the higher frequency region. The results showed that using frequency-domain techniques some of the problems described in [30] (Hill) using time-domain technique were eliminated. This is due to the fact that frequency-domain techniques allow direct estimation of the s-domain models which include the pure time delay as a parameter.

Kaufman and Ravi [32] present the identification of the dynamics of a General Electric Frame 7 gas turbine using the least squares method. Their approach utilized a black box model (ARX) and a sequence of square waves as input excitation to the system. The

dynamic relationship between fuel reference and engine power output as well as between inlet guide vane reference and exhaust temperature are investigated while the system is operating in closed loop control. In this work, the magnitude and the frequency range of the excitation square waves are assumed known from the knowledge of the physics of the system. The square wave excitation signal is superimposed on the actuator reference signal to generate the output data.

Merrill [40] described the application the Instrumental Variable/Approximate Maximum Likelihood (IV/AML) method, an open-loop identification technique, to closed-loop data of a F100 gas turbine engine. The multivariable model structure of engine was initially obtained via a mathematical method and subsequently fine tuned using various tests on open and closed loop data. The IV/AML method was applied to both open-loop simulation and closed-loop test data of an F100 turbofan engine. The data sets were obtained using a Bill of Material (BOM) controller, which consists of multiple single-loop controllers, and a multi-input multi-output (MIMO) controller. It was concluded that the resulting identified model showed acceptable performance when compared to the actual data. The model predicted the engine speeds fairly accurately, but has some discrepancy in the prediction of the engine thrust.

Chrysanthous et al. [11] discussed the main issues involved in developing multivariable models for gas turbines and presented typical results from actual engine tests. This paper briefly described a software package developed at the University of Salford to analyze data obtained from real plant. The author outlined the autoregressive model and the

recursive least square method used to estimate the model parameters. The limitation in the application of the recursive least square method was pointed out in the necessity for *a priori* information of a number of specified parameters such as model order, dead times in system components (actuators, sensors, plant states). The interactive nature of multivariable plants was also mentioned as a potential limitation to effectively using this identification method.

Hannet and Khan [27] presented the testing method used to obtain the model for gas turbine/control system in power generation application, and comparison of these models with a typical mathematical model found in the literature [51] (Rowen). The step response of the system was obtained by changing the turbine load (Megawatt) and measuring the turbine speed and power. Two different makes of turbine control systems are used in the tests, a General Electric Speedtronic and a Woodward Governor control system. The response from the model simulation is found to be more optimistic (more responsive) than actual measured response. It was concluded that the model structure provided by [51] (Rowen) is adequate with some minor modification.

A collection of papers presented at the UKACC International Conference on Control '98 cover various methods for modeling aircraft turbine engines. Evans [14] introduced the dynamic modeling of aircraft gas turbines. An outline of the engine construction and operation as well as basic requirements of a good engine model was discussed. A review of models and testing methods previously conducted in the field was also presented. Attention was paid to modeling the basic dynamic response of the engine and to

modeling thermal effects during large transient maneuvers. Arkov et al. [2] presented a method utilizing existing random disturbances created by the engine controller and operating environment during normal engine operation as the test source. An optimization technique of spectral analysis is derived providing high accuracy of identification. Optimal smoothing provides the compromise between the bias and variance of spectral estimate. An example of the turbofan engine model identification is considered demonstrating the viability of the proposed method. Borrel et al. [9] describes the estimation of parametric and non-parametric models of the fuel input to shaft speed output of a Rolls Royce Spey twin shaft engine using frequency domain techniques. Accurate models were estimated at several points along the turbine operating curve and the results of the parametric estimations are used to verify theoretical models derived from the thermodynamic relations of gas turbine. Norton et al. [42] presented the identification results for the same engine model as that in [9] (Borrel et al.). The presence of non-linearity and slow dynamics is inferred from the responses to a range of perturbation signals. Rodriguez-Vasquez and Fleming [49] demonstrated a practical application of a Genetic Programming approach in conjunction with a NARMAX (Non-linear ARMAX) model to obtain the relationship between the fuel input and shaft speed dynamics of a Rolls Royce Spey engine.

CHAPTER 3: GAS TURBINE THEORY OF OPERATION

3.1 General Description

The gas turbine engine is basically a heat engine which converts chemical energy (fuels) to mechanical energy in the form of shaft power (turboshaft engine) or propulsive thrust power (turbojet engine). The basic components of a gas turbine engine are the Gas Generator Unit (GGU) and an output turbine section.

The main function of a Gas Generator Unit (GGU) is to deliver a high-temperature, moderate-pressure gas stream to the output turbine section. The Gas Generator Unit consists of three components:

a) A compressor which takes ambient air and compresses it to a higher pressure level

b) A combustor or burner system where incoming fuel is mixed with the compressed air and the combined product is burned

c) A compressor-drive turbine whose primary function is to drive the GGU compressor.

The power output section consists of an additional turbine section, which produces output shaft power. In the single-shaft gas turbine engine, the compressor-drive turbine section and the output power turbine section are combined into a single turbine, which delivers the power to drive both the compressor and the external load. The single-shaft gas turbine has its compressor, turbine and load on a common shaft. In this arrangement, all

turbine components and the external load (a generator set in this study) rotate at the same speed. Figure 3.1 below illustrates the turbine components and the direction of the working fluid flow.

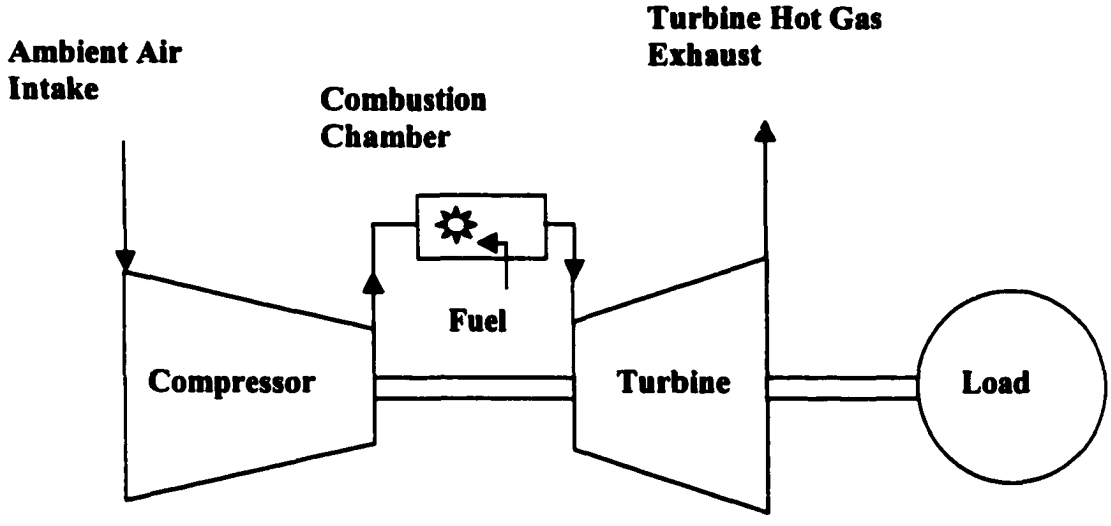

Figure 3.1 Single Shaft Gas Turbine Engine

Atmospheric air is initially compressed to a higher pressure in the compressor, heated by a combustion process to a much higher temperature in the combustion chamber, and then expanded in the GGU turbine to a lower pressure. The exhaust gas from the gas generator unit is then further expanded in the power turbine section, which provides shaft power to drive an external load (electrical generator). In any gas turbine, a large portion of the energy consumption is expanded in the GGU turbine to drive the compressors. The combustion product (working fluid) in any gas turbine is comprised of mainly air and a small amount of fuel.

3.2 Gas Turbine and Control Systems Functional Description

3.2.1 General

The gas turbine control system is responsible for controlling the speed and load of the turbine. It does so by controlling the amount of fuel going to the turbine combustion chamber. In a normal operating condition, the load on the turbine is at a fixed value and the turbine is running at a predetermined speed. This speed is 3600 RPM (revolution per minute) in typical power generation installations in the United States. As the electrical load demand on the turbine increases, additional torque is applied on the turbine shaft decreasing its speed. The control system responds to the change in speed by driving the fuel valve in the opening direction, admitting more fuel to the combustion chamber, to bring the speed back to the preset value. As the load demand decreases, lowering the torque applied on the turbine, allowing the speed to increase. The control system responds by driving the fuel valve in the closing direction, decreasing the fuel to the combustion chamber, to bring the speed back to the preset value.

The control system for a typical gas turbine in a power generation application carries out four primary functions: Start/Stop/Sequencing, Control, Protection, and Dispatching.

Start/Stop/Sequencing (SSS) Function: This part of the control system provides the discrete on/off signals to equipment such as motor starters, solenoid valves, indicating lights, and relays. The SSS function must provide the proper signals required for normal operation and also for safe operation and shutdown under all possible abnormal modes, including equipment or control system failures.

Control Function: This part of the control system is responsible for controlling the turbine speed, load, temperature, and other turbine parameters by means of continuously varying control signals. This is done primarily by controlling the fuel flow to the combustion chamber and by controlling the airflow through the system.

Protection Function: This portion encompasses the functions that prevent improper operation of the equipment, for example, over-speed, over-temperature, high vibration... The overriding requirement imposed on this function is to prevent injury to personnel. Secondary requirements include preventing damage to the equipment and surrounding facilities, maximizing overall availability, and minimizing maintenance costs. An example is the case when the turbine speed goes over the maximum design limit. The protection function, upon sensing this extreme over-speed condition, would command the fuel shutoff valve to go closed, thus preventing further increase in turbine speed.

Dispatching Function: This part of the system provides an interface between the turbine operator and the customer's operating or dispatching system. This is typical in situations where the turbine/generator system operates as part of a larger power grid system. The dispatching function basically is responsible for managing/sharing the load based on the power grid requirements.

3.2.2 Physics of Speed and Load Control

The turbine receives a flow of energy, which is transformed into developed torque (T_D). The load driven by the turbine yields an opposing load torque (T_L). When T_L matches T_D

the system is in a steady-state condition (constant speed). When there is a difference between T_D and T_L, the system is in transient condition (either accelerating or decelerating). Controlling this system involves maintaining a steady-state condition, and after a system disturbance occurs, returning the system to a steady state condition in the shortest possible time period with minimum change in speed. Figure 3.2 illustrates the balance between the turbine developed torque and load torque.

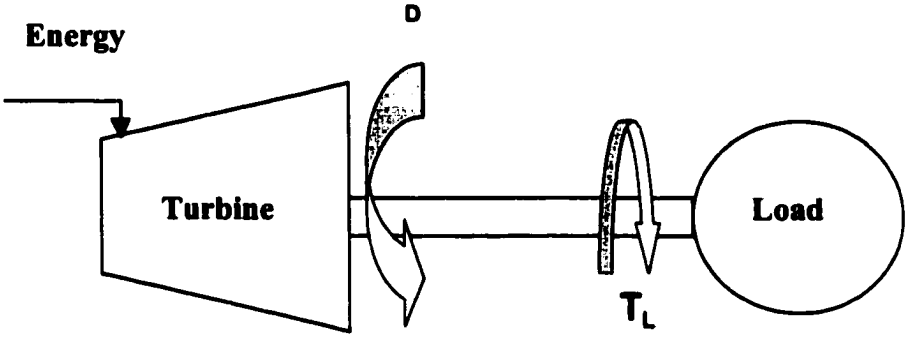

Figure 3.2 Developed Torque – Load Torque Balance

An increase in load results in an increase in fuel flow. This process cannot continue beyond the design limits of the turbine. The control system must modulate the maximum energy input to the turbine to limit the maximum power at various operating conditions.

3.2.3 Isochronous/Droop Operation in Power Generation Application

A speed control system can operate in either the isochronous mode or the droop mode. In the isochronous mode the control system maintains a constant steady-state speed, regardless of load. When a load change occurs, there is a momentary change in speed during the transient, but the speed will always return to the same value.

In the droop mode the steady-state speed varies with load. Speed decreases with an increase in load. If a generator operates at 5% droop, the frequency will decrease 5% when the load is increased from zero to 100%. For a generator set running at 60 Hertz at no load, the frequency will drop 5% (3 Hertz) to 57 Hertz when the load increases from zero to 100%. Again, during transient conditions, there will be momentary speed change, but, after the transient the speed will settle at a value determined by the droop line of frequency versus load.

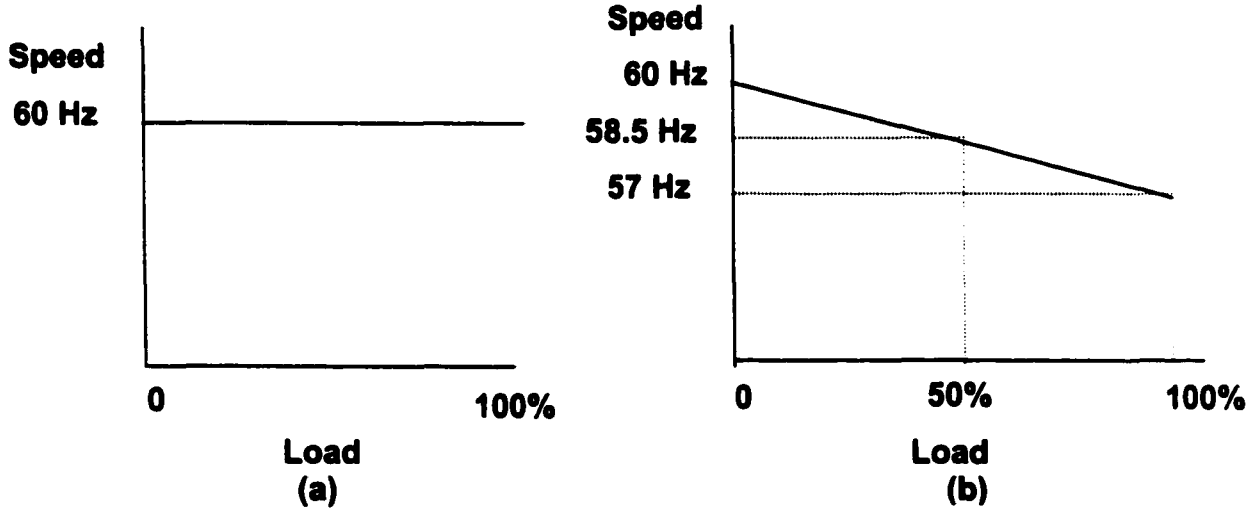

Figure 3.3 (a) Isochronous Operation (b) Droop Operation

A different term, synonymous to droop, is steady-state regulation. The term droop indicates the change in steady-state speed when the speed control system moves the fuel valve from zero fuel to maximum fuel. The term regulation is the change in steady state speed when the load is changed between rated speed/no load and 100% load.

3.3 Basics of Control Operation

3.3.1 Control of Light-off and Acceleration

The fuel control determines the fuel flow for ignition which is usually referred as light-off. After proper light-off is verified, the control increases fuel flow, which in turn accelerates the turbine to a preset speed where the speed governor takes over. During this acceleration period, the fuel control prevents excessive fuel flow, which could damage the turbine. This function is performed by the acceleration limiter and/or temperature limiter of the fuel control.

3.3.2 Control of Steady State Speed

Once the turbine reaches operating conditions, the fuel control must govern the steady state turbine speed. For industrial applications, this may be a constant speed for a generator application or a variable speed control for mechanical drives. For ship propulsion, the governor may set the turbine speed for constant power output with another control function on the variable pitch propeller.

3.3.3 Control During Transient Conditions

The turbine speed deviates from the steady state during load changes. The speed governor will rapidly increase or decrease fuel flow after such a load change to maintain steady state operation. The function of the acceleration limiter is to protect the turbine by restricting instantaneous increases in fuel flow. The deceleration limiter avoids flameouts due to a lean air/fuel ratio by controlling fast decreases in fuel flow.

3.3.4 Limit Maximum Power

An increase in load results in an increase in fuel flow. This process cannot continue beyond the design limits of the turbine. The control system must modulate the maximum energy input to the turbine to limit the maximum power according to several parameters, which determine maximum power and maximum temperature at various ambient conditions.

3.4 Dynamics of Speed Control of Gas Turbine

The gas turbine steady state stability and transient performances are affected mainly by the following turbine and load characteristics

- Time delay in the turbine between the moment the fuel valve takes a new position and the moment the turbine converts this new energy level into a new level of developed torque.
- Moment of inertia of all rotating parts of the turbine and load.
- Dynamic characteristics of the load.

Delay in developed torque: The following contribute to the delay in the developed torque

- Volume of the manifold/piping between the valve and the burner. Gaseous fuel can show considerable manifold delay.
- Combustion lag in the burner. This delay is associated with evaporating, mixing and burning of the fuel.
- Gas generator time constant and transition duct storage (for split shaft turbine)

Load Characteristics: The torque versus speed characteristics of the driven load can have significant impact to the steady state performance. For example, a load that has high speed to torque sensitivity, i.e. a small change in the applied torque causes a large change in speed can be very difficult to control.

Moment of Inertia: The moment of inertia of all rotating parts determines the off-speed and settling time after an increase or decrease in the setpoint or a change in load.

3.4 Temperature Control

An increase in power demand requires higher fuel flow, which results in an increase in turbine operating temperature. This temperature must be restricted when it reaches the maximum limit of the material used in the turbine. It is common to measure turbine outlet temperature (TOT) or exhaust gas temperature (EGT) using thermocouples. The temperature control compares this temperature signal with a reference signal and modulates fuel flow when the temperature reaches its reference setpoint. The dynamics of the temperature control loop is affected by the time constant of the thermocouple. This time constant is a measure of the delay in the thermocouple output after a step change in temperature. The magnitude of the delay determines the overshoot over the setpoint when a fast change in temperature is encountered. The time constant of the thermocouple is affected by the mass flow of gasses over the surface of the bimetal's protective well. A high mass flow will heat the surface faster. As a result, the time constant is smaller at high turbine speeds.

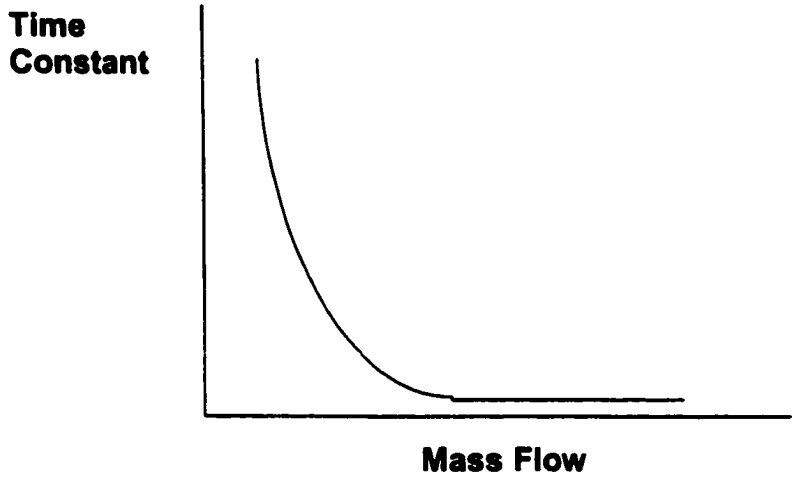

Figure 3.4 Thermocouple Time Constant vs. Turbine speed

3.6 Control of Turbine Maximum Power

When the demand for power increases, the speed governor increases fuel flow. At a certain point, the turbine reaches its maximum designed power level and a topping governor takes over the control of the fuel valve. For a single shaft turbine, this maybe the maximum speed setting, maximum fuel stop, or maximum temperature limiter. At this point, the turbine starts operating at a fixed power level. Any increase in power demand beyond this maximum level will result in a decrease in turbine speed.

The actual power level produced by a gas generator operating at constant speed or constant temperature varies with ambient temperature. As the ambient temperature decreases (higher air mass density) the power output of the turbine increases. At a certain ambient temperature, the power output of the gas generator reaches the maximum design limit of either the gas generator or the power turbine. If the turbine must operate at ambient temperature below this level, the fuel control must contain a power limiter.

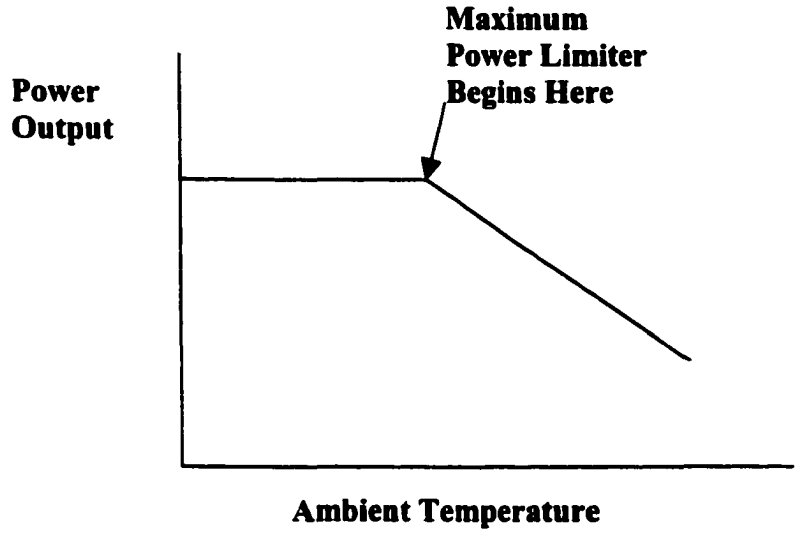

Figure 3.5 Effect of Ambient Temperature on Power Output

Another limitation may be compressor discharge pressure (CDP). With a decrease in ambient temperature, the mass flow increases and CDP increases. Depending on the turbine design, this CDP may reach its maximum safe limit. If this occurs, a CDP control must maintain this maximum CDP.

3.6.1 Acceleration and Deceleration Limiters

To avoid compressor surge during a sharp increase in fuel flow (acceleration), it is common to restrict maximum fuel flow as a function of a gas generator parameter such as speed, temperature, or compressor discharge pressure (CDP). The CDP limiter normally operates in an open-loop fashion limiting fuel flow as a function of the discharge pressure. The temperature limiter typically operates in a closed-loop mode, controlling the fuel flow with turbine exhaust temperature as the feedback parameter. The speed-controlled limiter, normally used in heavy industrial turbines, controls the rate of turbine acceleration as these machines have large inertia and rapid acceleration is not required.

The fuel control must also maintain a minimum fuel flow, which will sustain combustion at all times. Good transient response requires a decrease in fuel flow as fast as possible without causing a flameout. A simple deceleration limiter is a jump and rate limiter. This method allows an initial step decrease in fuel flow followed by a change as a function of time. Figure 3.6 illustrates the operating limits for a typical gas turbine engine.

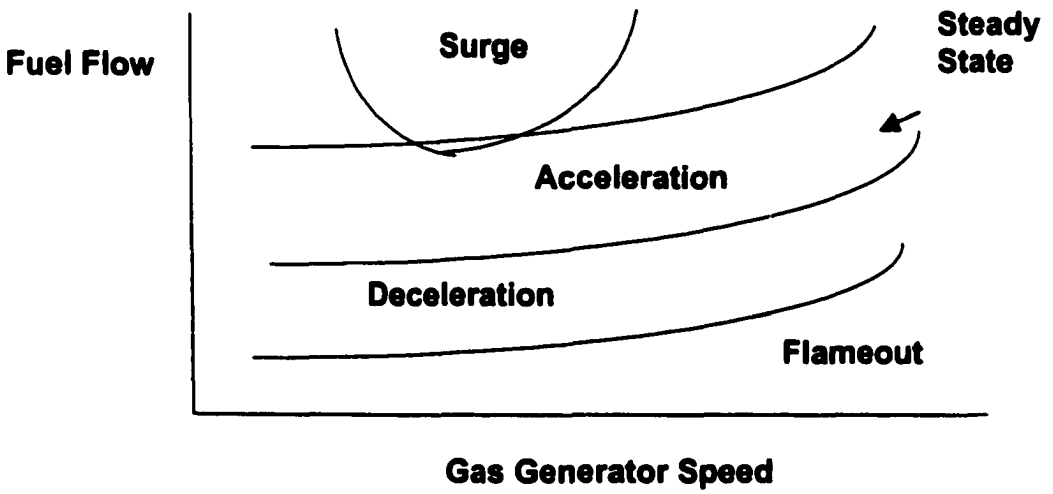

Figure 3.6 Turbine Fuel Control Operating Limits

3.7 Gas Turbine Mathematical Model

Bill Rowen [51] developed a linear mathematical model that represents a General Electric single-shaft industrial gas turbine. This model includes the turbine and fuel system dynamics as well as the speed/load controller, temperature controller, and acceleration controller. The system gains, coefficients, and time constants in this model were obtained from design and calculated values. These model parameters have been verified by test and actual field experience, which was accumulated from numerous installations in many different applications [51].

As part of a study to determine appropriate controller structure for gas turbines, the data generated by the above linear model was compared against that of actual experimental data [27] (Hannett, L.N. and Afzal Khan). The results show that in general the response from the simulation model is slightly faster than that of the actual system. However, it was determined that the structure of the simulation model represented the real system adequately in this study.

The linear mathematical model developed by [51] is used in the present study for the purpose of identifying the dynamics of the gas turbine and its fuel systems. As the dominant dynamics of the turbine are identified when the turbine is in the speed control mode, the temperature and acceleration controller were omitted. Figure 3.7 represents the turbine simulation model and the speed controller. Figure 3.8 is the block diagram representing the turbine and fuel system elements. The gas turbine system is essentially a linear device with the exception of the rotor time constant. There is a small transport delay associated with the combustion reaction time, a time lag associated with the compressor discharge volume, and a delay associated with the transport of the fuel gas from the combustion system through the turbine. The flow rate of the fuel gas is proportional to the product of the speed controller output and the turbine speed. There are two time constants in the fuel system. The first is associated with the valve positioning system and the second is the volumetric time constant associated with the piping and fuel distribution manifold. The controller output to the fuel valve has a maximum and a minimum limit. The maximum limit normally acts as a backup to the

temperature controller preventing over-fueling condition. The minimum limit is chosen to allow adequate fuel flow to insure that flame is maintained within the gas turbine combustion system.

The block diagrams depict a normalized gas turbine and controller model; i.e. the model parameters are scaled from 0 to 1. For example, turbine speed is scaled from 0 to 1 corresponding to 0-3600 rpm. Similarly, turbine load (MW) is scaled from 0 to 1 for the entire range of rated turbine MW output. The turbine speed controller is a simple proportional and integral (PI) controller. The representation of the speed controller is suitable for either droop or isochronous control and operates on the speed error formed between a reference made up of one normalized speed setpoint plus an excitation signal, compared with actual turbine rotor speed. Reference [51] lists a range of values for the parameters in this mathematical model representing different turbine model numbers and fuel types (gas or liquid). The particular turbine selected for this study is the General Electric model 7001E, which is a gas-fueled engine operating nominally at 3600 RPM and at a rated power output of 75 megawatts. The following model parameters correspond to this particular General Electric gas turbine

Turbine Model Parameters:

a ,b,c = Fuel valve/actuator transfer function parameters

a = 1; b = 0.05; c = 1

Fuel command limits (normalized): Max = +1.5, Min = -0.1

Tf = Fuel Piping Volume Time Constant (0.40 seconds)

Tc = Combustion delay (0.01 seconds)

Ted = Turbine exhaust delay (0.04 seconds)

Tcd = Compressor discharge volume time constant (0.20 seconds)

Ti = Turbine/Generator rotor time constant (12.2 seconds)

$$Ti = 5.98 \frac{WR^2}{P_{max}} \left(\frac{N_r}{3600} \right)^2$$

where

WR^2 = Rotating weight moment of inertia in lb-ft^2 (153,000 lb-ft^2)

P_{max} = Maximum power in KWatts (75,000 KWatts)

N_r = Rated speed in RPM (3600 RPM)

The turbine torque calculation is given by

$$f(u) = 1.3(Wf - 0.23) + 0.5(1 - n)$$

Wf = Fuel flow (normalized)

n = Turbine speed

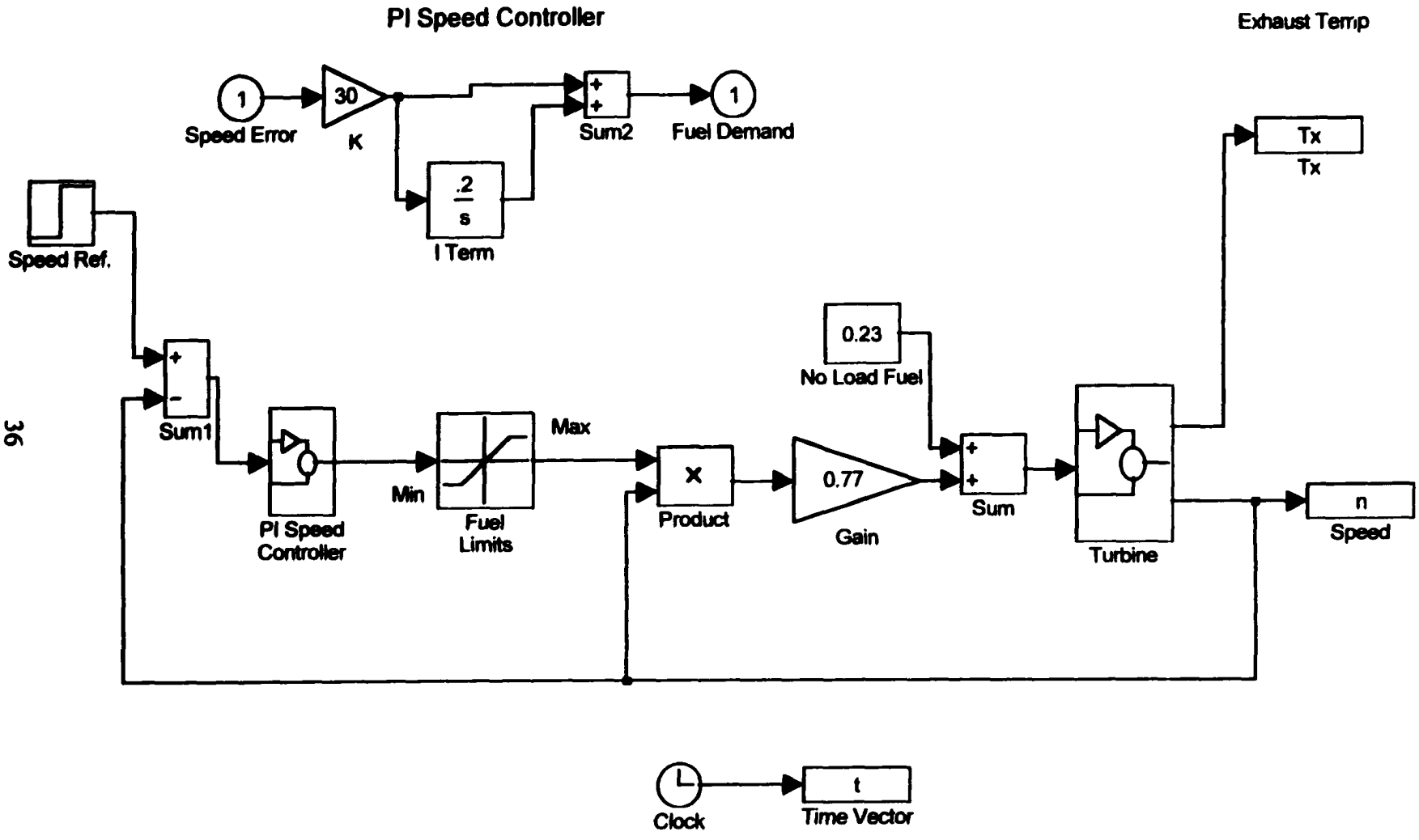

Figure 3.7 Single-Shaft Gas Turbine Mathematical Model

Student Version of MATLAB

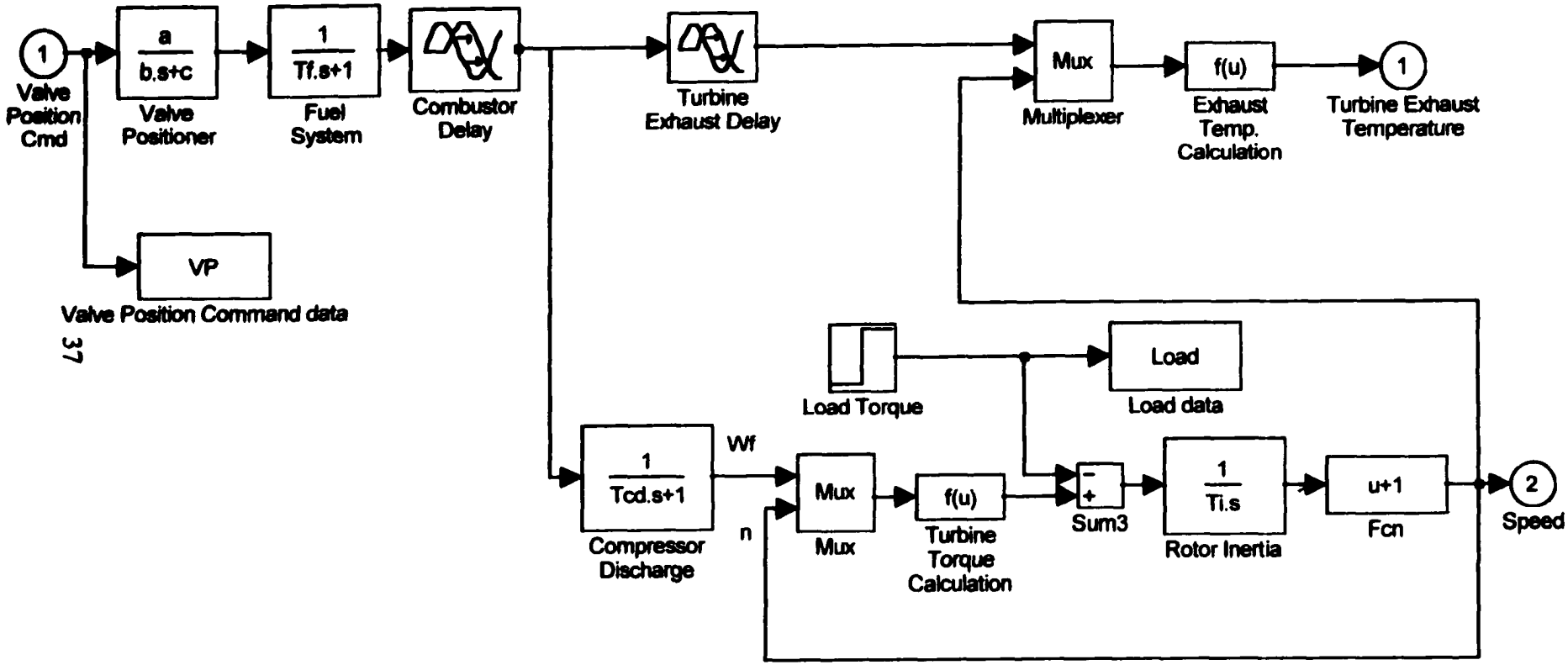

Student Version of MATLAB

Figure 3.8 The Gas Turbine and Fuel System Model

CHAPTER 4: DESIGN OF THE IDENTIFICATION EXPERIMENT

4.1 Objective

This experiment is geared toward identifying the open-loop dynamics of the single-shaft gas turbine, including the dynamics of the fuel metering system, while the machine is in closed- loop operation. The system simulations will be performed at steady state, full-load condition. Under this condition, it is necessary to operate the turbine in closed loop control for safety consideration. The final objective is to produce a mathematical model, using the collected data, which will adequately represent the dynamics of the turbine and fuel system. In essence, we are looking to characterize the dynamic relationship (open-loop dynamics) of the fuel valve position command (input) to the turbine speed (output).

4.2 System Configuration

For the purpose of this research project, a gas-fueled single-shaft turbine and a Proportional and Integral (PI) speed control system are assumed. The typical liquid-fueled turbine is different from the gas-fueled turbine only in the basic hydro-mechanical design of the fuel distribution system. There is essentially no difference for either type of fuels in the experiment setup and signal analysis for system identification purposes. The theory of operation of the gas turbine and its control systems has been discussed in Chapter 3. Figure 4.1 shows the gas-fueled distribution system components. Figure 4.2 depicts a representative block diagram of the gas turbine and its speed control system for the purpose of data measurement description.

4.2.1 Gas Fuel System Basic Elements

Modeled elements include:

Fuel Filter: Filter out the contaminants present in the fuel, preventing clogging of gas fuel valves and injector passages, and to protect pumps and other components.

Shutoff Valve: Used to provide absolute shutoff of gas fuel to the turbine.

Throttle (Control) Valve: regulates the flow of gas fuel to the turbine.

Pressure Regulation Valve: regulates the fuel inlet pressure to the fuel-metering valve.

Fuel Manifold (not shown): The manifold is located downstream of the fuel-metering valve. It distributes the fuel to multiple fuel injectors.

Fuel Injectors (not shown): The fuel injectors are located at various locations around the combustion chamber. It supplies the fuel gas to the combustion chamber so that the flame pattern and temperatures are controlled.

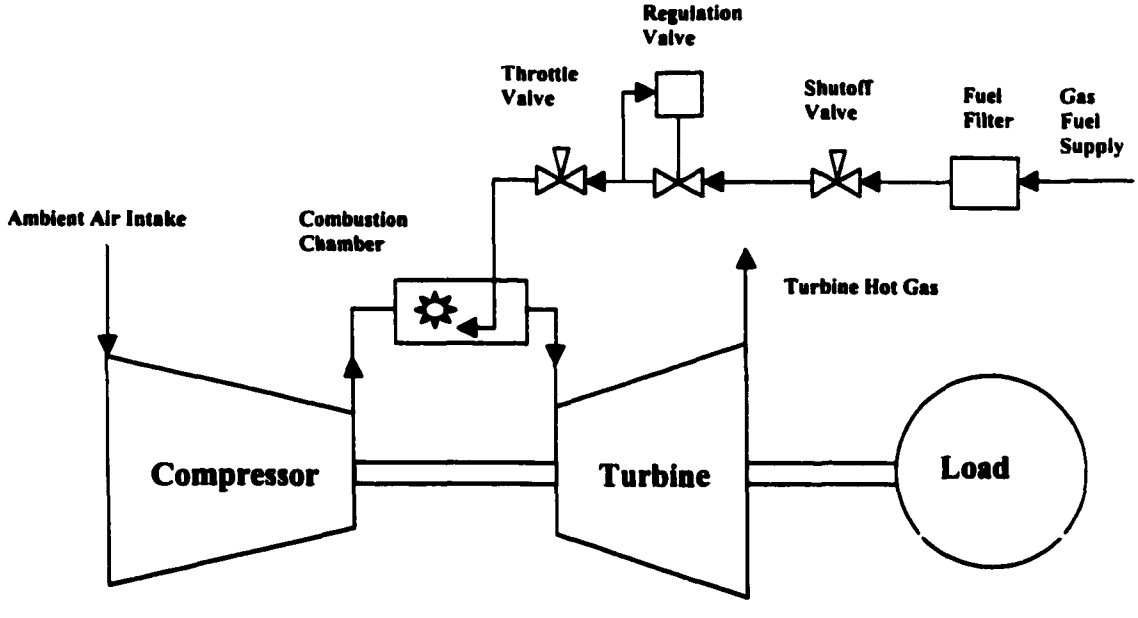

Figure 4.1 Turbine and Gas Fuel System

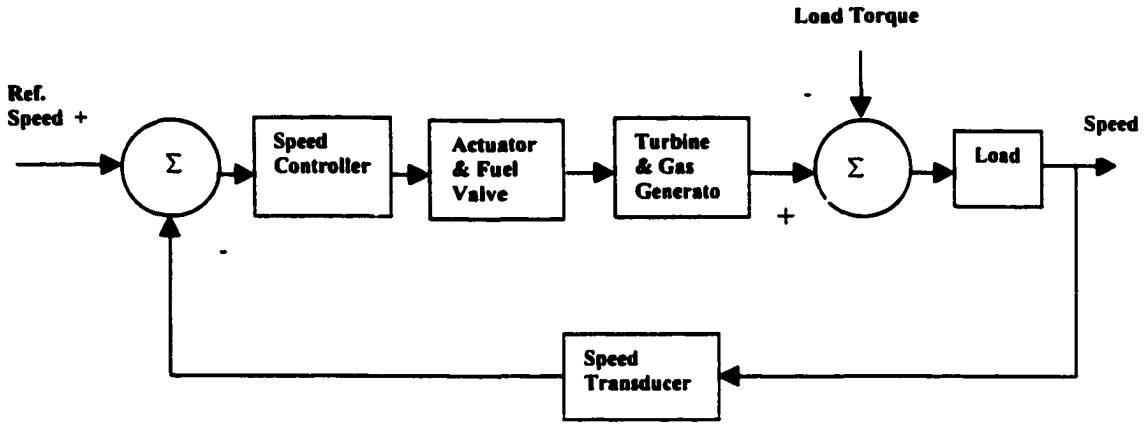

Figure 4.2 Block Diagram of the Turbine & Speed Control System

4.2.2 Turbine Control System

The typical industrial gas turbine control system is comprised of a digital programmable controller, consisting of a Central Processing Unit (CPU) and various plug-in input/output (I/O) modules. The CPU is responsible for executing the control and data acquisition algorithms and the I/O modules are mainly responsible for signal measurement and conditioning. The data to and from the turbine are handled through the I/O modules and they in turn communicate with the CPU via an internal bus structure. The CPU and the modules are typically located in the same chassis [67] (Woodward).

In the normal control mode, turbine speed is measured by a magnetic pickup (MPU) whose output is brought into a speed input module for conditioning. The controller compares this signal with the speed reference (setpoint) and makes corrective action accordingly based on the value of the error. The resulting corrective control signal is then sent to an output module that conditions the signal to an appropriate form to drive the fuel valve actuator. Since the speed control is a critical control loop in the system, it operates

at the fastest sampling rate available. Typical industrial distributed control systems (DCS) for gas turbine updates at 5 milliseconds intervals [67] (Woodward).

The actuator positions the fuel valve according to the input signal coming from the electronic module. In a typical fuel valve actuator, an attached position transducer indicates the position of the actuator. The position indication maybe a voltage or 4-20 mA signal which is proportional to actuator position and is available for external measurement or for feedback to the electronic controller.

4.3 Signal Measurements

For turbine model identification purposes, the data collection will consist of the following measurements. Each measurement point will have an associated time stamp.

Speed Reference: The speed error signal will be recorded and synchronized with the system clock.

Turbine Speed: This is the output of the speed magnetic pickup. It is assumed that the speed signal has already been filtered and conditioned for further processing

Fuel Valve Position Command: This is the output signal coming out of the turbine speed controller.

4.4 Excitation Signal Design

4.4.1 General

The following section describes the process of designing an optimal excitation signal for the turbine dynamic model identification. It is known that the input signal for

identification has to be sufficiently rich in excitation signals to adequately bring out the dynamic modes of the gas turbine system under consideration. Although it is not as obvious in time-domain identification as in frequency response identification, the excitation must be rich in frequency content to excite all the modes of the system. In order to arrive at an acceptable excitation, i.e. an input that is rich in the spectrum of frequencies of interest, the system modes are analyzed using *a priori* data about the gas turbine and fuel system. In cases where the data is not readily available, design and application experience must be utilized to determine a reasonable range of frequency. In this study, however, a different approach is used; the system modes and time delay are estimated using an on-line step response.

4.4.2 Estimate of System Characteristics

When designing a suitable test signal it is important that the amplitude of the signal be as large as possible but within a linear operating range of the gas turbine systems. This is especially an important consideration for our case since we intend to use linear discrete black-box models to represent the turbine dynamics. Furthermore, since we have assumed that the turbine is operating in full production mode, it is necessary to avoid excessively upsetting the turbine operation. In addition to signal amplitude consideration, there are two other important properties of a suitable excitation signal: signal power and signal bandwidth [45] (Porch).

Signal Amplitude: For our purpose, safety practice and the need to stay within the linear operating range of the gas turbine systems require that the input signal does not exceed +/-5% of the nominal speed setpoint which is 3600 RPM.

Signal Power: During the identification experiment it is necessary to inject as much power into the turbine system as possible. This can be achieved by using a large signal amplitude (which is proportional to the energy). However, in order to stay within acceptable operating limit, the power should be distributed over the frequency range of the input signal. In a parametric model a mathematical transfer function describes the system with a limited number of parameters. These parameters include the information available from all frequencies and they need to be accurately estimated using the parametric modeling approach. The optimum power spectrum of the excitation signal in the parametric model should contain the high energy levels at those frequencies where it contributes most to the knowledge about the parameters of the model [55] (Schoukens et al.).

Signal Bandwidth: To determine an appropriate bandwidth for the excitation signal, it is proposed that a small step response be initially generated. This step response is induced by applying a 5% increase in the speed setpoint while the turbine is operating at steady state full load conditions. From this step response data, the system time constant and time delay can be estimated. The time constant is estimated as the time it takes for the turbine speed to reach 63.3% of the final value after the fuel valve position command changes. The time delay is estimated as the time elapsed between a change in the fuel valve command and the change in turbine speed. The corner frequency (in Hertz) is then

the reciprocal of the time constant (in seconds). Assume that the corner frequency ω_c and the time delay T_d have been obtained from the step response data. The input signal bandwidth required for turbine excitation can be specified by the minimum frequency, ω_{min}, and the maximum frequency ω_{max} where

$$\omega_{min} < \omega_c < \omega_{max}$$

From turbine application experience, it is reasonable to assume that

$$\omega_{min} = 0.02\omega_c \quad \text{and} \quad \omega_{max} = 2\omega_c$$

The following section presents the results of the step response experiment using the GE turbine simulation model discussed in the previous chapter. The turbine operation is initiated at time t = 0 second with the turbine speed setpoint at the nominal value of 1 and with 100% load. After the turbine settles to the steady state condition at time t = 20 seconds, a step input of 5% (of the nominal setpoint) was generated and superimposed onto the setpoint. Values of the speed setpoint, turbine speed, and fuel valve position command are recorded for a period of 50 seconds. Figure 4.3 below shows the 5% step response of the turbine system and Figure 4.4 provides a zoomed-in window of the response for time t =18 to 24 seconds. The initial nonlinear transient seen in both plots is due to the fuel valve position being limited at the upper end. The larger the speed error the more likely the controller output will reach the fuel limit setting. For smaller step, for example, 1% of the speed setpoint, the transient response of the fuel is basically linear. The fuel limit setting is shown in the turbine simulation model in the previous chapter. From the plot data, the time constant of the system (the time it takes to reach 63% of the final speed of 1.05) is calculated to be 1.406 seconds. The time delay between the speed

setpoint signal and turbine speed as well as the delay between the fuel valve position command and turbine speed is approximately 71 milliseconds.

The corner frequency in Hertz is the reciprocal of the system time constant

$$\omega_c = 1/1.406 \text{ seconds} = 0.7 \text{ Hz}$$

The time delay is

$$T_d = 0.071 \text{ seconds}$$

The minimum and maximum frequency of the desirable excitation signal can then be determined from the corner frequency ω_c

$$\omega_{min} = 0.02\omega_c = 0.014 \text{ Hz} \qquad \text{and} \qquad \omega_{max} = 2\omega_c = 1.4 \text{ Hz}$$

The values of ω_{min} and ω_{max} will be used later for the design of the multi-sine excitation signal. The value of T_d will be used to formulate the structure of the black-box models in the subsequent sections.

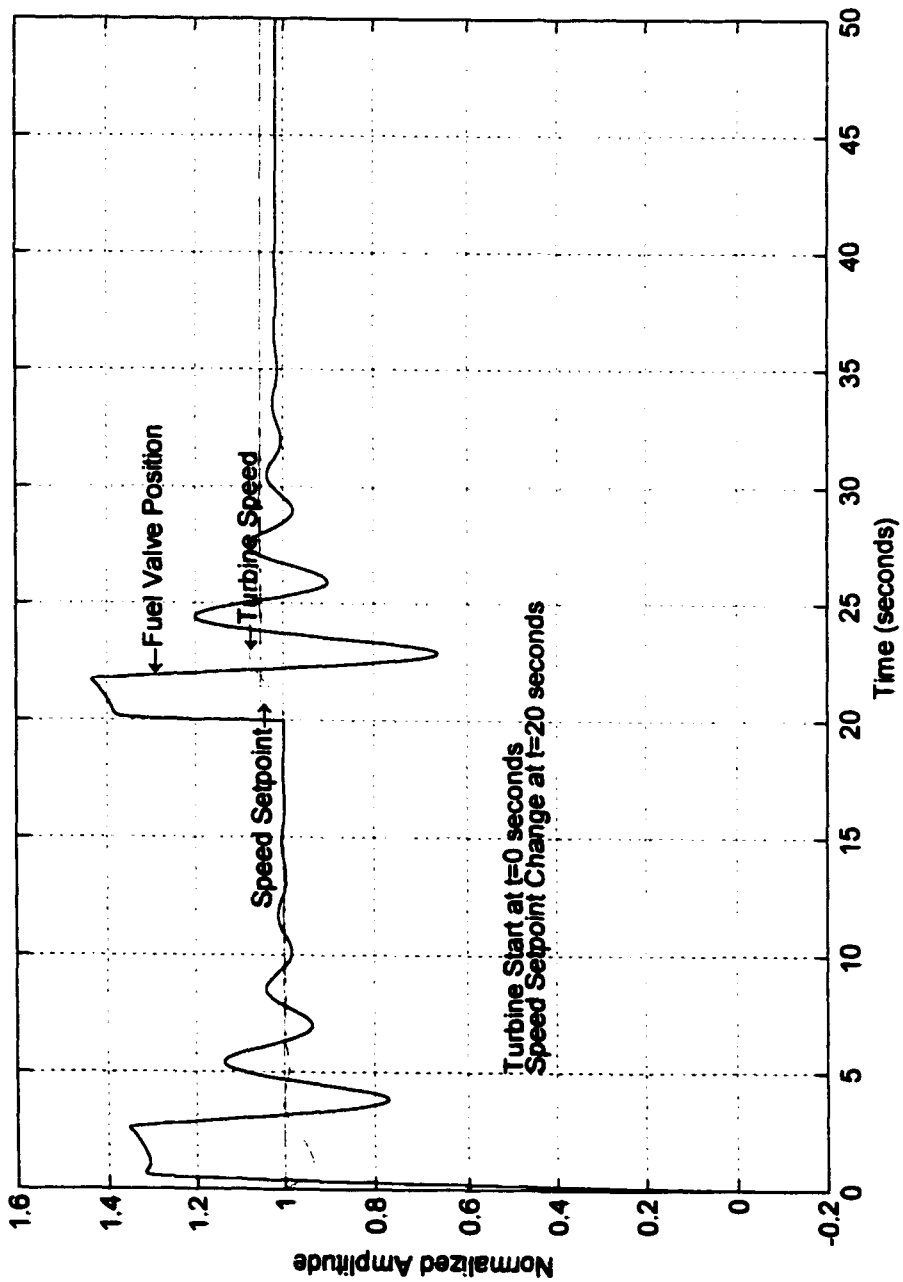

Figure 4.3 Response to a 5% Step Input

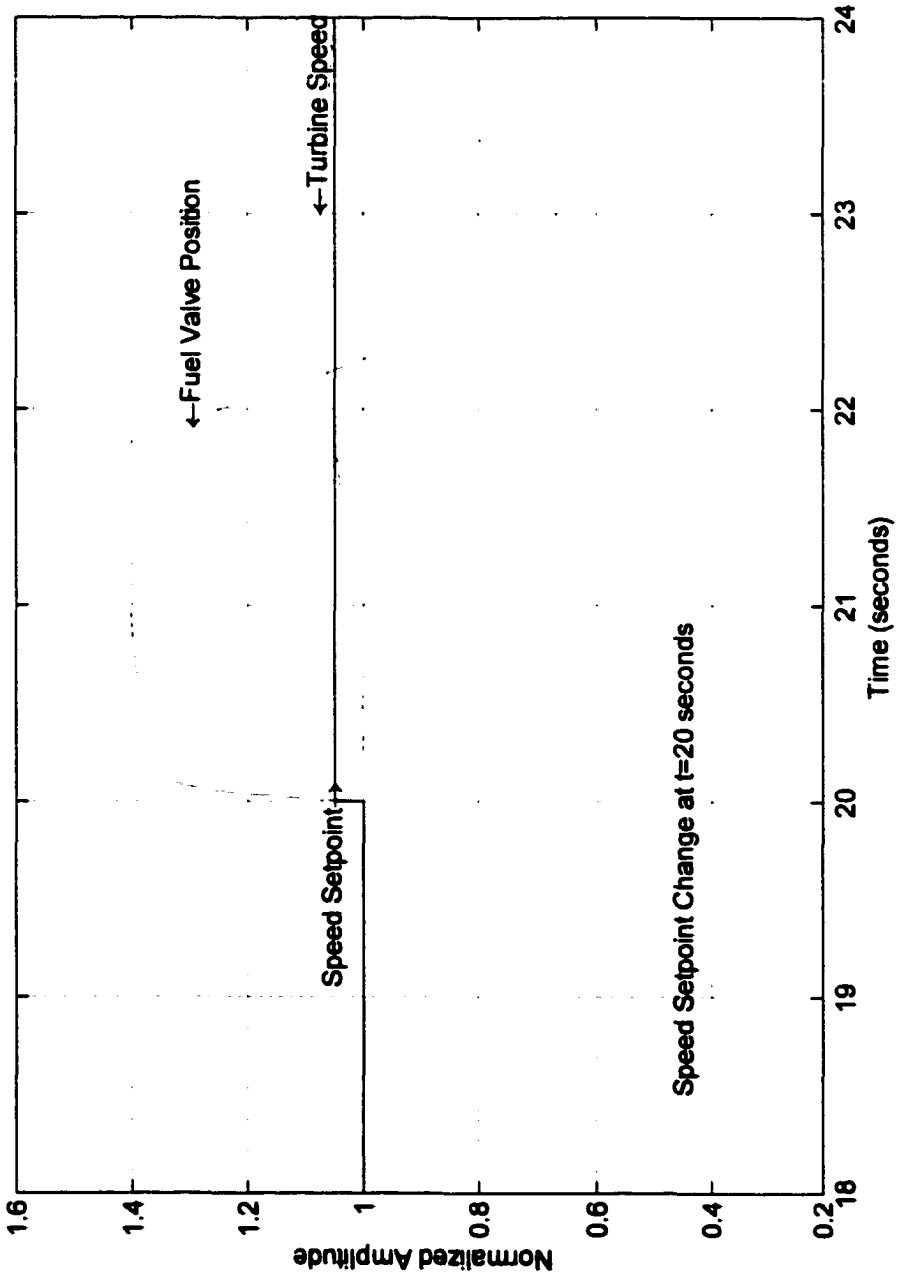

Figure 4.4 Zoomed View of the Step Response to a 5% Input

4.4.3 Multi-Sine Signal Design

Examples shown in Schoulken et al. [54] and others illustrate that the multi-sine signal, which is a periodic signal consisting of the sum of a set of harmonically related sinusoids, always generates a suitable excitation in all situations. The inherent properties of the multi-sine provide the flexibility to configure the frequency and amplitude spectrum as required by the application. For these reasons, the multi-sine is the signal of choice for this turbine identification experiment.

When designing an excitation it is desirable to have as much input power as possible across the frequency band of interest, i.e. maximum possible amount of energy injected into the system at all frequencies. However, in practice, this is limited by the input amplitude constraint. The goal here is to design an optimal excitation for the experiment where "optimal" means that maximum accuracy is obtained in a fixed measurement time for a specified peak value of the excitation signal. Optimization with respect to time domain behavior maximizes the injected power of the excitation signal by compressing it. This results in an improved signal-to-noise (S/N) ratio, and hence greater accuracy in the parameter estimates [54]. It was also shown by Schoulken et al. [54] that the energy could be maximized for an extreme value of the excitation signal by using different compression techniques. The two most important features of a test signal are a minimum crest factor and a minimum time factor. Low crest factor is indicative of a high energy level and low distortion in the signal, whereas low time factor is indicative of the overall quality of the signal with respect to measurement accuracy [54]. Further description and analysis of the crest factor and minimum time factor are presented in Appendix B.

The basic requirement in the design of the multi-sine is the specification of the frequency range and amplitude spectrum. Once this is done, an iterative mathematical algorithm can be utilized to calculate a signal that has a minimum crest factor. The input frequency range of 0.014 Hz to 1.4 Hz was determined previously from the step response data. The appropriate number of components in this frequency range and the amplitude for each component has been determined by trial and error in this study. In general, it was found that having 10 or more components at equal intervals tends to improve the richness of the data for identification purposes. To improve the likelihood that all turbine system dynamic frequencies are included, 100 components in the frequency range of 0.014 Hz to 1.4 Hz have been used. It was also found that signal amplitudes of 0.2 or lower for each frequency component generate an acceptable multi-sine signal in the time-domain, i.e. one that stays within the +/-5% of the speed setpoint. Figure 4.5 shows the amplitude spectrum of this test signal.

The clipping algorithm (described in Appendix B) is used to calculate the multi-sine signal using the above specification. For this experiment, a total of five periods of the test signal is generated. This is intended to have sufficient data points for subsequent analysis. Figure 4.6 shows the resulting excitation signal in the time-domain having five repeating periods. From the plot, it is obvious that using the compression technique in the clipping algorithm, the time-domain amplitude has been reduced significantly. The reduction is from the level of 0.2 specified initially to the level of about 0.0025. The signal, however, appears to have a rich excitation across the frequency range. Having the signal amplitude at such a small level reduces the risk of upsetting the turbine operation.

Next, the excitation signal from Figure 4.6 is superimposed on the turbine speed setpoint during steady-state operation. During this time, fuel valve position command and turbine speed are collected at an interval of 0.001 seconds. Figures 4.7 shows the recorded data. Note that the total experiment time for five periods of excitation occurred in approximately 350 seconds.

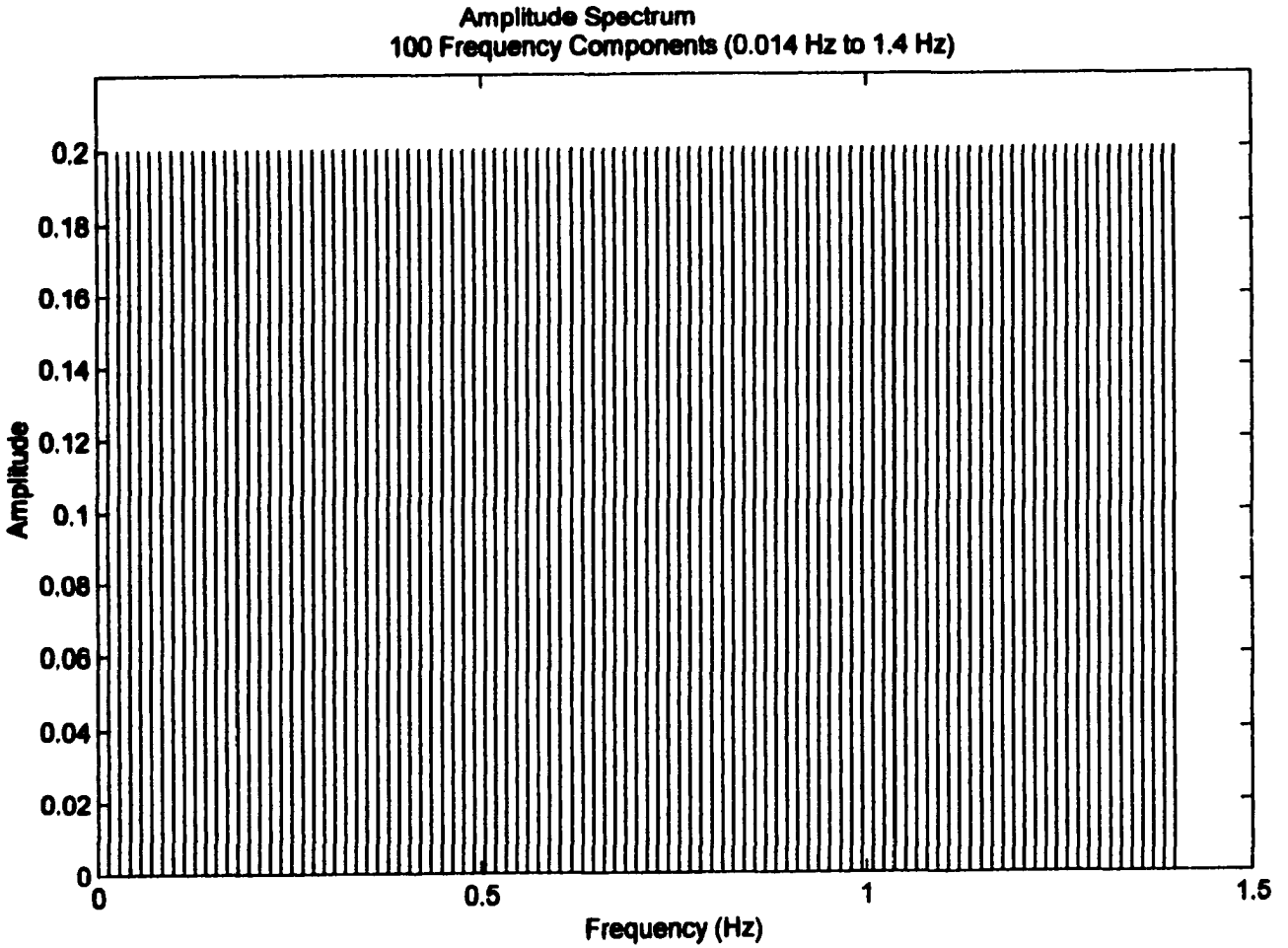

Figure 4. 5 Frequency Spectrum of the Excitation Signal

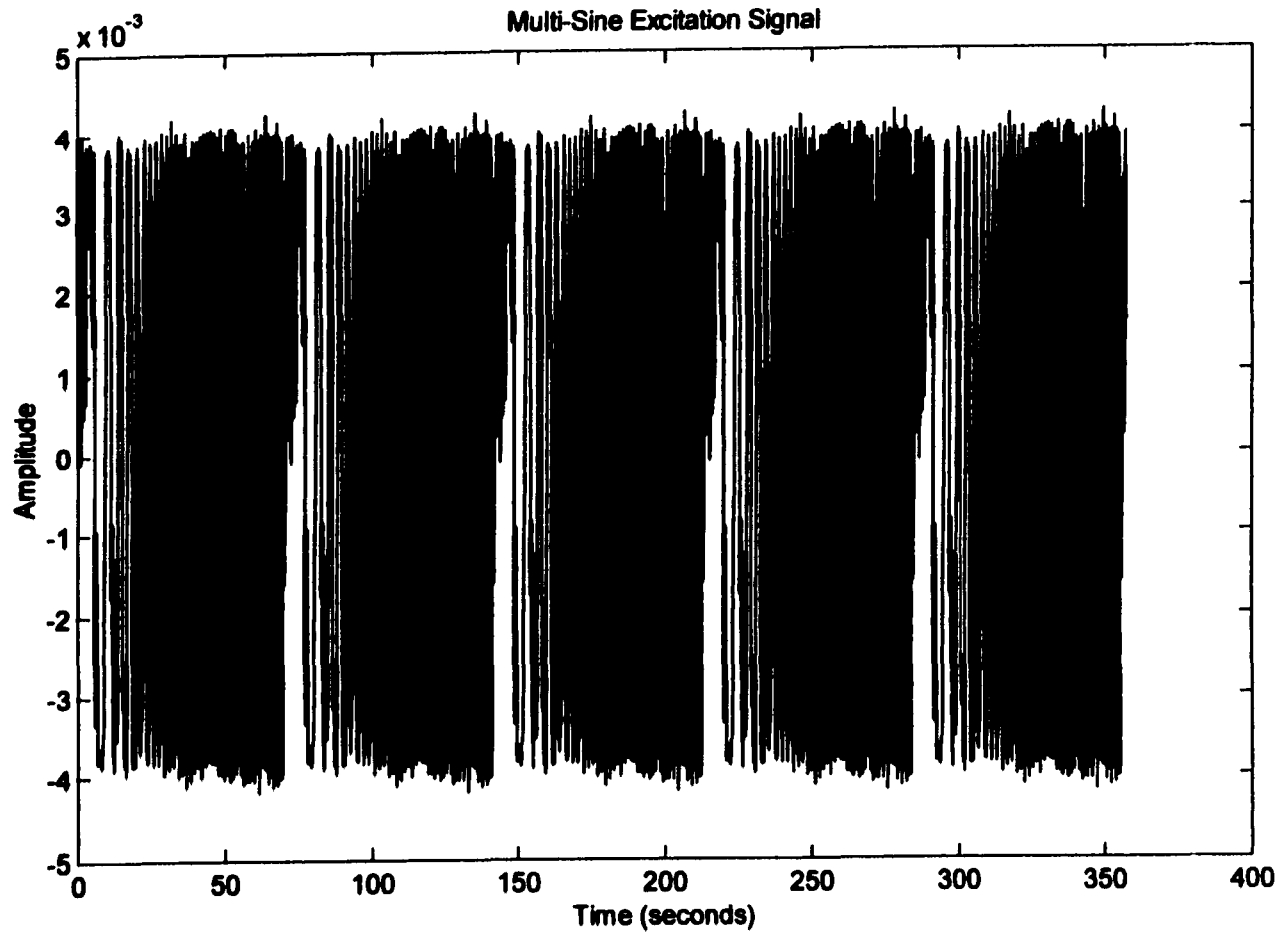

Figure 4.6 Multi-Sine Excitation Signal

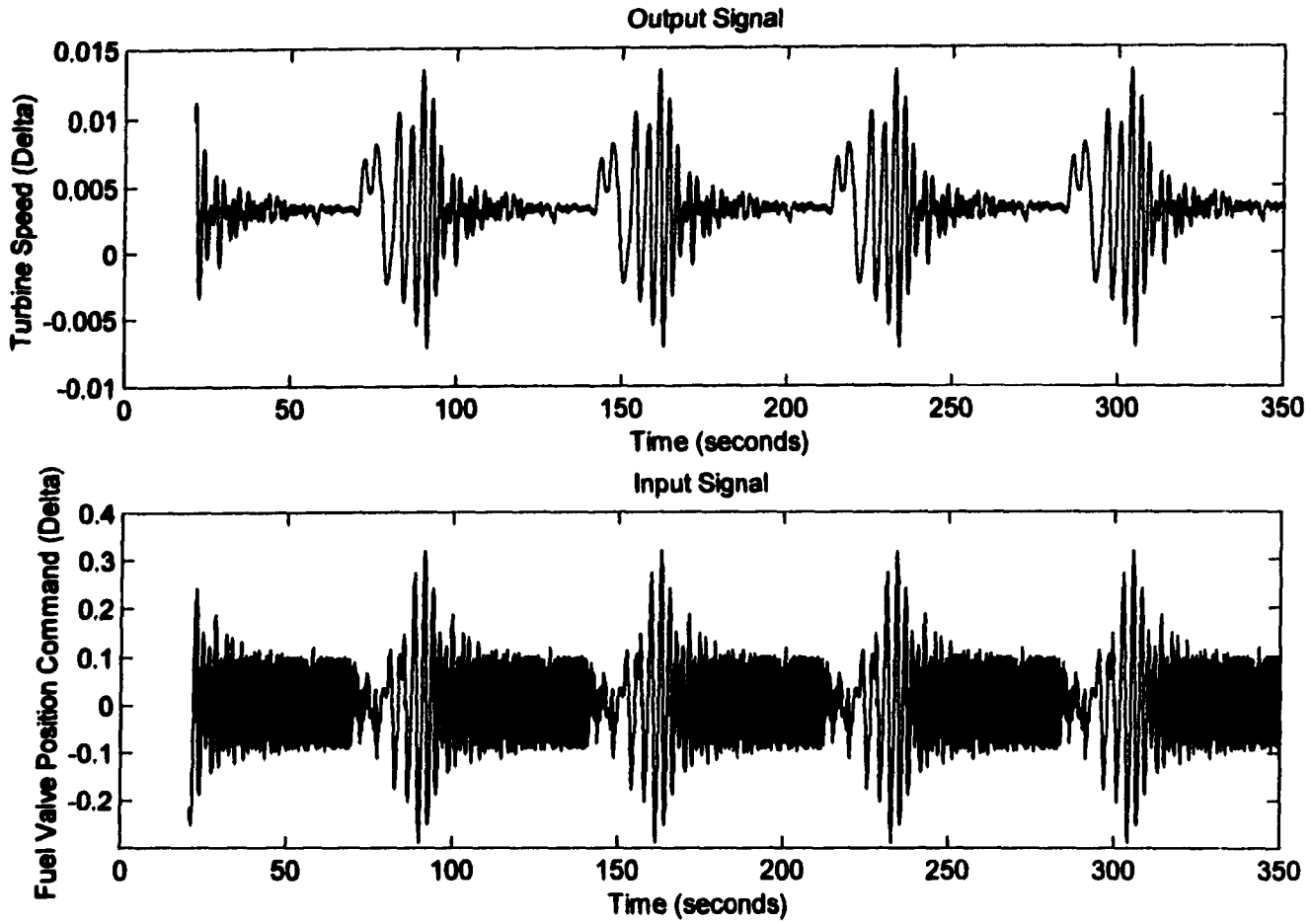

Figure 4.7 G.E. Turbine Model Input/Output Data

4.4.4 Selection of Sampling Interval and Number of Data Points

The issue of selecting appropriate sampling interval will be addressed later in the section on model validation. As noted in the experiment, the data has been collected using a time interval of 0.001 second (1 KHz sampling rate) for a total of five excitation periods (350 seconds total). The fast sampling rate is used to capture all possible information available in the input/output data. For analysis purpose, however, re-sampling at a longer time interval may be required to reduce the computational effort. From a practical viewpoint, a minor interruption of 350 seconds would be acceptable during normal turbine operation.

From a theoretical viewpoint, the choice of sampling interval is linked to the time constants of the system. Sampling that is significantly faster than the system dynamics produces data redundancy and relatively small information value in the new data points. Also, sampled models with very small sampling intervals compared to the system time constants can cause numerical sensitivity during parameter computation [35] (Ljung). Sampling that is slower than the system dynamics leads to serious difficulties in determining the parameters that describe the dynamics. A rule of thumb is to choose a sample frequency at least 10 times the bandwidth of the system [54] (Schade) and [35] (Ljung). The accuracy in parameter estimation for most identification methods is usually improved with larger number of data points. The tradeoff is between the time required to perform the experiment and better accuracy in the parameter estimates. In a power generation production environment, it is typically not desirable to perturb the process more than what is necessary. Fluctuations in turbine speed result in corresponding swings in the electrical voltage which can cause damage to the users' equipment.

4.4.4 Experimental Procedure

To summarize the steps in the identification experiment

Step 1:

Set up data acquisition equipment (or in software) to measure the speed setpoint, fuel valve position command and turbine speed.

Step 2:

Start the turbine and bring it up to rated speed and full load. Apply a 5% step input to the speed setpoint and measure turbine speed and fuel valve position command. Determine the turbine system time constant and time delay. Calculate the corner frequency ω_c using the time constant value. Calculate the minimum and maximum frequency for the excitation signal using the guideline: $\omega_{min} = 0.02\omega_c$, $\omega_{max} = 2\omega_c$

Step 3:

Design excitation signal (multi-sine for this case) to include 100 components at equal intervals in the signal bandwidth. The bandwidth is determined by ω_{min} and ω_{max} from Step 3 above. Use amplitude of 0.2 for all frequency components.

Step 4:

Determine the sampling frequency based on the system time constant. Set the number of data points to be collected.

Step 5:

Superimpose the excitation signal onto the speed setpoint during turbine steady-state operation. Collect the data for turbine speed and fuel valve position command for further analysis.

CHAPTER 5: TURBINE MODEL STRUCTURE SELECTION

5.1 General

The objective of this research effort is to develop a simple but robust turbine model that can be used to tune the controller's parameters so as to maintain/improve the system performance even as the performance of the components deteriorate over time. In general, for both on-line and off-line computation, linear black-box models (difference equations) appear to be appropriate from the viewpoint of computational and algorithmic complexity required to calculate the model parameters from experimental data. In this section, different forms of linear black-box models are reviewed for applicability to the problem of estimating the model of the single-shaft gas turbine engine.

It is well understood that the higher the order of the model the better it can fit to the data. However, higher-order models result in excessive computational effort and pose the risk of losing particular physical meaning of the model. In situations where there is noise on the measurements, additional parameters can give a better fit to the measurements. However, the introduction of the extra parameters increases the covariance matrix and reduces numerical stability [54] (Schoukens, J. and R. Pintelon). The essential trade-off is between a good fit of the model to the experimental data and the complexity of the required computation.

5.2 Model Structure Selection

General black-box models are quite often used in system identification and controller synthesis problems. The usual approach is to use linear regression models with stochastic noise inputs for dynamic systems to represent the system structure. The general model structure discussed widely in the identification literature is as follows

$$y(t) = G(q^{-1};\theta)u(t) + H(q^{-1},\theta)e(t) \qquad (5.1)$$

y(t) is the output at time *t* and *u(t)* is the input. *e(t)* is a sequence of independent and identically distributed random variables with zero mean (white noise) and q^{-1} is the delay operator. For the problem at hand where the experimental data is collected while the system is in closed-loop control, the perturbation caused by the feedback signal and the action of the controller can reasonably be considered as noise in the system under test. As a result, special cases of the general model structure known as ARMAX and ARX are appropriate. These model structures are described below

For a single input single output (SISO) systems the general model structure above can be written as an ARMAX model

$$\begin{aligned} &A(q^{-1})y(t) = B(q^{-1})u(t) + C(q^{-1})e(t) \\ &\textit{where} \\ &A(q^{-1}) = 1 + a_1 q^{-1} + \ldots + a_{na} q^{-na} \\ &B(q^{-1}) = b_1 q^{-1} + \ldots + b_{nb} q^{-nb} \\ &C(q^{-1}) = 1 + c_1 q^{-1} + \ldots + c_{nc} q^{-nc} \end{aligned} \qquad (5.2)$$

The model parameter vector is

$$\theta = (a_1 \ldots a_{na} b_1 \ldots b_{nb} c_1 \ldots c_{nc}) \qquad (5.3)$$

Equation (5.2) can be written explicitly as the difference equation

$$y(t)+a_1y(t-1)+\ldots+a_{na}y(t-na)=b_1u(t-1)+\ldots+b_{nb}u(t-nb)+e(t)+c_1e(t-1)+\ldots+c_{nc}e(t-nc) \quad (5.4)$$

Equation (5.4) can also be written to include a time delay from the input to the output signal. Assume that the time delay is equal to a number of *nk* samples. This would make some leading coefficients of polynomial $B(q^{-1})$ zeros. The expression for $B'(q^{-1})$ below is then used in the difference equation (5.4)

$$B'(q^{-1})=b_{nk}q^{-nk}+b_{nk+1}q^{-nk-1}\ldots+b_{nk+nb-1}q^{-nk-nb+1}=q^{-nk}B(q^{-1}) \quad (5.5)$$

Examining equation (5.2), the ARMAX model can be interpreted as the noise *e(t)* and input *u(t)* are subjected to the same dynamics (same poles) in $A(q^{-1})$. This is a reasonable interpretation if the dominating disturbances enter early in the process (together with the input) [37] (Ljung, L. and Torkel Glad). This interpretation is also applicable to the case of system under closed-loop control where the noise *e(t)* is treated as the disturbances generated by the controller and/or feedback effect.

The case when the previous values of the noise *e(t)* do not contribute to the dynamics of the output *y(t)* is the ARX model, which can be written as

$$y(t)+a_1y(t-1)+\ldots+a_{na}y(t-na)=b_1u(t-1)+\ldots+b_{nb}u(t-nb)+e(t) \quad (5.6)$$

The ARX model is the easiest to estimate since the corresponding estimation problem is of a linear regression type. Ljung, L. and Torkel Glad [37] recommends that the ARX should be used as a starting point because of its simplicity. However, it is cautioned that

the ARX model can result in incorrect estimates of the system dynamics because the $A(q)$ polynomial also has to describe the disturbance properties. In this case, to improve accuracy, higher order in polynomials $A(q)$ and $B(q)$ may be required. The ARMAX model is certainly the most used black-box model because it gives extra flexibility to handle disturbance modeling with the additional terms in the $C(q)$ polynomial.

5.3 Model Structure Validation

This is the problem of determining the "best" model within a chosen model structure. Given a model structure, it is always possible to use the data set obtained in the experiment to evaluate whether the selected model will serve its purpose [35] (Ljung). This study has selected the black-box models as the model structure of choice, and within this family the ARX and the ARMAX are being considered. The remaining issue is to determine the better between the ARX and the ARMAX models. As explained previously, there is general consensus in the identification community that the model validation is done by several ways: using a priori knowledge about the system, using the experiment data, and possibly using the experience of working with the model.

The model's ability to reproduce the measured output data is obviously a necessary criterion for comparison. This is the basic tool that will be used to compare between ARX and ARMAX models in the section on Turbine Model Validation. The other recommended tool is the Residual Analysis, which involves looking at the covariance between residuals (errors), $\varepsilon(t)$, and past inputs, $u(t-\tau)$, where

$$\varepsilon(t) = y(t) - y^*(t \mid \theta_N^*) \qquad (5.7)$$

$$\hat{R}_{\omega}^{N}(\tau) = \frac{1}{N}\sum_{t=1}^{N}\varepsilon(t)u(t-\tau) \qquad (5.8)$$

If these numbers are small it is reasonable to assume that the model could have relevance also when it is applied to other inputs [35] (Ljung). The covariance of signals is discussed in appendix A of this work.

The mean square error (MSE) between the measured output and the predicted output is another measure of the how well the selected model structure can reproduce the output data

$$MSE = \sqrt{\frac{1}{N}\sum_{t=1}^{N}\left(y(t) - y_p(t)\right)^2} \qquad (5.9)$$

N is the length of the data record, $y(t)$ is the recorded output data, and $y_p(t)$ is the predicted output using the model. The MSE is typically calculated over the entire length of the data record.

There are other standard criteria that determine the suitability of a model structure and the parameter values within the structure. The best known technique is the Akaike's Final Prediction Error (FPE) criterion and his closely related Information Theoretic Criterion (AIC) [1]. Both of these criteria simulate the cross validation scenario, where the model is tested on a different data set. The FPE is formulated as

$$FPE = \frac{1+\frac{n}{N}}{1-\frac{n}{N}} * V \qquad (5.10)$$

n is the total number of estimated parameters, N is the length of the data record, and V is the quadratic fit loss function for the model structure under consideration. The AIC criterion is formed as

$$AIC \approx \log\left[\left(1+\frac{2n}{N}\right)*V\right] \qquad (5.11)$$

According to Akaike's theory, the model with the smallest FPE or AIC value should be selected.

5.4 Model Order Selection

This is a problem of selecting the "correct" model order that can best represent the system dynamics. Although there are heuristic and analytical approaches in determining the appropriate model order, there is a general consensus in the system identification community that the model order can best be determined through experimentation. In general, certain model structure and order are selected, the identification experiment is carried out and then the model predicted output (using the same input signal) is used to calculate the error from the measured system output. Statistical tests can then be carried out on the prediction error to determine whether the model order has any validity. Typical validation procedures also recommend plotting out the model predicted output data for comparison with the measured system output. The subsequent section on model validation will basically employ these steps outlined in this section. For most cases, the "correct" model can be thought of as the simplest one that explains all the data well enough.

The model order is a result of the intended use. For requirements to gain physical insights into the physics of the system, complex models maybe required. For control design purposes, often a simple low-order model would suffice. Furthermore, the more complicated the model the more difficult it is to design the controller. Again, the question of computational complexity versus ease of use is the primary issue. In our present study, it is assumed that the models ARX and ARMAX should be at most a 4^{th}-order system.

CHAPTER 6: IDENTIFICATION METHOD

6.1 Prediction Error Methods

The prediction error methods are basically procedure to calculate the prediction of the output at time t given input/output data up to time $t-1$. This predicted output is calculated using the selected model $M(\theta)$ as discussed in the previous chapter. The question of identifiability and accuracy of various methods for identifying the open-loop characteristics of dynamic systems using closed-loop data has been addressed extensively in the technical literature [25], [26], [33], [35], [61], [65]. The analysis presented in the above references lead to the conclusion that it is possible to identify the open-loop dynamics from the data collected under feedback. The underlying assumption is that the data is sufficiently informative and that the model set under consideration contains the true system. The general recommendation from these studies is that the prediction error methods (PEM) should be the prime choice for identifying system model with closed-loop data.

The prediction error method works especially well in the direct identification configuration. This is the configuration where the system is operating in the closed loop with the controller in action. The input/output data for the open-loop system is measured and treated as though they were obtained from an open-loop experiment, ignoring any feedback and not using the loop reference signal. Detailed studies by Gustavsson et al. [25] and Soderstrom et al. [62] show that the direct identification is the simplest

approach to employ for a closed-loop system and that it works regardless of the complexity of the controller. Ljung [35] further illustrates that the direct identification does not require knowledge about the character of the feedback or special algorithms and software. Ljung [35] also shows that the direct identification will result in consistency and optimal accuracy if the model structure contains the true system.

The PEM methods are closely related to the maximum likelihood (ML) method which is a very general method for parameter estimation. The basic idea in the maximum likelihood method is to construct a function of the data and the unknown model parameters called the likelihood function. The estimate is then obtained as the parameter values which maximizes the likelihood function. By definition, the likelihood function is essentially the probability density function of the observations. To determine the likelihood function it is necessary to have *a priori* knowledge that makes it possible to write the conditional probability of the observed data. This usually means that the probability distribution of the observations must be known in advance. The determination of this conditional distribution is essentially a prediction problem and the likelihood function can be expressed as a product of the conditional densities of the prediction errors. This relation to the prediction problem leads to an alternative formulation of the parameter estimation, which involves a prediction model and a criterion, which is a function of the prediction errors. In both the PEM and ML methods, the similarity exist in the optimization (maximization or minimization) of a function. However, the criterion function is formulated in a different way in each of the two methods. The criterion function in the ML approach is formulated based on probability

theory whereas the criterion function in the PEM is formulated with no probabilistic assumption. Astrom [5] stated that the PEM and the ML methods have the advantage that they can be applied to a large variety of model structures and experimental conditions and that they have been shown to have good asymptotic properties in many cases. It was also stated in the same reference that the drawback of these methods is that they often require substantial numerical calculations. However, with the existing computing power, this has become less of an issue.

In this study, no *a priori* knowledge has been assumed about the observations. Hence it is difficult to use the maximum likelihood method for lack of the knowledge about the probability density function of the data and the parameters. Therefore, it is reasonable to choose the prediction error methods as the procedure to identify the open-loop dynamics of the turbine using closed-loop data. A description of the prediction error methods is discussed in Appendix C of this document.

6.2 Prediction Error Method Applied to Turbine Model Parameterization

The parameter estimation principle for discrete model of the turbine system is illustrated in Figure 6.1. A discrete-time model with adjustable parameters is implemented on the computer. The error between the turbine speed (output) at instant t, $y(t)$, and the output predicted by the model $y_p(t)$ is used by a parameter adaptation algorithm which, at each sampling instant, will modify the model parameters in order to minimize this error. The parameter adaptation algorithm inherently contains a criterion function which is used as the basis for minimizing the prediction error. The parameter adaptation algorithm shown

in the block diagram is essentially the Prediction Error Method (PEM) that has been discussed above. Examining the block diagram in Figure 6.1, the PEM can be implemented either in on-line or off-line mode. Our approach here is to perform the identification procedure off-line (batch mode) which means that all the data are collected before the analysis is carried out.

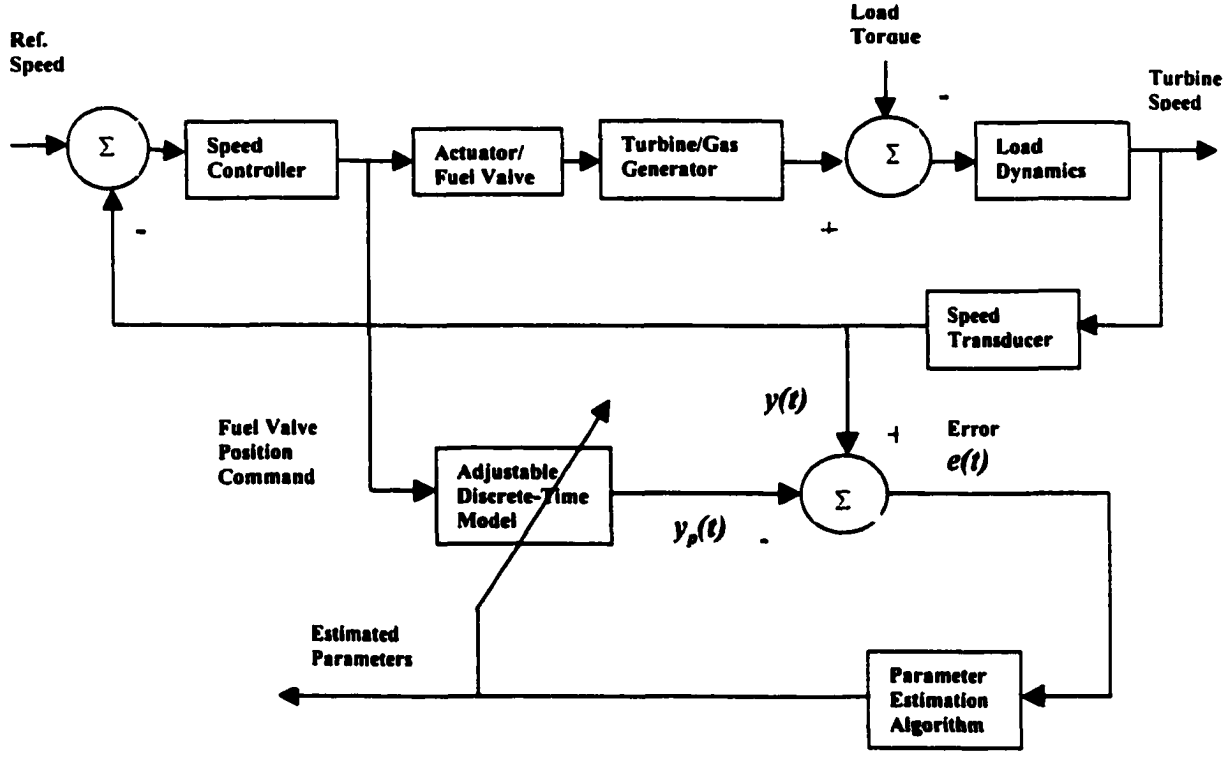

Figure 6.1 Turbine Model Parameter Estimation

6.3 Convergence of the Prediction Error Methods

The prediction error approach is described in detail in appendix C and repeated here for clarity. Given a vector D^N which contains the input and output data

$$D^N = [y(1), u(1), y(2), u(2), y(3), u(3), \ldots, y(N), u(N)]$$

and the model structure $M(\theta)$ containing the unknown parameter vector θ. The approach is to minimize a criterion function $V_N(\theta, D^N)$ so that the prediction error is as small as

possible. The prediction error is defined as the difference between the measured output and the predicted output provided by the model $M(\theta)$ when $M(\theta)$ is subjected to the same measured input $u(t)$

$$e(t, \theta) = y(t) - y^*(t|\theta)$$

where $y(t)$ = measured output

$y^*(t)$ = predicted output provided by $M(\theta)$

It has been proven in [35] (Ljung, Chapter 8) and [62] (Soderstrom et al., Chapter 7) that under proper conditions, the prediction error method will always lead to convergence of the parameter values θ as the number of measurement N approaches infinity. The assumed conditions are as follow

1. The selected model structure contains the "true system"
2. The collected data set is informative enough, or in other words, the input signal used in the experiment is persistently exciting
3. The selected model structure is linear and stable
4. The criterion function is a quadratic function in nature

Under these assumptions, it was shown in the above references that the estimate θ^* is the minimizing argument of the criterion function $V^*(\theta)$ as with probability of 1 as N approaches infinity

$$\theta^* \rightarrow \arg\min(V^*(\theta)) \qquad \text{with probability of 1 as } N \rightarrow \infty$$

where θ^* is the estimates and $V^*(\theta)$ is the average of the square of the prediction error over the ensemble of the data values. In other words, the estimate will converge to the best possible approximation of the system that is available in the model set.

CHAPTER 7: TURBINE MODEL VALIDATION

7.1 Validation Approach

As discussed in previous sections, the model structures under consideration are the ARX and the ARMAX models having at most 4^{th}-order dynamics. Discussion on the pros and cons of various identification methods also lead to the decision to use the prediction error method with a quadratic criterion for computing the model coefficients. Furthermore, using *a priori* knowledge of the single-shaft gas turbine, it is also determined that these discrete models should not contain any numerator dynamics, i.e. there is no zeroes in the discrete transfer function. The models then consist of the denominator dynamics (poles), noise dynamics (only in ARMAX models), and an appropriate time delay.

The general approach is to use the input/output data generated with the multi-sine excitation signal for computing the model coefficients. For clarity this set of input/output data will be called the estimation data and it is shown in Figure 7.1. Recall that the estimation data in Figure 7.1 is collected while the turbine is operating at full load. The resulting models are then validated employing different sets of data, which will be referred to as the validation data. From practical experience, an appropriate validation signal is a periodic ramp which has a frequency around 0.5 Hz. This validation data is obtained by applying a ramp signal having amplitude of 0.02 at 0.5 Hz to the speed setpoint in the General Electric turbine model. During this time, the fuel valve position command (input data) and the turbine speed (output data) are recorded for 100 seconds. In order to validate the estimated models at different operating condition, the validation

data for the 0.5 Hz ramp are collected at both full load and also at 25% load conditions. Both sets of validation data are shown in Figure 7.2.

Examining the validation data in Figure 7.2, it is obvious that when the turbine is operating at lighter loads, it does not require as much fuel input to effect the same turbine speed change demand, i.e. less torque is required to cause the same speed change. The nonlinear response due to the fuel command limits is again seen in Figure 7.2. At 100% load, where the fuel valve is operating at the high end of the flow, the maximum limit is causing the response to saturate at the top. At 25% load, the opposite is true, where the lower limit is causing the response to saturate at the bottom end.

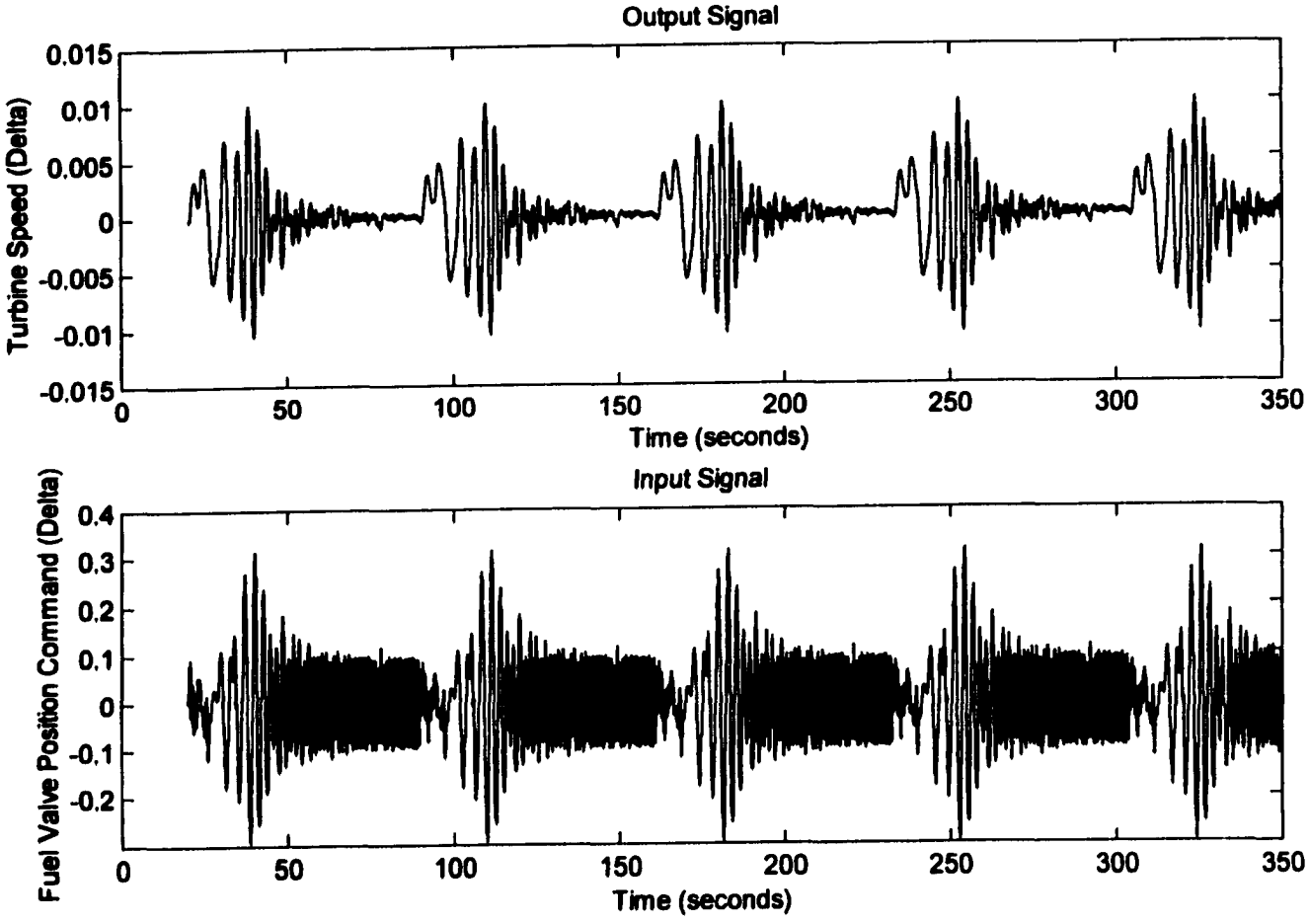

Figure 7.1 Estimation Data –Multi-Sine Excitation (5 Periods)

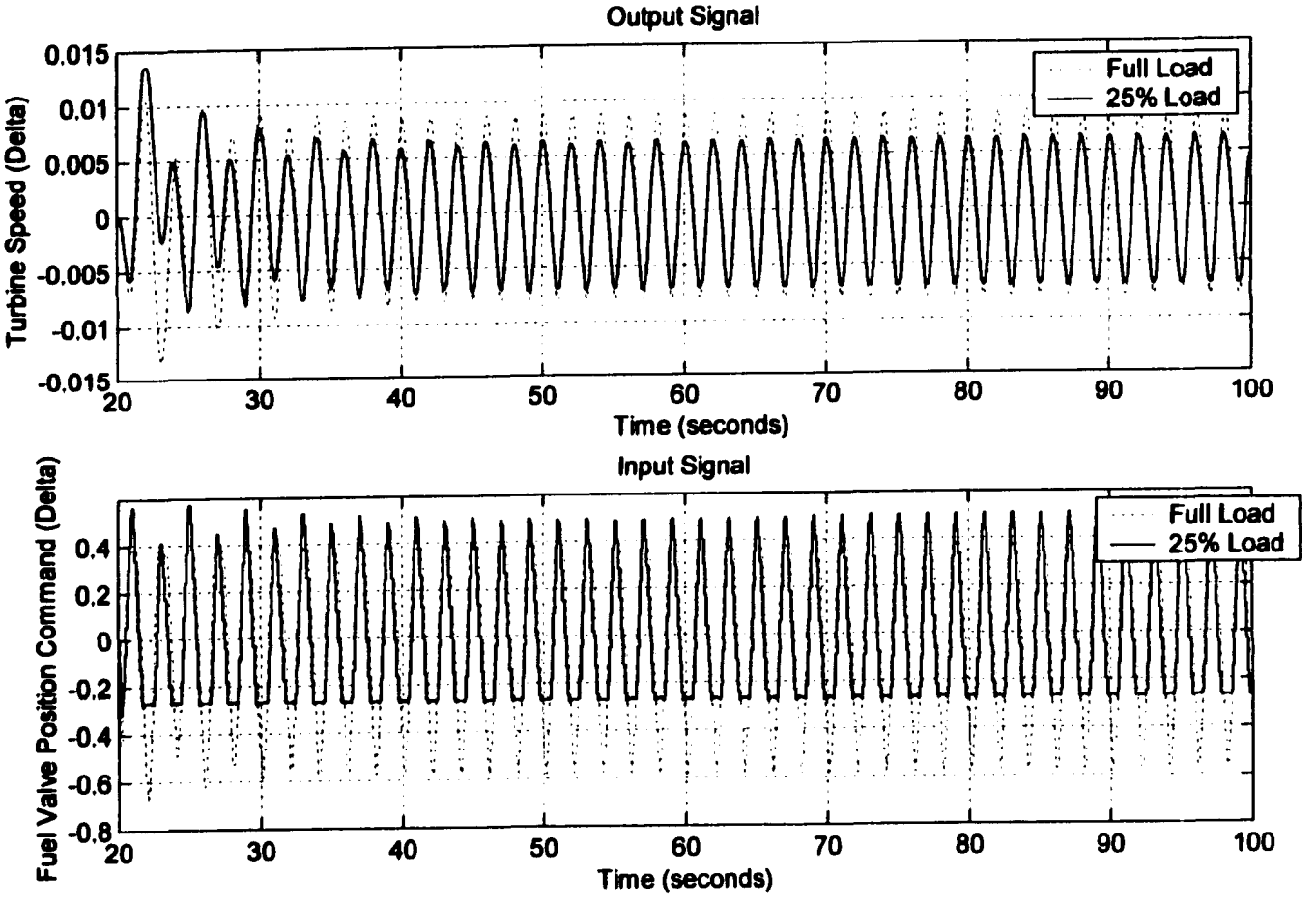

Figure 7.2 Validation Data – 0.5 Hz Ramp Signals

7.2 Data Handling

Recall that during the experiment the turbine input/output data are collected at the rate of 1 kHz. During the identification process, it was necessary to re-sample the data at a lower frequency to avoid aliasing effects and to avoid having the poles of the discrete models being very close to the +1 point on the unit circle. The lower sampling rate also reduces the number of data points which reduces the computation time in the prediction error algorithm significantly. Recall that the bandwidth of the turbine system was estimated at 0.7 Hz using the step response data. For this reason, it is appropriate to use the sampling rate of 10 Hz, which is approximately 10 times the bandwidth. This choice of the sampling rate is in good agreement with standard practice in industry and certainly widely recommended in control systems and identification literature. As discussed in the sections below, the optimum sampling rate is 10 Hz. Lowering the sampling rate to 5 Hz causes the numerical calculations to become unstable (divergent). It appears that, if the sampling rate is less than 10 Hz, much longer data record will be required to improve the convergence of the method. Higher sampling rates, for example, 20 Hz, do not seem to improve the model fit but certainly requires longer computation time.

7.3 Results

To facilitate the ensuing discussion, recall the formulation of the ARMAX and the ARX black-box models from equations 5.4 and 5.6, respectively

ARMAX:
$$y(t)+a_1y(t-1)+\ldots+a_{na}y(t-na)=b_1u(t-1)+\ldots+b_{nb}u(t-nb)+e(t)+c_1e(t-1)+\ldots+c_{nc}e(t-nc)$$

ARX:
$$y(t)+a_1y(t-1)+\ldots+a_{na}y(t-na)=b_1u(t-1)+\ldots+b_{nb}u(t-nb)+e(t)$$

For systems with a time delay the models can be written as

ARMAX: $$y(t)+a_1y(t-1)+\ldots+a_{na}y(t-na)=b_1u(t-nk)+\ldots+b_{nb}u(t-nk-nb+1)+e(t)+c_1e(t-1)+\ldots+c_{nc}e(t-nc)$$

ARX: $$y(t)+a_1y(t-1)+\ldots+a_{na}y(t-na)=b_1u(t-nk)+\ldots+b_{nb}u(t--nk-nb+1)+e(t)$$

where *nk* is an integer that is a multiple of the sampling interval

Both of the models relate the current output *y(t)* to a finite number of past outputs *y(t-k)* and inputs *u(t-k)*. For the ARMAX model, the structure is completely define by *na*, *nb*, *nc*, and *nk*. In this structure, *na* is the order of the denominator of the discrete transfer function (number of poles), *nb-1* is the order of the numerator (number of zeroes), *nc* is the order of the noise model, and *nk* is an integer multiple of the sampling time *T* representing the time delay. For sampled system, as can be seen in the above model equations, *nk =1* represents no time delay in the system. The ARX model structure has identical definition for *na*, *nb*, and *nk*, but since there is no noise dynamics, *nc* is always equal to zero.

For the problem at hand, where we already assumed there is no numerator dynamics in the transfer function for the turbine model, *nb* is set to 1 for both the ARMAX and the ARX models. The value of *nk* is dependent on the sampling time *T*. For example, when the data is sampled at 10 Hz, the sampling time is 100 milliseconds. Recall from the estimated time delay from the step response data collected earlier, the time delay was 71 ms. Hence *nk* is initially set at 2, which represents 100 milliseconds time delay. The next increment of *nk =3* represents a time delay of 200 milliseconds and so on.

The estimation data is used with the prediction error method to calculate the coefficients for both ARX and ARMAX models with increasing order and varying time delay. For each model, the Akaike Final Prediction Error and the Mean Square Error are calculated for comparison purposes. These values are shown in Tables 7.1 and 7.2 below. Recall that "better" model structure has lower the Akaike FPE value, where as the MSE is a measure of how well the model can reproduce the output data with the given validation data.

Figures 7.3 through 7.9 show the dynamic characteristics of the "correct" models of the ARX and ARMAX models, i.e. ones that have comparatively best combination of Akaike FPE and MSE values.

Table 7.1 – Akaike FPE and Mean Square Error for ARX Models

ARX Models			Normalized Akaike	Normalized Mean Square Error (Fit)	
na	*nb*	*nk*	FPE	Full Load	25% Load
2	1	1	104.08	2.11	2.13
2	1	2	72.16	1.05	1.01
2	1	3	63.18	0.63	0.61
3	1	1	93.28	1.70	1.58
3	1	2	71.71	0.99	0.95
3	1	3	61.79	0.66	0.65
4	1	1	93.28	1.76	1.65
4	1	2	70.07	1.16	1.14
4	**1**	**3**	**49.57**	**0.87**	**0.87**

Table 7.2 – Akaike FPE and Mean Square Error for ARMAX Models

ARMAX Models				Normalized Akaike FPE	Normalized Mean Square Error (Fit)	
na	*nb*	*nc*	*nk*		Full Load	25% Load
2	1	2	1	84.67	2.08	2.13
2	1	2	2	53.18	0.93	0.90
2	1	2	3	37.88	0.56	0.39
3	1	3	1	35.85	3.4E03	49.2E03
3	**1**	**3**	**2**	**24.38**	**0.66**	**0.39**
3	1	3	3	35.94	0.58	0.39
4	1	4	1	22.53	1.05	0.71
4	1	4	2	20.00	0.89	0.57
4	1	4	3	30.86	0.56	0.39

7.4 Discussion

In general, both the ARX and ARMAX models require the inclusion of at least one sampling interval of time delay (100 milliseconds). This is apparent from examining the Akaike FPE and the MSE in Tables 7.1 and 7.2. These values are reduced as much as 100% from no time delay (*nk*=1) to 100 milliseconds delay (*nk*=2). This is encouraging in the sense that our original time delay estimate of 71 milliseconds is not much off from the time delay of 100 milliseconds. For the ARX models, increasing time delay and model order appear to improve the model performance somewhat significantly. The higher model order (*na*=4) and longer time delay of 200 milliseconds (*nk*=3) seem to provide the best fit.

For the ARMAX models, the larger time delay (*nk*>2) and larger model orders (*na* >3, *nc*>3) provide a better fit to the validation data. However, the impact on the Akaike FPE seems negligible. In fact when the model order is increased above 3, the Akaike FPE

actually decreases indicating possible over-fitting situation. In general, the ARMAX is less tolerant with incorrect time delay. When no time delay is modeled, the ARMAX provides relatively high values in Akaike FPE and MSE. The model with (*na*=3, *nc*=3, *nk*=1) is especially sensitive to the incorrect time delay. This is evident in the very high MSE values for this particular model structure.

In general, the ARMAX provides better fit than the ARX model having the same denominator dynamics (same *na*). Increasing the ARX model order, however, can improve the fit. This can be explained by the fact that there is presence of noise in the estimation data. The source of the noise can come from the controller actions or the effect of feedback. The higher the order in the ARX the better it can model the noise effect in the data. It is apparent from the Akaike FPE and the MSE values that the 3rd-order ARMAX model (*na*=3, *nc*=3) having 100 milliseconds time delay (*nk*=2) provides the best overall performance.

Figures 7.3 through 7.6 show the response to the ramp signals for the best ARMAX and ARX models. It is apparent that both can track the 0.5 Hz ramp signals (full-load and 25% load) quite well with the ARMAX model performing slightly better. The MSE values show that the ARX model has the same fit in both load cases where as the ARMAX model has better fit to the 25% load ramp signal. Since the ability to track a ramp signal in the range of 0.5 Hz is often a requirement for typical industrial single-shaft gas turbines. It can be concluded that the obtained models would provide reasonable estimate for turbine controller design.

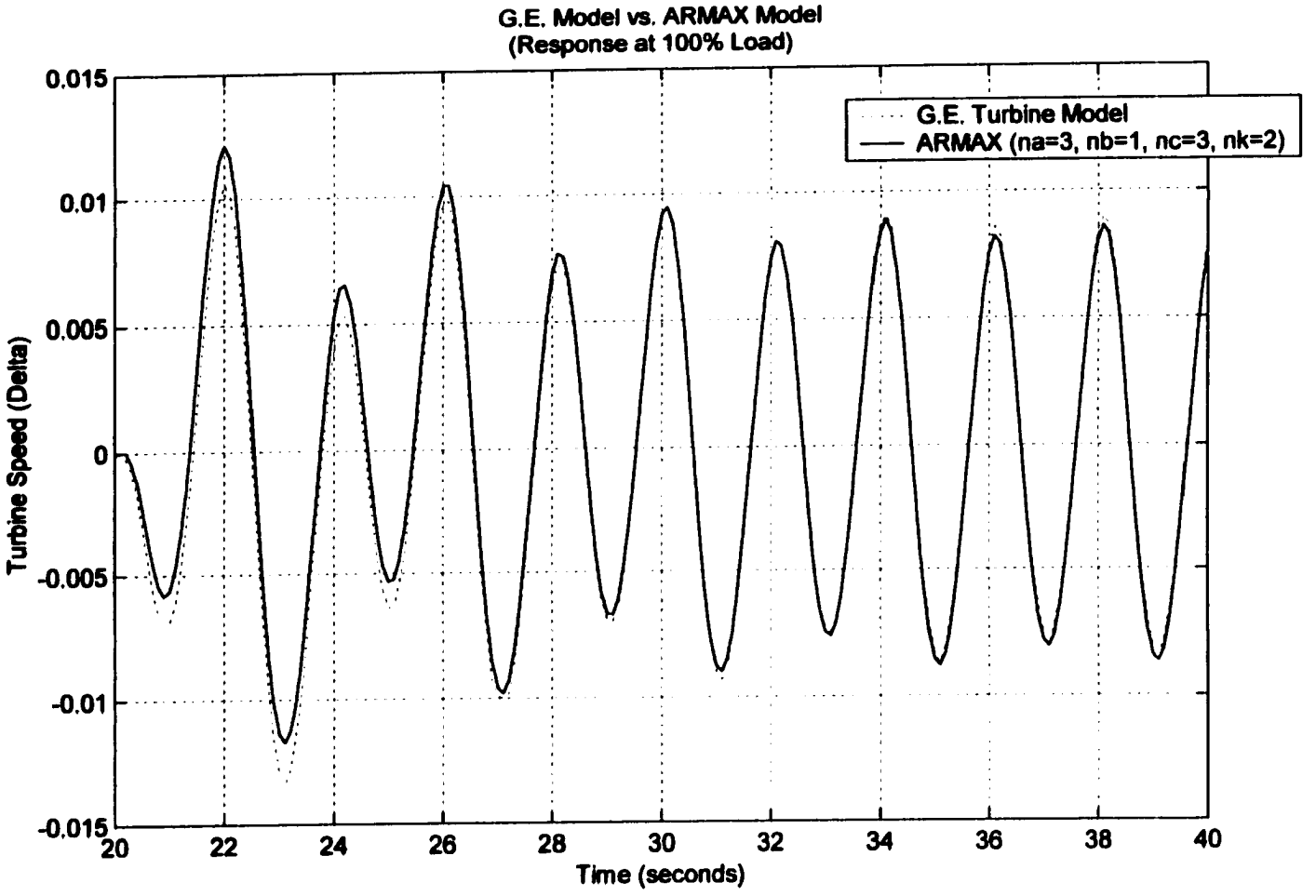

Figure 7.3 G.E. Model vs. ARMAX Model – 100% Load

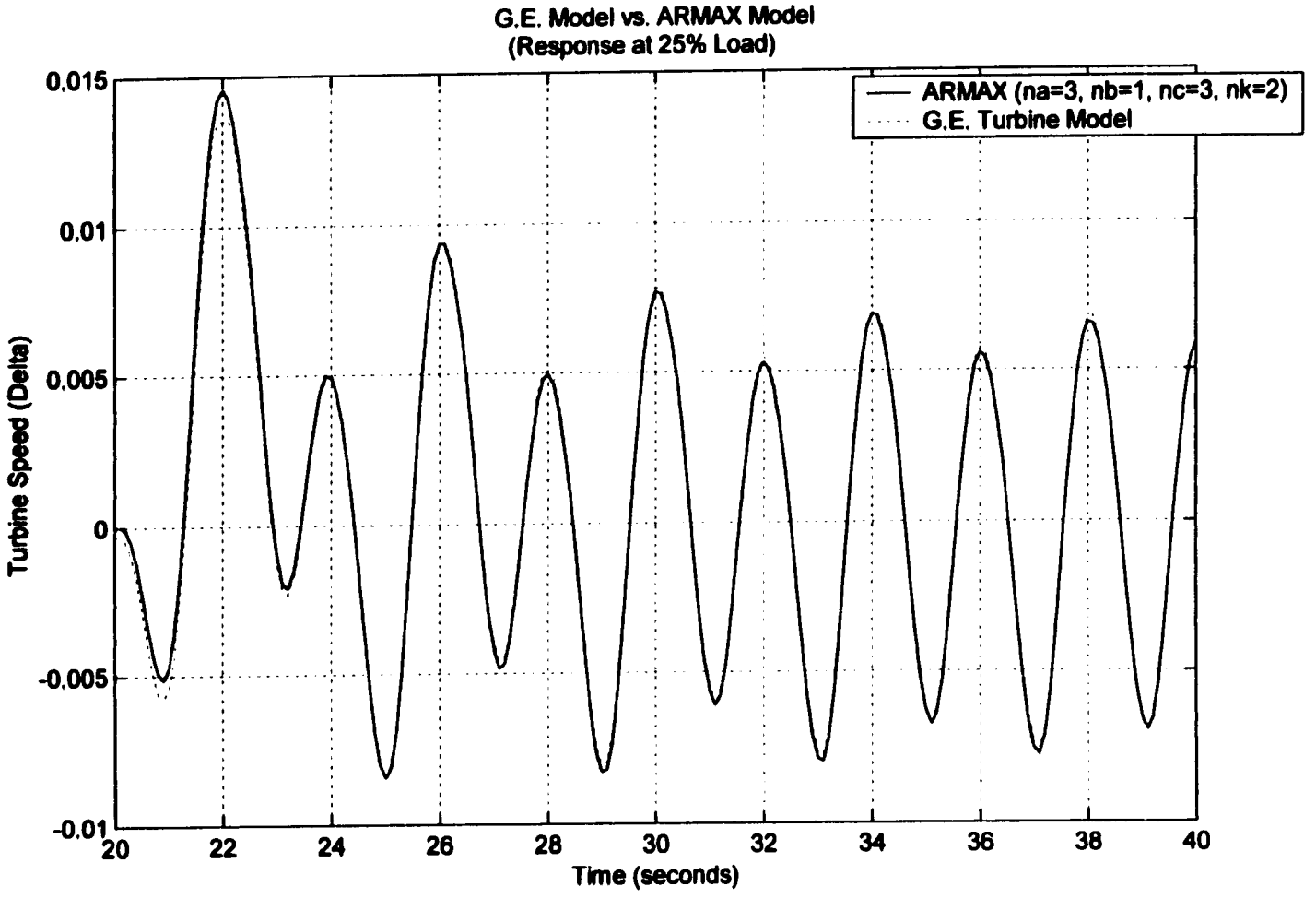

Figure 7.4 G.E. Model vs. ARMAX Model – 25% Load

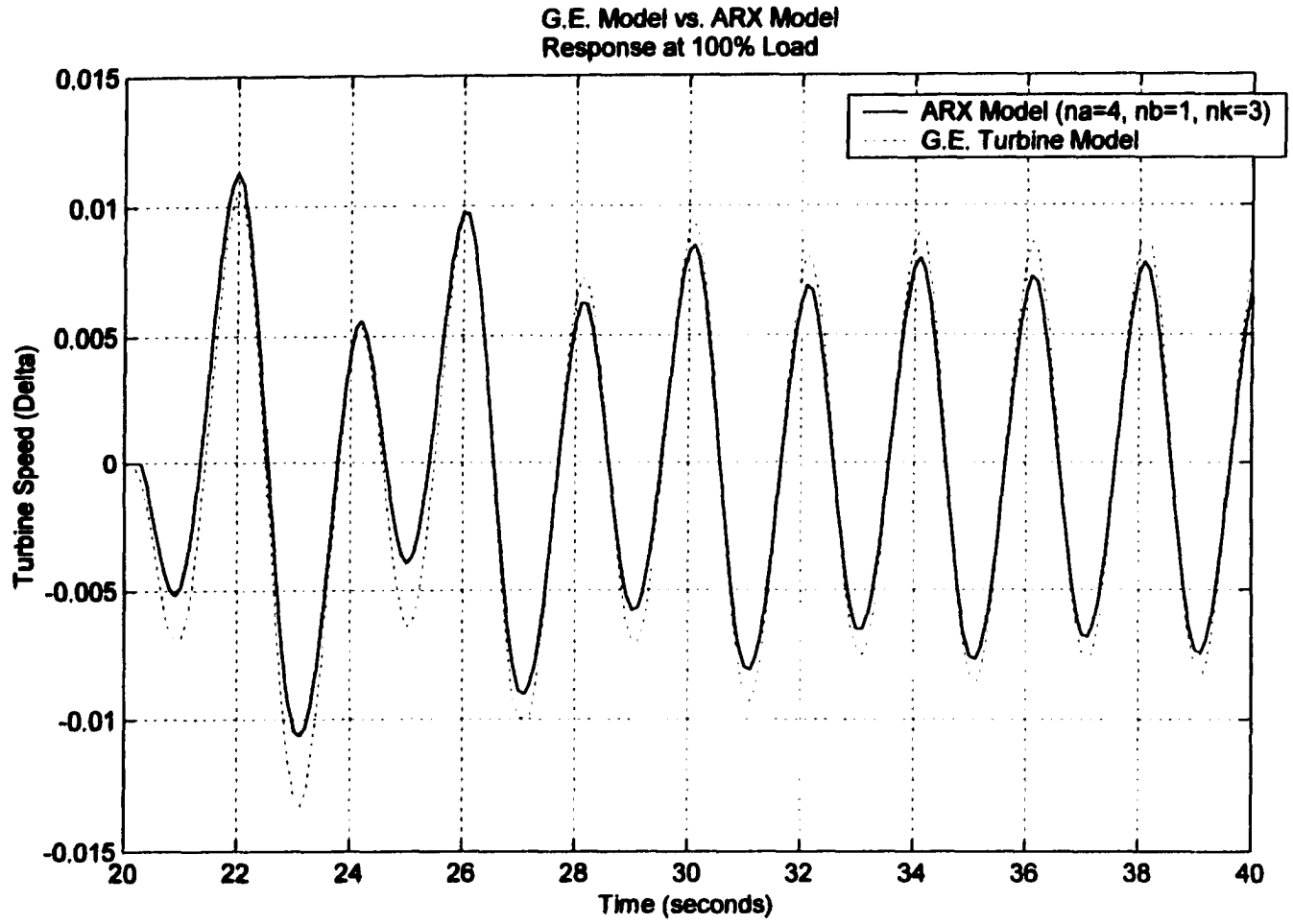

Figure 7.5 G.E. Model vs. ARX Model – 100% Load

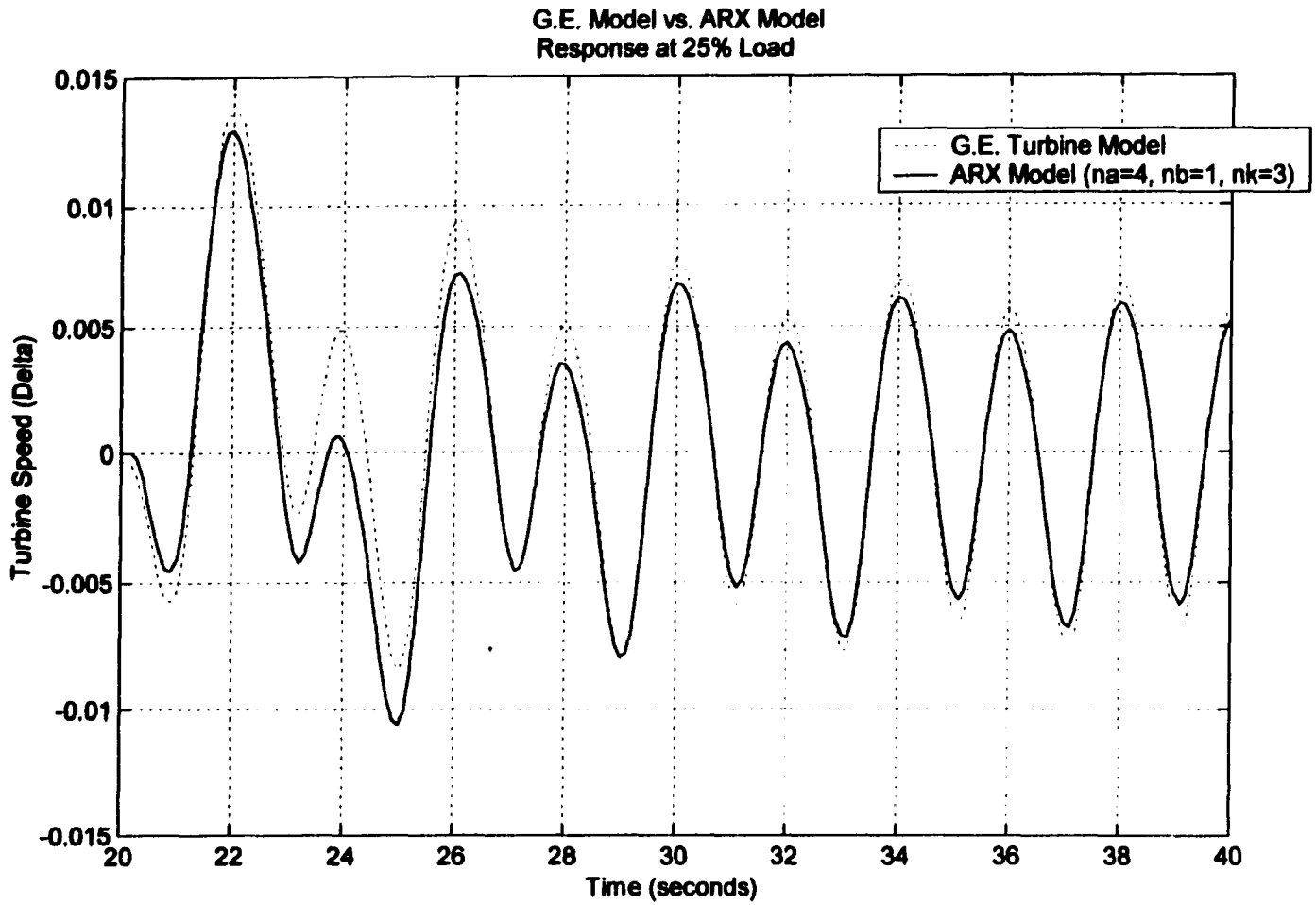

Figure 7.6 G.E. Model vs. ARX Model – 25% Load

Reviewing the plots of the poles and zeroes in Figures 7.7 and 7.8 for both models, it can be seen that all of the poles are inside the unit circle, which indicates that the transfer functions are stable. This is an important requirement if these models are to be used for controller design. In both cases, there are some poles that occur close to the +1 point on the unit circle. This is due to the effect of sampling. The higher the sampling rate the closer the poles are to this point on unit circle. During the experiment, it was verified that the proximity of the poles to the unit circle is determined by how fast the sampling rate is. When the original data set, which is sampled at time interval of 0.001 seconds (1 kHz), is used to estimate the models, all of the poles tend to cluster about the +1 point. Having all the poles clustered together at the point +1 would cause difficulty in designing the controller using the models. This is because it requires substantially more accurate calculation in the controller design to be able to distinguish one pole from the other.

In this study, the numerator dynamics has been ignored (no zeroes in the model). If the numerator dynamics were included, all of the zeroes of the models would fall outside the unit circle. This is understood as the artifact of modeling since the zeroes were forced into the model structure. This reinforces the knowledge that the turbine dynamics has no zeroes (as seen in the turbine simulation model) and it is well reflected in the estimation data.

The remaining performance comparison is the Residual Analysis. The plot shows the auto-correlation of the input signal and the cross correlation between the input and output signals. The plot also shows the 99% confidence interval which is a statistical measure of

the degree of confidence that the true values of the parameters are found around the estimates. The rule of thumb is that if the correlation functions go significantly outside this confidence interval, the model would not be a good description of the system [35] (Ljung). With respect to this relative measure of performance, the ARMAX model appears better than the ARX model since the ARMAX stays closer to the confidence limits than the ARX.

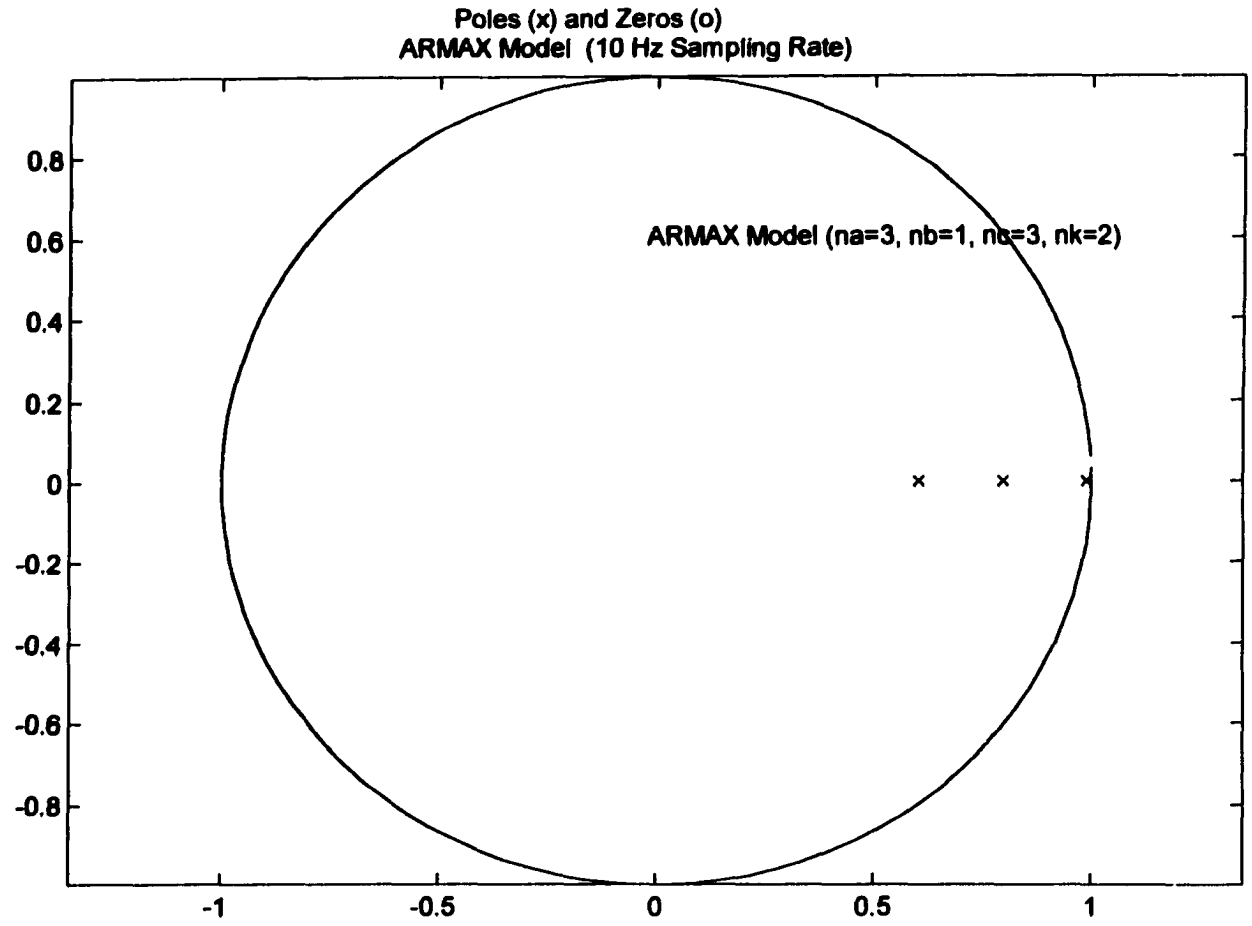

Figure 7.7 ARMAX Model – Location of Poles

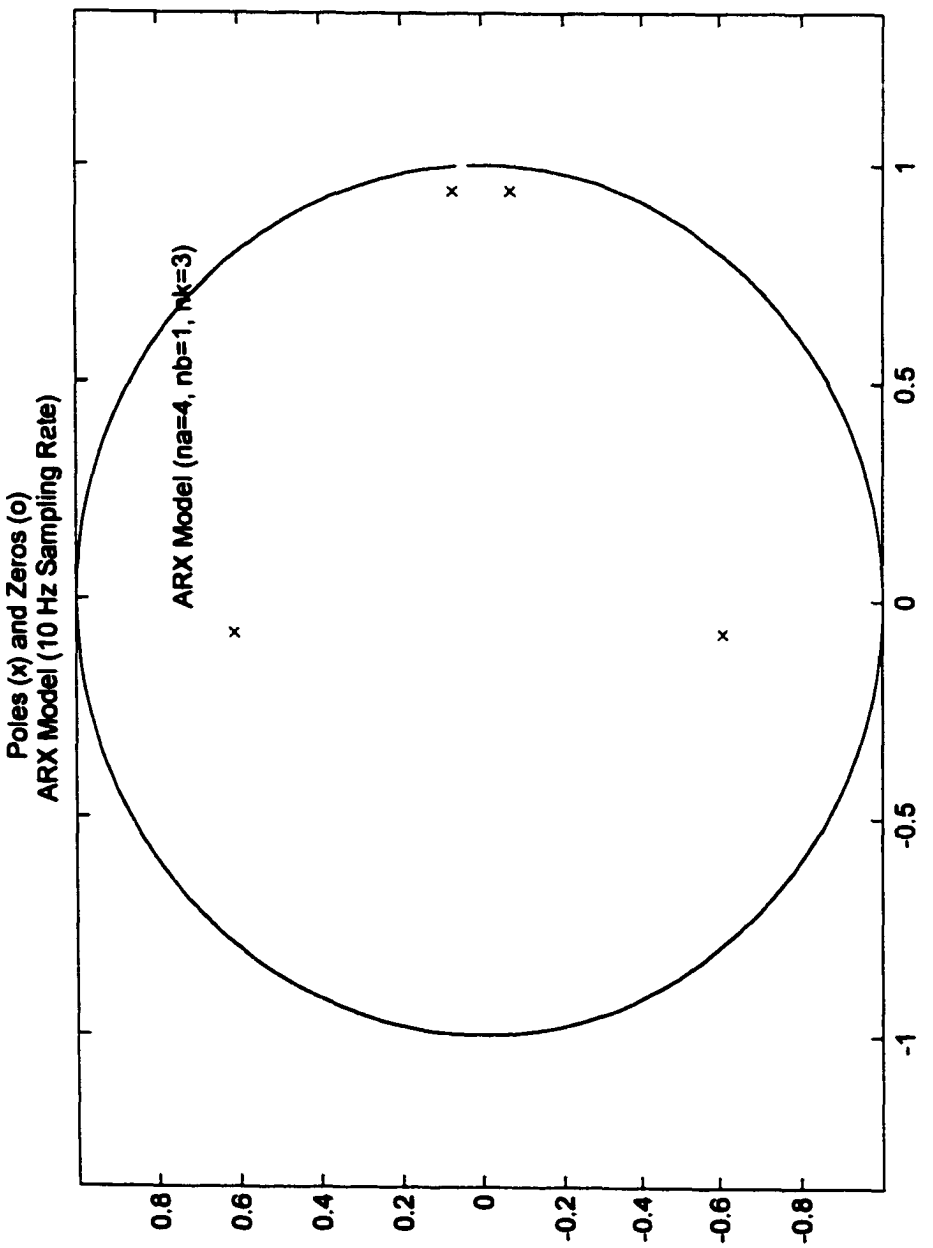

Figure 7.8 ARX Model – Location of Poles

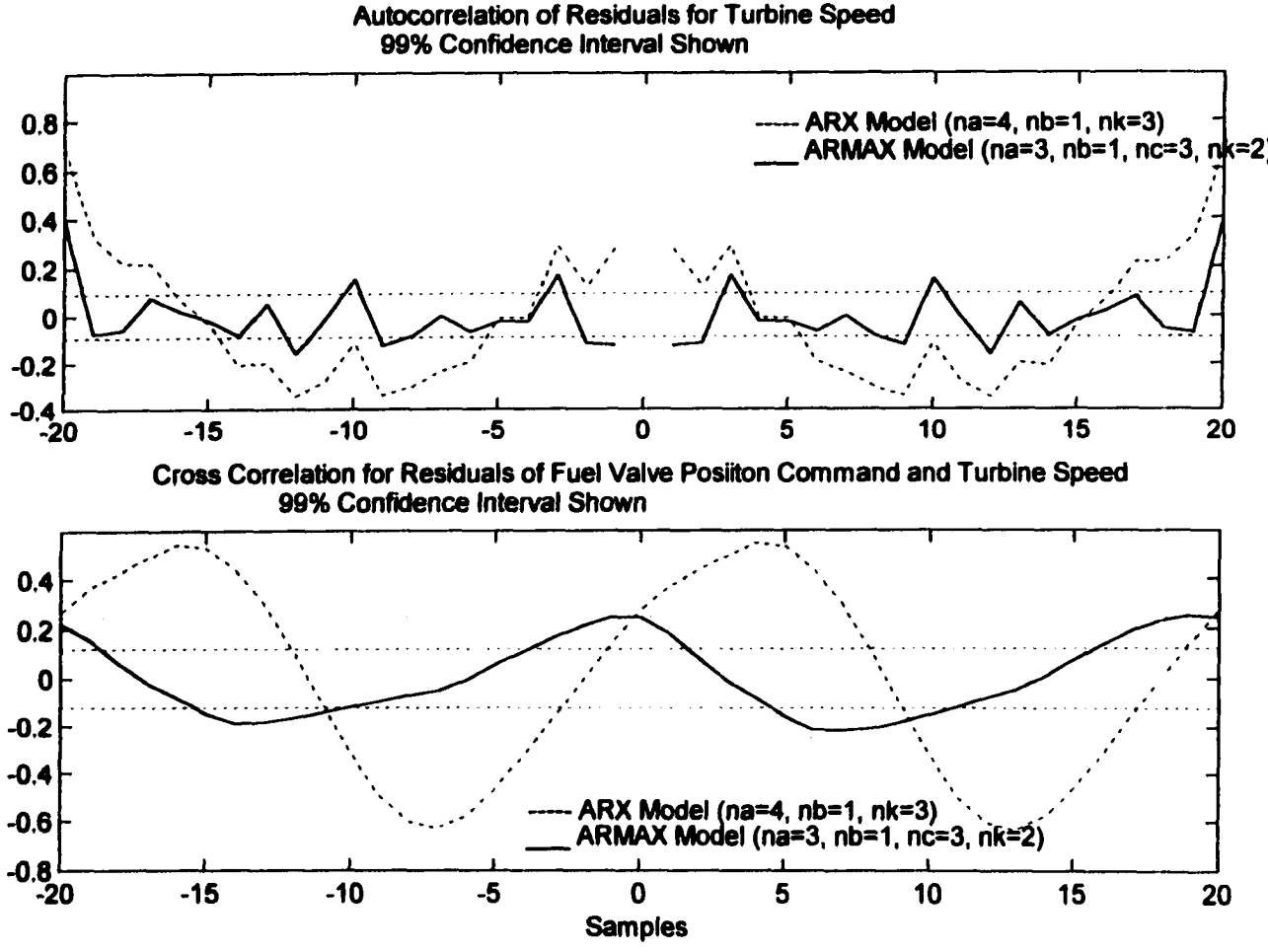

Figure 7.9 Residuals of ARMAX and ARX Models

CHAPTER 8: IMPLEMENTATION GUIDELINES

This following section specifies the guidelines to implement the experimental procedure and the identification algorithms presented thus far. It is assumed that the procedure would be implemented as part of the turbine control system and requires no other external data acquisition equipment. It is further assumed that the turbine speed PI controller has been roughly tuned so that the turbine can operate in a stable mode. The control software should have routines to sample the fuel valve command signal and the output of the magnetic speed pickup at a minimum sampling rate of 500. The fuel valve command signal is the signal that comes out of the actuator final driver (amplifier) and the turbine speed is the signal at the speed-input card.

Step 1: Start up the gas turbine and apply 100% load.

Step 2: After the turbine has reached steady state (no fluctuation in speed can be detected), apply a +5% step input superimposed on the turbine speed setpoint, and at the same time, measure the fuel valve command signal and turbine speed. The data should be sampled as fast as possible (500 Hz). Collect the data for 100 seconds and store it in temporary memory.

Step 3: Compute the turbine step response characteristics (time constant and time delay). Time constant is defined as the time it takes for the turbine speed to reach 63.3% of the final value. For example, for a turbine that operates at 3600 RPM, the final value due to a +5% step input is 3780 RPM. The time constant is the time required for the turbine speed to go from the steady-state 3600 RPM to 3714 RPM. The time delay is computed as the time elapsed from the moment the fuel valve position command signal changes to the

moment the change in turbine speed is detected. Compute the approximate bandwidth ω_c of the turbine system using the reciprocal of the time constant. The bandwidth value is in Hertz and theoretically represents the corner frequency of a first-order dynamic system. Round the value of ω_c to the nearest tenth to facilitate subsequent calculations.

Step 5: The data sampling rate ω_s is determined by multiplying the bandwidth ω_c by 10. Round this value up to the closest integer.

Step 6: Apply an anti-aliasing filter with a cut off frequency at $2*\omega_s$ (Nyquist frequency) to the input/output data obtained in Step 4.

Step 7: Re-sample the data from Step 6 at frequency ω_s.

Step 8: Use the (round-off) approximate bandwidth calculated in the Step 4 to calculate the frequency range for the excitation signal. The frequency range is defined by the lower and upper limits, ω_{min} and ω_{max}, respectively.

$$\omega_{min} = 0.02\omega_c \quad \text{and} \quad \omega_{max} = 2\omega_c$$

Step 9: Specify 100 frequency components at equal intervals from ω_{min} to ω_{max}. The amplitude of each frequency components should be 0.2. This information is then used to design the multi-sine signal using the procedure in Appendix B. There are commercial software programs such as the MATLAB Frequency Domain Identification ToolBox that have the routines to calculate the multi-sine signal. Generate 5 periods of the signal and store the data in temporary memory.

Step 10: During steady state operation of the turbine, apply this sequence of data from Step 9 to the turbine speed setpoint. Record the fuel valve position command and turbine speed for the length of five periods of the excitation signal and store the data in a temporary memory space.

Step 11: Use the data from Step 10, apply the anti-aliasing filter and the re-sampling process as in Steps 6 and 7.

Step 12: Use the data sequence in Step 11 and apply the Prediction Error method to search for the model coefficients. The Prediction Error algorithm is outlined in Appendix C, but different optimization routines are available commercially. The System Identification Toolbox in MATLAB has an ARMAX routine that computes the ARMAX model coefficients using the PEM algorithm. When implementing the PEM search, the ARMAX model should be of 3rd order in both the $A(q^{-1})$ and $C(q^{-1})$ polynomials. The time delay should be a multiple of the sampling interval and as close to the time delay estimated during the step response as possible. The ARMAX model should not have any numerator dynamics.

CHAPTER 9: CONCLUSION AND RECOMMENDATION

The identification method presented thus far agrees well with the state-of the-art techniques for estimating open loop dynamics from closed loop data. This has been clearly illustrated in the current literature and thoroughly discussed in this dissertation. Within the system identification community, the general consensus is that the Direct identification approach using the prediction error method is the best choice for closed loop identification.

The 3rd-order ARMAX model represents the single-shaft gas turbine dynamics reasonably well. It provides the capability to accurately track a 0.5 Hz ramp signal for two different load conditions. This is an important feature since the tracking capability is a typical requirement for the control systems of the turbine type under consideration. In addition to having accurate turbine dynamics representation, the 3rd-order ARMAX model does not require excessive computation to determine the model coefficients. This is an added benefit in terms of implementation of the identification algorithm. The prediction error method is clearly an effective and robust algorithm that converges to the model coefficients in an acceptable amount of time.

The multi-sine signal is an effective excitation. It provides the ability to excite different modes (frequencies) of the turbine dynamics and also provides the ability to limit the signal amplitude to required levels. The ability to compress the large amplitudes helps in keeping the turbine response within linear operating range, which facilitates usage of the

linear estimation models. This is probably the most important aspect during turbine operation where the excitation signal is required to be small but also required to generate sufficiently informative data for model identification.

The ARMAX model obtained in this study is useful for the design and analysis of the control for the single-shaft gas turbine. The model can be used to simulate the turbine step response, which is useful for simple PID controller design. It can also be very useful for implementing different control strategies such as state feedback control where the poles of the difference equation are used in the controller design procedure. The next logical step to consider is to use the model in a model reference adaptive control (MRAC) system. This is a control design approach where the output of the model is continuously compared with the turbine output, and the control parameters are continuously updated to provide control action to meet specific system performance specification.

Another potential application of the method described thus far is the identification of the dynamics between fuel valve position command to the exhaust temperature of a single-shaft gas turbine engine. Controlling the turbine exhaust temperature is an important function of the control system since the exhaust temperature indicates when the turbine design limits have been reached. For this problem, the same approach can be utilized to obtain the dynamic model of the turbine exhaust temperature as a function of fuel valve position command. In this scenario, the ARMAX model may be simplified to a 2^{nd}-order system since the dynamics of the turbine rotor inertia is no longer present. In a real turbine system, however, there exists a coupling between the turbine exhaust temperature

and the turbine speed. In addition to having the speed controller active, it is necessary to use a temperature controller for controlling the exhaust temperature during the identification process. For more accurate identification, this problem should be considered as a multivariable system in which both turbine speed and turbine exhaust are the outputs, and fuel valve command and the air flow control signal are the driving inputs.

A possible improvement to the robustness of the identification method described in this dissertation is the implementation of the delta operator δ. The delta operator, defined as $\delta = 1 - q^{-1}$, can be used in place of the delay operator q^{-1} in the ARMAX model structure to reduce possible numerical errors in the optimization algorithm. Middleton and Goodwin [41] have shown that the delta operator can provide well-conditioned model parameterization so that round-off or other numerical errors are avoided. The delta operator has been utilized in industrial digital control systems to reduce the risk of introducing numerical errors in the control calculation [54] (Schade).

REFERENCES

1. Akaike, H. (1981). Modern Development of Statistical Methods. *Trends and Progress in System Identification, Chapter 6, Eykhoff P. (editor).* Pergamon Press.
2. Arkov, V.Y, G.G. Kuikin and P. J. Fleming (1998). Dynamic Model Identification of Gas Turbines. *UKACC International Conference on Control '98.*
3. ASME Gas Turbine Division (1978). *Basic Gas Turbine Engine Technology.*
4. ASME Gas Turbine Division. *Basic Gas Turbine Engine Technology, Home Study Course.*
5. Astrom, K.J. (1981). Maximum Likelihood and Prediction Error Methods. *Trends and Progress in System Identification, Chapter 5, Eykhoff P. (editor).* Pergamon Press.
6. Beltrami, E. (1987). *Mathematics for Dynamic Modeling.* Academic Press.
7. Bettocchi, R., P. R. Spina and F. Fabbri (1996). Dynamic Modeling of Single-Shaft Industrial Gas Turbine. *1996 International Gas Turbine & Aeroengine Congress & Exhibition, Birmingham, UK.* ASME Paper 96-GT-332.
8. Blotenberg, W. (1993). A Model for the Dynamic Simulation of a Two-Shaft Industrial Gas Turbine with Dry Low NOX Combustor. *International Gas Turbine and Aeroengine Congress and Exposition, 1993,* ASME Paper 93-GT-355.
9. Borrell, A., Ceri Evans and David Rees (1998). Identification of Aircraft Turbine Dynamics Using Frequency-Domain Techniques. *UKACC International Conference on Control '98.*
10. Bos van den, Adriaan (1993). Periodic Test Signals – Properties and Use. *Perturbation Signals for System Identification, Chapter 4,* Godfrey, K.R. (Editor, 1993). Prentice Hall International.
11. Chrysanthou, A., A. H. Jones and B. Porter (1986). Identification of Gas Turbine Dynamics. Colloquium on "Gas Turbine: Control Theory and Practice", *IEE Computing and Control Division.*
12. Cottington, R.V. and C.B. Pease (1979). Dynamic Response Testing of Gas Turbines, *ASME Journal of Engineering for Power,* January 1979, Vol. 101, pp. 95-100.
13. Davies, W. D. T. (1970). *System Identification for Self-Adaptive Control.* Wiley-Interscience, John Wiley and Sons, Ltd.
14. Evans, D.C. (1998). Testing and Modelling Aircraft Gas Turbines: an Introduction and Overview. *UKACC International Conference on Control '98.*
15. Evans, D.C., Antoni Borrell and David Rees (1998). Testing and Modelling Gas Turbines Using Multisine Signals and Frequency-Domain Techniques. *International Gas Turbine & Aeroengine Congress & Exhibition,* Stockholm, Sweden, 1998. ASME paper 98-GT-98.
16. Evans, D.C., D. Rees, D.L. Jones and D.C. Hill (1994). Measurement and Identification of Gas Turbine Dynamics in the Presence of Noise and Nonlinearity. *IMTC '94, IEEE Publication,* pp. 609-614, 1994.

17. Evans, D.C., D. Rees, D.L. Jones and D.C. Hill (1994). Time and Frequency Domain Identification of Jet Engine Dynamics: Problems and Solutions. *10th IFAS Symposium of System Identification*, Session CL3, Copenhagen.
18. Eykhoff, P. (1974). *System Identification, Parameter and State Estimation*. John Wiley and Sons.
19. Godfrey, K. (1993). Introduction to Perturbation Signals for Frequency-domain System Identification. *Perturbation Signals for System Identification, Chapter 2*, Godfrey, K.R. (Editor, 1993). Prentice Hall International.
20. Godfrey, K. (1993). Introduction to Perturbation Signals for Time-domain System Identification. *Perturbation Signals for System Identification, Chapter 1*, Godfrey, K.R. (Editor, 1993). Prentice Hall International.
21. Godfrey, K.R. (1980). Correlation Methods, *Automatica*, Vol. 16, pp. 527-534, 1980.
22. Godfrey, K.R. and D.J. Moore (1974). Identification of Processes Having Direction Dependent Responses, with Gas Turbine Engine Applications. *Automatica*, Vol. 10, pp. 469-481.
23. Goodwin, G.C. and Kwai Sang Sin (1984). *Adaptive Filtering Prediction and Control*. Prentice-Hall Information and System Sciences Series.
24. Goodwin, G.C. and R.L. Payne (1977). Dynamic System Identification: Experiment Design and Data Analysis. Academic Press, New York.
25. Gustavsson, I., L. Ljung, and T. Soderstrom (1977). Identification of Processes in Closed Loop – Identifiability and Accuracy Aspects, *Automatica*, Vol. 13, pp. 59-75.
26. Gustavsson, I., L. Ljung, and T. Soderstrom (1981). Choice and Effect of Different Feedback Configurations. *Trends and Progress in System Identification, Chapter 5, Eykhoff P. (editor)*. Pergamon Press.
27. Hannett, L.N. and Afzal Khan (1993). Combustion Turbine Dynamic Model Validation From Tests, *IEEE Transactions on Power Systems*, Vol. 8, No. 1, February 1993.
28. Hartley, T.T., G.O. Beale and S.P. Chicatelli (1994). *Digital Simulation of Dynamic Systems: A Control Theory Approach*. Prentice Hall.
29. Hill D.C. (1994). *System Identification of Gas Turbine Engines*, Ph.D. Thesis, Birmingham University School of Electrical and Electronic Engineering, UK.
30. Hill D.C. (1997). Identification of Gas Turbine Dynamics: Time-Domain Estimation Problems. *ASME 97-GT-31, International Gas Turbine & Aeroengine Congress & Exhibition*, Orlando, Florida, USA.
31. Johnson, R.C. Jr. (1988). *Lectures on Adaptive Parameter Estimation*. Prentice Hall Advanced Reference Series.
32. Kaufman, H. and R. Ravi (1994). Identifying a Dynamic Model for a GE Frame 7 Gas Turbine. *ASME Paper 94-GT-117*, 1994 International Gas Turbine & Aeroengine Congress & Exhibition, The Hague, Netherlands.
33. Kurz, H. and R. Isermann (1975). Methods for On-line Process Identification in Closed Loop. *Proceedings of the IFAC 6th World Congress*, Boston, Massachusetts, U.S.A., August 24-30, 1975, Section 11.3, pp. 1-14.
34. Landau, I.D. (1990). *System Identification and Control Design*. Prentice-Hall, New Jersey.
35. Ljung L. (1999). *System Identification: Theory for the User*. Prentice Hall, New Jersey.

36. Ljung, L. and T. Soderstom (1983). *Theory and Practice of Recursive Identification*. The Massachusetts Institute of Technology Press.
37. Ljung, L. and Torkel Glad (1994). *Modeling of Dynamic Systems*. Prentice-Hall Information and System Sciences Series.
38. Maybeck, P.S. (1979). *Stochastic Models, Estimation, and Control*. Academic Press, Inc.
39. Mehra, R.K. (1981). Choice of Input Signals. *Trends and Progress in System Identification, Chapter 9, Eykhoff P. (editor)*. Pergamon Press.
40. Merril, W.C. (1983). Identification of Multivariable High-Performance Turbofan Engine Dynamics from Closed-Loop Data. *First Annual NASA Aircraft Controls Workshop*, October 24-26, 1983.
41. Middleton, R.H. and G.C. Goodwin (1990). Digital Control and Estimation. Prentice Hall, New Jersey.
42. Norton, J.P., P. T. Ladlow and D. C. Hill (1998). Identification of Large-Transient Effects in Aircraft Gas-Turbine Dynamics. *UKACC International Conference on Control '98*.
43. Oppenheim, A.V., Alan S. Willsky, and Ian T. Young (1983). *Signals and Systems*. Prentice-Hall Signal Processing Series.
44. Polonyi, M.G. (1991). *Power and Process Control Systems*, McGraw-Hill Inc.
45. Porch, H.R. (1993). Application of Multi-frequency Test Signals to an Industrial Water Boiler. *Perturbation Signals for System Identification, Chapter 14*, Godfrey, K.R. (Editor, 1993). Prentice Hall International.
46. Rake, H. (1980). Step Response and Frequency Response Methods, *Automatica*, Vol. 16, pp. 519-526, 1980.
47. Rees, D. and D.L. Jones (1993). Design and application of Non-binary Low-peak-factor Signals for System-dynamic Measurement. *Perturbation Signals for System Identification, Chapter 12*, Godfrey, K.R. (Editor, 1993). Prentice Hall International.
48. Richalet, J. (1981). The Model Method. *Trends and Progress in System Identification, Chapter 1, Eykhoff P. (editor)*. Pergamon Press.
49. Rodriguez-Vazquez, K. and P. J. Fleming (1998). Multiobjective Genetic Programming for Gas Turbine Engine Model Identification (1998). *UKACC International Conference on Control '98*.
50. Rolls-Royce plc (1986). *The Jet Engine*, 4th edition.
51. Rowen, W.I. (1983). Simplified Mathematical Representations of Heavy-Duty Gas Turbines. *ASME Journal of Engineering for Power*, October 1983, Vol. 105, pp. 865-869.
52. Rowen, W.I. (1991). Simplified Mathematical Representations of Single Shaft Gas Turbines in Mechanical Drive Service. *Unpublished document.*
53. Sawyer's Gas Turbine Engineering Handbook, *Volumes I-III, Turbomachinery International Publications*, 3rd Edition, 1985.
54. Schade, W.J., Woodward Governor Company, Private Communication, 1998.
55. Schoukens, J. and R. Pintelon (1991). *Identification of Linear Systems: A Practical Guideline to Accurate Modeling*. Pergamon Press, 1991.
56. Schoukens, J., P. Guillaume and R. Pintelon (1993). Design of Broadband Excitation Signals. *Perturbation Signals for System Identification, Chapter 3*, Godfrey, K.R. (Editor, 1993). Prentice Hall International.

57. Schoukens, J., R. Pintelon and H. Van Hamme (1994). Identification of Linear Dynamic Systems Using Piecewise Constant Excitation: Use, Misuse and Alternatives. *Automatica*, Vol. 30, No. 7, pp. 1153-1169.
58. Schroeder, M.R. (1970). Synthesis of Low-Peak-Factor Signals and Binary Sequences With Low Autocorrelation. *IEEE Transactions on Information Theory*, pp. 85-89.
59. Schweppe, F.C. and R.D. Masiello (1975). System Identification for Electric Power Systems. *Proceedings of the IFAC 6th World Congress*, Boston, Massachusetts, U.S.A., August 24-30, 1975, Section 31.1, pp. 1-6.
60. Sinha, N.K. and B. Kuszta (1983). *Modeling and Identification of Dynamic Systems*. Van Nostrand Reinhold Company.
61. Smith, M.S. (1987). Mathematical Modeling and Digital Simulation for Engineers and Scientists, 2nd Edition. John Wiley & Sons, Inc.
62. Soderstrom, T. and P. Stoica (1989). *System Identification*. Prentice Hall International (UK) Ltd.
63. Sutherland, P. and R.W. Walker (1975). Correlation Techniques Applied to the Identification of Boiler Dynamics. *Proceedings of the IFAC 6th World Congress*, Boston, Massachusetts, U.S.A., August 24-30, 1975, Section 2.2, pp. 1-8.
64. The MathWorks Inc. SIMULINK & MATLAB manuals, 1992.
65. Van der Ouderaa, E., J. Schoukens, and J. Renneboog (1988). Peak Factor Minimization Using a Time-Frequency Domain Swapping Algorithm. *IEEE Transactions on Instrumentation*, Vol. 37, No. 1, March 1988.
66. Wellstead, P.E. (1977). Reference Signals for Closed Loop Identification. *Int. J. Control*, Vol. 26, No. 6, pp. 945-962.
67. Woodward Governor Company. *Description of System Operation, Simplex NetCon Digital Control System for Gas Turbine Generator Unit*. Private Communication, 1998.
68. Ljung, L., Forssell, U. (1999). An Alternative Motivation for the Indirect Approach to Closed-Loop Identification, *IEEE Transaction on Automatic Control*, Vol. 44, No. 11, November 1999.
69. Ljung, L., Forssell, U. (1999). Closed-loop Identification Revisited, *Automatica*, Vol. 35, No. 7, pp. 1215-1241, 1999.
70. Zhou, Y., Tugnait, J.K. (1999) Closed Loop Linear Model Validation and Order Estimation Using Polyspectral Analysis, *Proceedings of the American Control Conference*, San Diego, California, June 1999, pp. 341-345.
71. Tontiruttananon, C., Tugnait, J.K. (1998). Parametric Identification of Closed-loop Linear Systems Using Cyclic-Spectral Analysis, *Proceedings of the American Control Conference*, Philadelphia, Pennsylvania, June 1998, pp. 3597-3601.
72. Landau, I.D., Rolland, F. (1994). An Approach for Closed Loop System Identification, *Proceedings of the 33rd Conference on Decision and Control*, Lake Buena Vista, Florida, December 1994, pp. 4164-4169.
73. Van Baars, G.E., Bongers, P.M.M. (1994). Closed Loop System Identification of an Industrial Wind Turbine System: Experiment Design and First Validation Results, *Proceedings of the 33rd Conference on Decision and Control*, Lake Buena Vista, Florida, December 1994, pp. 625-630.

74. Sun, L., Liu, W., Sano, A. (1997). Over-sampling Approach to Closed Loop Identification, *Proceedings of the 36th Conference on Decision and Control*, San Diego, California, December 1997, pp. 1253-1258.
75. Pasadyn A.J., Qin, S.J., Valle-Cervantes, S. (1999). Closed-loop and Open-loop Identification of an Industrial Waste Water Reactor, *Proceedings of the American Control Conference*, San Diego, California, June 1999, pp. 3965-3969.
76. Van den Hof, Paul (1998). Closed-loop Issues in System Identification, *Annual Reviews in Control*, Vol. 22, 1998, pp. 173-186.
77. Forssell, U., Chou, C.T. (1998). Efficiency of Prediction Error and Instrumental Variable Methods for Closed-loop Identification, *Proceedings of the 37th IEEE Conference on Decision and Control*, Tampa, Florida, December 1998, pp. 1287-1288.
78. Ljung, L., Forssell, U. (1997). Variance Results for Closed-loop Identification Methods, *Proceedings of the 36th Conference on Decision and Control*, San Diego, California, December 1997, pp. 2435-2440.
79. Fatehi, F., Smith, J.R., Pierre, D.A. (1996). Robust Power System Controller Design Based on Measured Models, *IEEE Transaction on Power Systems*, Vol. 11, No. 2, May 1996, pp. 774-780.
80. Van der Klauw, A.C., et al. (1994). Closed loop Identification of a Distillation Column, *Proceedings of the Third IEEE Conference on Control Applications*, Vol. 1, 1994, pp. 275-280.
81. Ditmar, W.P.A., Henrichs, S., Pettitt, R.R. (1994). Application of Multi-Frequency Test Signals to Closed Loop System Identification, *IEE Control'94*, March 21-24, 1994, pp. 303-308.
82. Gexin, M., Dali, Z., Yanda, L. (1996). Fuzzy Neural Networks in Nonlinear System Identification, *Proceedings of the IEEE International Conference on Industrial Technology*, 1996, pp. 375-379.

APPENDICES

Appendix A: Properties of Signals and Processes

The following material serves to supplement the analysis of the identification method and model validation presented in the main body of this study. Various definitions and derivations presented here are available in most textbooks on Probability and Statistics and System Identification.

A1. Expectation and Covariance Matrix of a Random Process

Let e be a random variable, which describes the possible numerical outcomes of experiments whose results can not be exactly predicted beforehand. The probability of the numerical values falling in between the values a and b is expressed by the probability density function (PDF) $f_e(x)$:

$$P(a \le e < b) = \int_a^b f_e(x)dx \tag{A.1}$$

For a random vector

$$e = \begin{bmatrix} e_1(t) \\ \vdots \\ e_n(t) \end{bmatrix} \tag{A.2}$$

a corresponding PDF $f_e(x) = f_e(x_1,\ldots,x_n)$ from $\mathbf{R}^n$ to $\mathbf{R}$ is defined and

$$P(e \in B) = \int_{x \in B} f_e(x)dx \tag{A.3}$$

where B is a subset of $\mathbf{R}^n$ and P(A) means "the probability of event A"

The expectation or mean value of e is defined as

$$Ee = \int_{\mathbf{R}^n} x f_e(x)dx \tag{A.4}$$

and the covariance matrix of e is defined as

$$Cov(e) = E(e-m)(e-m)^T ; m = Ee \qquad (A.5)$$

A2. Transfer Function of a Linear System with Additive Disturbance

The basic assumption here is that all systems are single input and single output (SISO) Linear Time Invariant (LTI) systems. This means that given a system as shown in Figure A1 the output response *y(t)* to a certain input *u(t)* does not depend on absolute time. It is said to be linear if its output response to a linear combination of inputs is the same linear combination of the output responses of the individual inputs. Furthermore, it is said to be causal if the output at a certain time depends on the input up to that time only.

Figure A1 System with Input/Output

It is well known that a linear, time-invariant, causal system is completely described by its impulse response (or weighting function) $g(\tau)$ as follows

$$y(t) = \int_{\tau=0}^{\infty} g(\tau)u(t-\tau)d\tau \qquad (A.6)$$

thus, knowing $g(\tau)$ and knowing $u(s)$ *for* $s \leq t$, we can consequently compute the corresponding output $y(s)$, $s \leq t$ for any input.

In this study we have dealt exclusively with observations of inputs and outputs in discrete time, since this is the typical data-acquisition mode in the identification process. It is

thus assumed $y(t)$ is observed at the sampling instants $tk = kT$, k=1,2,..., where T is the sampling interval. It is further assumed that the sampling instants are equally spread over time and that the input *signal* $u(t)$ is sampled and kept constant between sampling instants

$$u(t) = u_k, \qquad kT \le t \le (k+1)T \tag{A.7}$$

Equation (A.6) can then be written as follows

$$y(kT) = \int_{\tau=0}^{\infty} g(\tau)u(kT-\tau)d\tau \tag{A.8}$$

Inserting (A.7) into (A.8) gives

$$y(kT) = \int_{\tau=0}^{\infty} g(\tau)u(kT-\tau)d\tau = \sum_{j=1}^{\infty} \int_{\tau=(j-1)T}^{jT} g(\tau)u(kT-\tau)d\tau = \sum_{j=1}^{\infty}\left[\int_{\tau=(j-1)T}^{jT} g(\tau)d\tau\right]u_{k-j} = \sum_{j=1}^{\infty} g_T(j)u_{k-j} \tag{A.9}$$

where $$g_T(j) = \int_{\tau=(j-1)T}^{jT} g(\tau)d\tau \tag{A.10}$$

The expression in (A.9) indicates that it is sufficient to know the sequence $g_T(j)$ to compute the response to the input at the sampling instants.

Assuming that T is one time unit and using t to indicate the sampling instants, we can describe (A.9) as

$$y(t) = \sum_{j=1}^{\infty} g(j)u(t-j) \qquad t = 0,1,2,... \tag{A.11}$$

For realistic physical systems, disturbances need to be considered for analysis and design purposes. Disturbances can be simply illustrated as in Figure A2

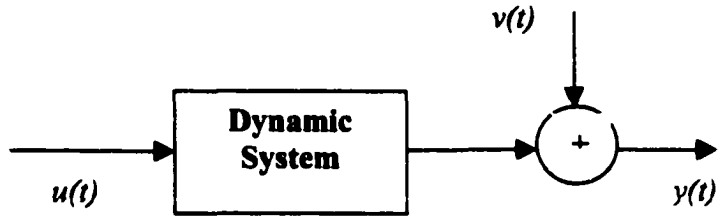

Figure A2 System with Disturbance

The sources and causes for such a disturbance may be the result of measurement noise or possibly uncontrollable inputs such as those due to the environment in which the system is located. In our case, where the input and output signals are measured while the system is operating in closed loop control, the disturbance can be considered the additional effect that the feedback and controller has on the inputs. Within the linear system assumption the disturbance can reasonably be lumped into an additive term at the output as shown in Figure A2

$$y(t) = u(t) + v(t) \tag{A.12}$$

or, from equations (A.8) through (A.11)

$$y(t) = \sum_{j=1}^{\infty} g(j)u(t-j) + v(t) \tag{A.13}$$

The disturbance *v(t)* is assumed to be a random stochastic signal and can be represented by

$$v(t) = \sum_{j=0}^{\infty} h(j)e(t-j) \tag{A.14}$$

where *e(t)* is white noise, i.e., a sequence of independent random variables with certain probability density function as described above

Introducing the backward shift operator q^{-1}

$$q^{-1}u(t) = u(t-1); \qquad q^{-1}e(t) = e(t-1)$$

Equation (A.11) can be written as

$$\begin{aligned} y(t) &= \left[\sum_{j=1}^{\infty} g(j)q^{-j}\right]u(t) = G(q)u(t) \\ G(q) &= \sum_{j=1}^{\infty} g(j)q^{-j} \end{aligned} \tag{A.15}$$

and, similarly, (A.14) can be written as

$$\begin{aligned} v(t) &= \left[\sum_{j=0}^{\infty} h(j)q^{-j}\right]e(t) = H(q)e(t) \\ H(q) &= \sum_{j=1}^{\infty} h(j)q^{-j} \end{aligned} \tag{A.16}$$

Substituting (A.15) and (A.16) into (A.12)

$$y(t) = G(q)u(t) + H(q)e(t) \tag{A.17}$$

which is the basic description for a linear system with additive disturbances.

Appendix B: Design of Multi-Sine Excitation Signal

B1. General

It is well known fact that to obtain good estimates from an identification experiment the collected data should be informative, i.e. the input excitation signal used in the experiment has to be persistently exciting of a certain order. This usually means that the input contains sufficiently many distinct frequencies which, at the minimum, consist of all possible critical frequencies of the system under test. This is so that the applied input signal would excite all dynamic response modes of the system, which then produces informative data for the identification process.

It is also known that the asymptotic properties of the estimate (bias and variance) depend only on the input power spectrum and not the waveform of the input. This usually means that the excitation signals used in an identification experiment need to have a high signal-to-noise (S/N) ratio. For most cases, the input power is inversely proportional to the covariance matrix of the estimates, where the covariance matrix is an indication of the consistency and convergence of the estimates. It can be shown that the smaller the covariance matrix the better the estimates, thus using sufficiently high input signal power can improve the chance of obtaining good estimates of the system dynamics. Theoretically the S/N ratio of a signal can be achieved by augmenting the energy of the signal, i.e. increasing the amplitudes of the signal components. However, in practice, there are limitations to the extreme values or peaks of the input signals, e.g. to avoid saturation and non-linearity in the system under test. So the problem is to put as much energy as possible in a signal with given maximum amplitude. The magnitudes of the

individual signal components are also important to allow all the modes of interest to be excited [64] (Van der Ouderaa et al.).

In summary, a good input excitation signal for an identification experiment that produces informative data to obtain good model estimates should have as much energy as possible at all necessary frequency components without causing saturation, non-linearity or operational upsets in the system under test. A survey by Schoukens et al. [55] compared the properties of different excitation signals and concluded that the multi-sine signal is indeed the best signal, which has all necessary properties to improve the chance of obtaining good estimates in an identification experiment. The multi-sine signal has also been found to be the most flexible signal with optimal properties that facilitate implementation in real systems.

B2. Multi-Sine Signal Description

The multi-sine is a band-limited signal consisting of a finite sum of harmonically related sinusoids. Let $f(t)$ be the multi-sine signal described in the time domain. The Fourier series for $f(t)$ can be written as

$$f(t) = \sum_{j=1}^{N} a_j \cos(\omega_j t + \phi_j) \qquad \text{(B.1)}$$

with j the harmonic number, a_j the amplitude of the j^{th} component, ω_j the signal frequency and ϕ_j the phase of the j^{th} component. All of the components in $f(t)$ are related by a fundamental frequency ω_j. The total amount of energy contained in the signal $f(t)$ is represented by E^2_{rms} in which

$$E_{eff} = \sqrt{\sum_{j=1}^{N} \frac{a_j^2}{2}} \qquad \text{(B.2)}$$

Assuming M^+ and M^- are the largest positive value and the most negative value of $f(t)$, respectively, the *crest factor* C_r of the signal is defined as

$$C_r = \frac{M^+ - M^-}{2E_{eff}} \qquad \text{(B.3)}$$

The crest factor represents the amount by which the amplitude of the signal is compressed. From the discussion above, a desirable characteristic of an excitation signal is to have as much energy possible without having the amplitude peaks that can cause problems in the system under experiment. Crest factor minimizing algorithms, which will be discussed in following paragraphs, have been employed to minimize the amplitude peaks in the excitation signal but, at the same time, maintain the energy spectrum of the original signal. Consequently, a good signal waveform is one that has a small crest factor. For signals having a large number of components ($N = \infty$), it is easily seen from equations (B.1) and (B.2) that a binary and symmetric signal has the crest factor of 1, which is the best that can be attained. Similarly, from equations (B.2) and (B.3) it can also be seen that the crest factor of a pure sine wave is $\sqrt{2}$. The binary signal, having a crest factor of 1, appears to have a theoretical advantage over other type of signals. However, there are some practical limitations in using binary signals in identification experiment [35] (Ljung).

The multi-sine signal represented by equation (B.1) has all the signal power in the specified harmonics given the appropriate parameters. The derivation of the power spectrum of the multi-sine signal has been shown in [35] (Ljung) and [61] (Soderstrom, T. and P. Stoica) and listed below

The power spectrum (power density) Φ_f of the deterministic signal *f(t)* can be defined as the discrete Fourier transform of the covariance function

$$\Phi_f(\omega) = \sum_{j=1}^{N} R_f(\tau) e^{-i\tau\omega} \qquad \text{(B.4)}$$

where $R_f(\tau)$ = covariance function of the signal *f(t)*

τ = time variable

It was shown in [35] and [61] that

$$\Phi_f(\omega) = 2\pi \sum_{j=1}^{N} \frac{a_j^2}{4} [\delta(\omega - \omega_j) + \delta(\omega + \omega_j)] \qquad \text{(B.5)}$$

where δ is the Dirac pulse function

B3. Multi-Sine Signal Design

Examining the equation (B.5) for the signal power spectrum it is seen that with N, a_j and ω_j the signal power can be placed very precisely to desired frequencies. In addition, all possible information matrices can be obtained within the family of equation (B.1) for large enough N [35] (Ljung). It is apparent from the above description of the multi-sine signal that even though the input spectrum can be arbitrarily shaped, but the crest factor can potentially become very high. For example, from equation (B.2), the power of the

signal is $\sum a_j^2/2$. If all the sinusoids are in phase, the squared of the amplitude will be $\left(\sum a_j\right)^2$. The crest factor can thus be up to $\sqrt{2N}$ (if all a_j are equal). The way to control the crest factor is to choose the phases ϕ_j so that the cosines are "as much out of phase" as possible [35] (Ljung). Shroeder [57] developed a formula to adjust the phase angles of a periodic signal with a given input spectrum to minimize its peak-to-peak amplitude (crest factor). The given formula for the phase angles yields in general low crest factors comparable to that of a single sinusoidal signal of equal power.

Schroeder's phase: ϕ_1 is chosen arbitrary

$$\phi_j = \phi_1 - \frac{j(j-1)}{N}\pi \quad ; \; 2 \le j \le N$$

Van der Ouderaa et al. [64] presented an algorithm to minimize the peaks in the time-domain of band-limited Fourier signals. This method has the ability to effectively compress the signals without disturbing their spectral magnitudes. This is an iterative method to optimize the phases of the multi-sine signal to achieve a time signal that has a minimum peak value for a given amplitude spectrum. The basic idea is a clipping procedure in which the time-domain signal is clipped at a certain value related to its extreme value to cut off the peaks. The concept is illustrated in Figure B1 below

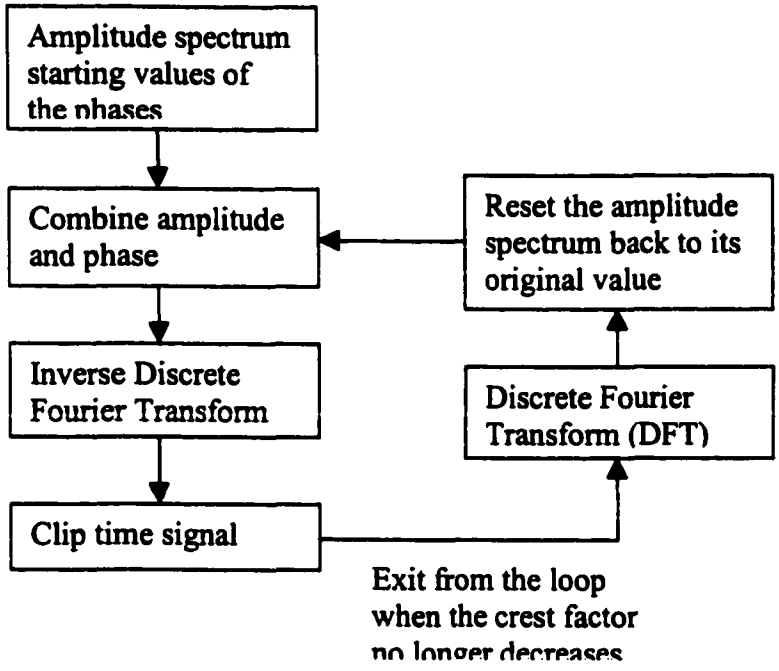

Figure B1 Minimization of the crest factor of a multi-sine: clipping algorithm [53], [62]

The above iteration procedure starts from a given amplitude spectrum and uses arbitrary phases as starting values. Using the inverse Discrete Fourier Transform (DFT) the signal is calculated at a set of equidistant times. Clipping off all the values greater than a given maximum then generates a new time signal. Van der Ouderaa et al. [64] recommends a clipping levels between 75 to 95 percent of the extreme value of the time signal at each iteration. Clipping levels higher than 95 percent will result in low convergence speed, and clipping levels lower than 75 percent may cause divergence of the algorithm because the heavy clipping greatly alters the spectral magnitude [64] (Van der Ouderaa et al). Next, the new modified spectrum and phases are calculated using DFT. The new phases are kept as a first approximation to the solution, but the desirable (original) amplitude spectrum is used in place of the modified spectrum. This iteration is repeated until there is no significant improvement (reduction) in the value of the crest factor. This algorithm

is used in the MATLAB Frequency Domain Identification Toolbox for designing multi-sine signals and it is used to generate the minimum crest factor signal in the following example.

Example:

Consider a multi-sine signal that consists of 100 frequency components equally spaced and ranging from 0.014 Hz to 1.4 Hz. Each component of the signal has amplitude of 0.2 and zero phase. The magnitude spectrum of the multi-sine signal is plotted as a function of frequency in Figure B2. The objective here is to generate a time-domain signal that has all the specified frequency components but having the signal peaks as small as possible. Recall from the discussion above, the resulting time-domain signal would retain all the power and frequency spectrum characteristics but would have minimal peaks in the time domain.

Figure B3 shows the time-domain plot of the multi-signal. The period of the signal (~71.43 seconds) is equal to the reciprocal of the lowest frequency (0.014 Hz). As observed from Figure B2 with all the phases at zero, there are peaks that are many times more than the originally specified magnitudes of 0.2. Obviously, this signal can not be used as an excitation signal in practical applications.

Using Schroeder's phase equation, Figure B4 illustrates that the time-domain peaks are compressed significantly to much lower values. Further improvement in the amplitude compression can be made using the clipping algorithm. This is shown in Figure B5.

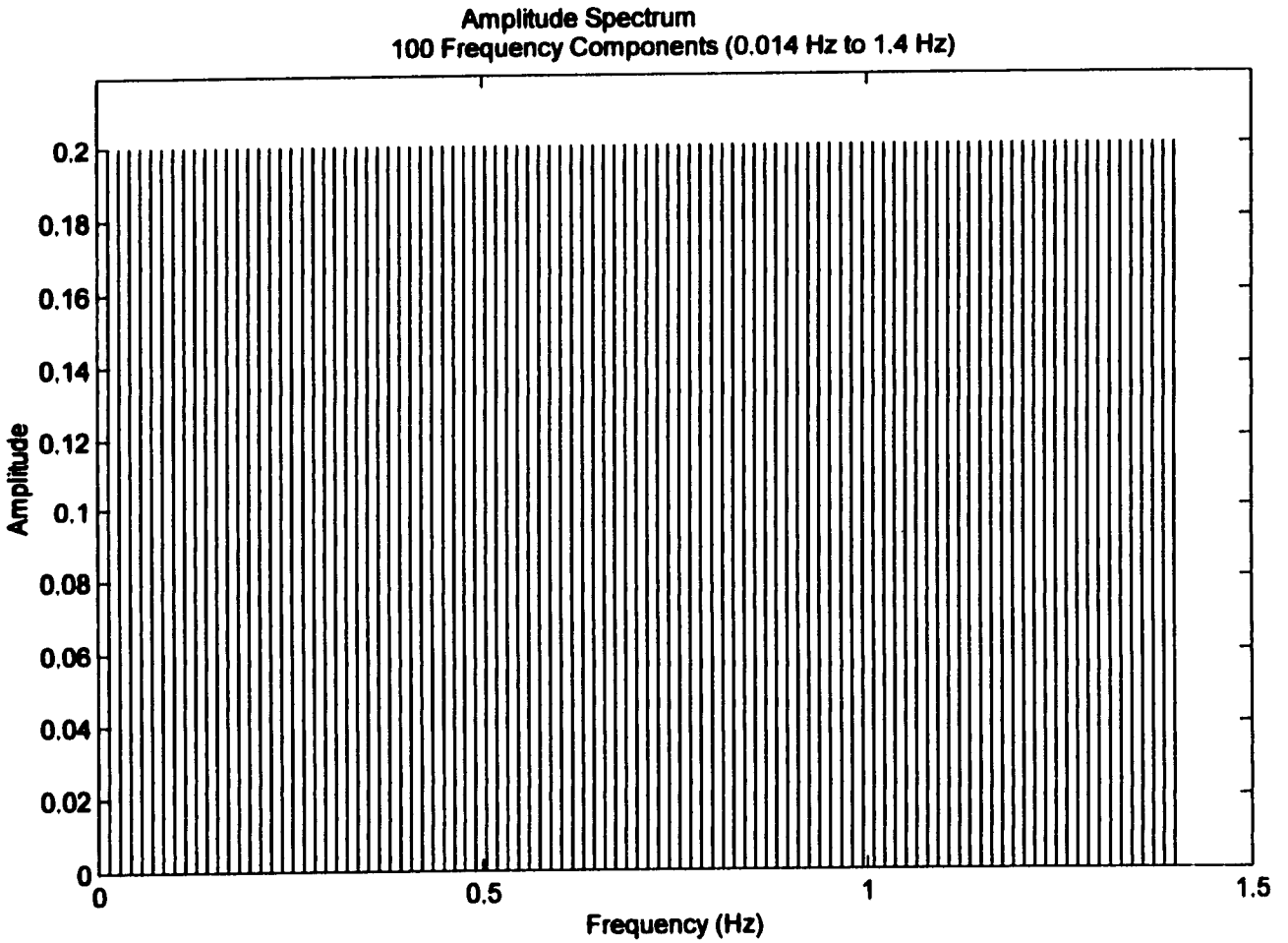

Figure B2 Amplitude Spectrum of the Multi-Sine Signal

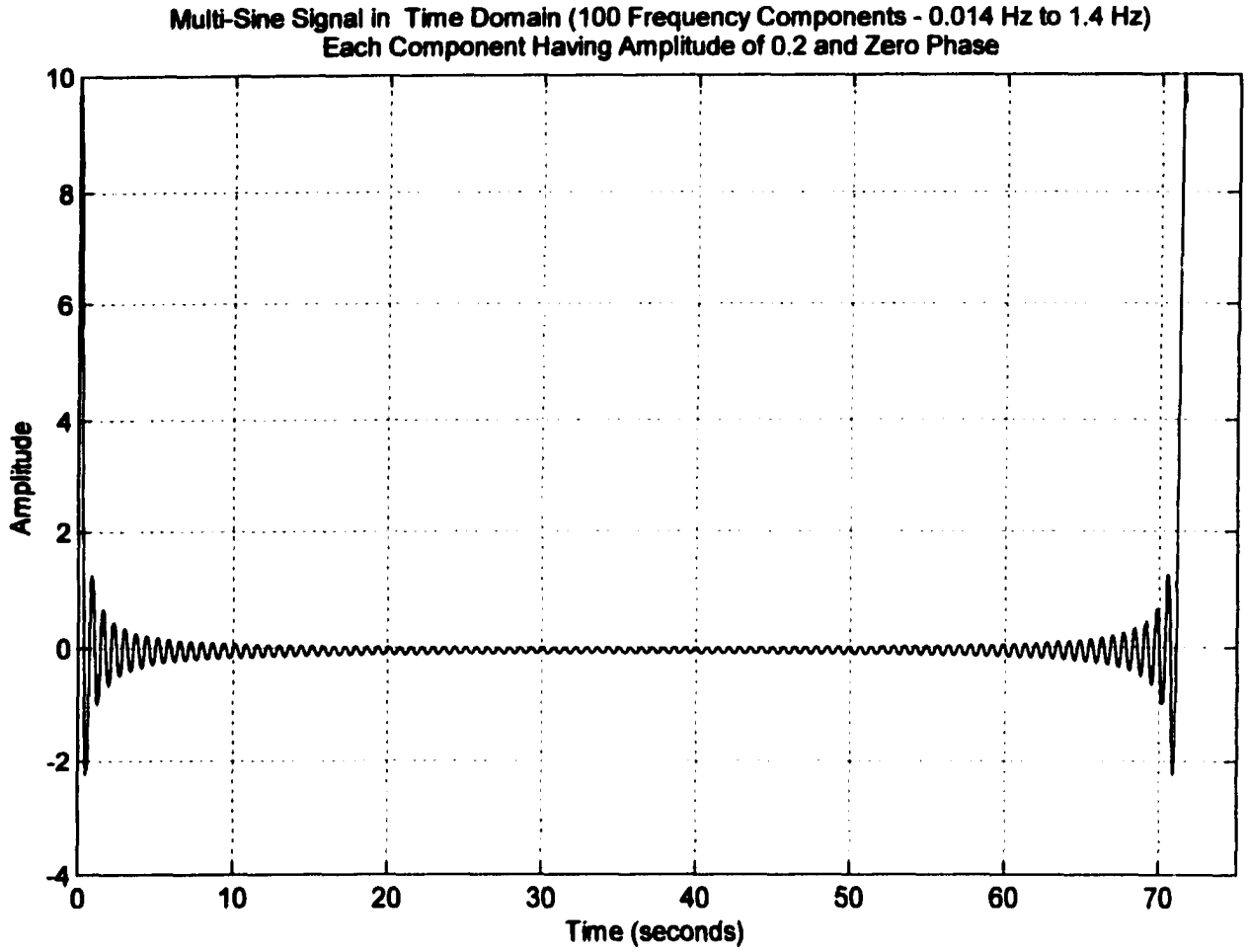

Figure B3 Time Domain Plot of the Multi-Sine Signal

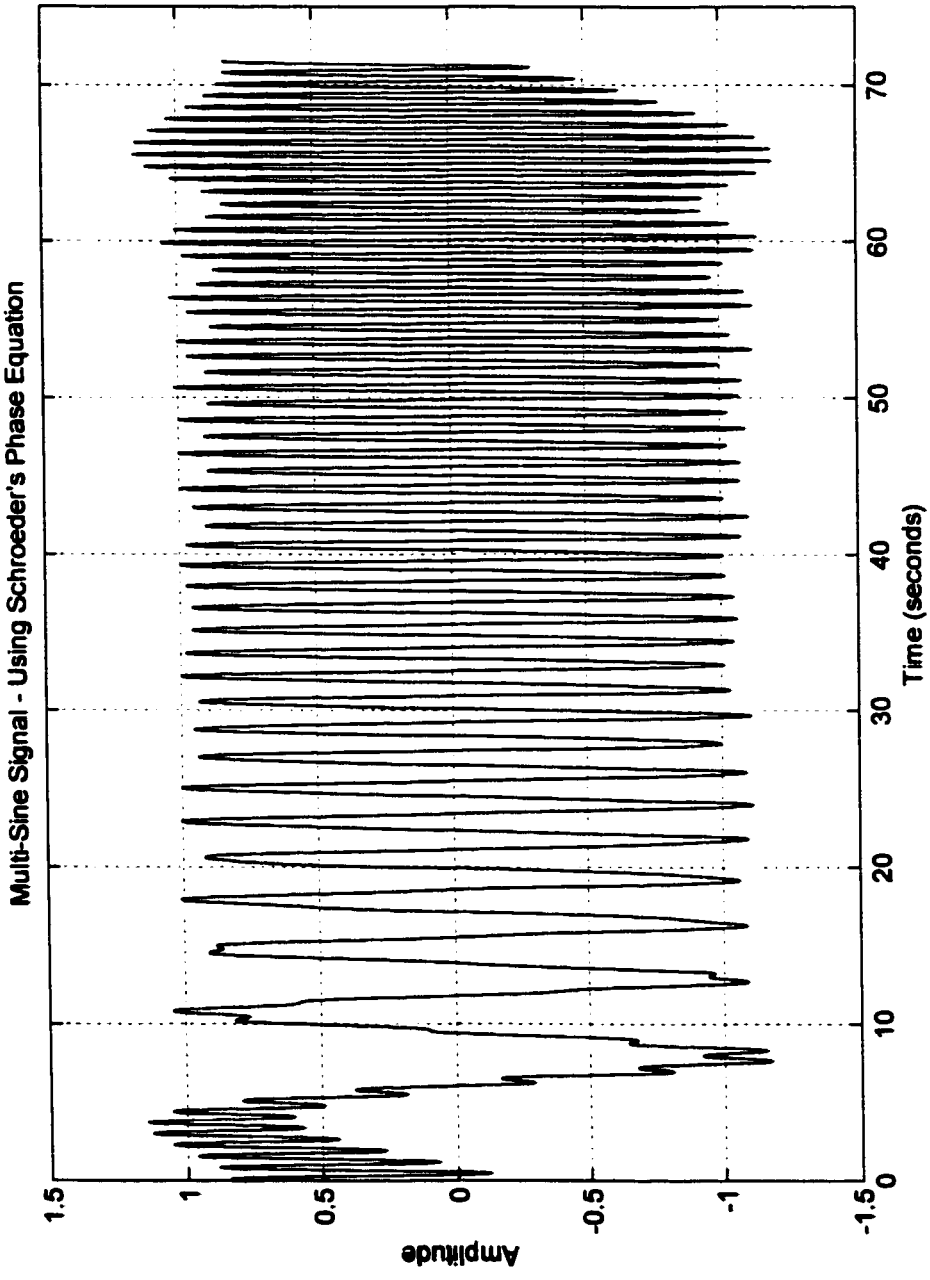

Figure B4 Multi-Sine Signal Using Schroeder's Phase Design

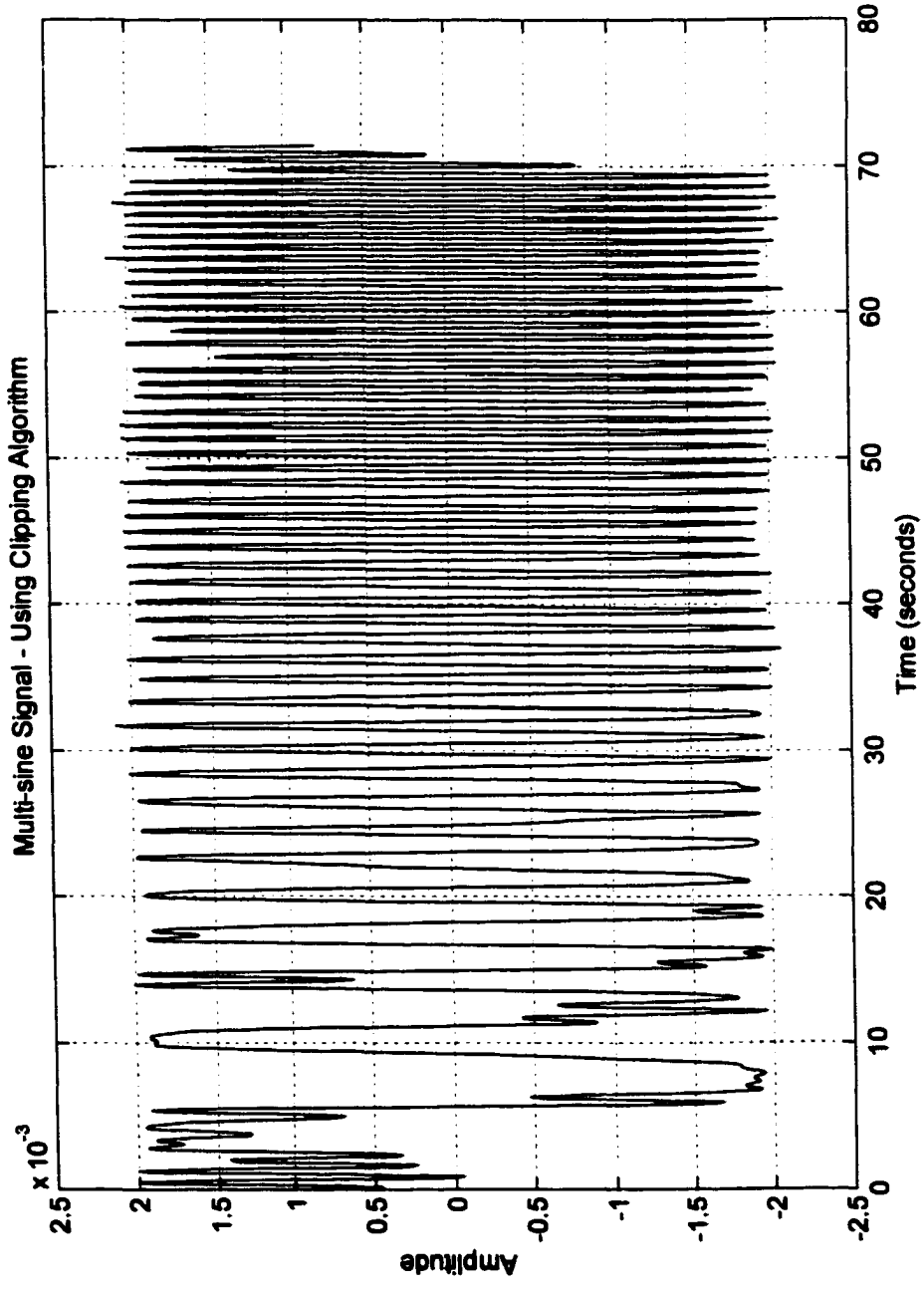

Figure B5 Multi-Sine Signal Using the Clipping Algorithm

Appendix C: Prediction Error Methods

C1. General Description

Given a set of observed data D^N and a candidate model $M(\theta)$ which contains the model parameter (coefficient) vector θ, the question is how to use the information contained in D^N to select proper values of the model parameter vector θ. This is in essence the principle of the parameter estimation method. A specific case of a parameter estimation is the prediction error method and is described below

Let D^N be the vector containing the measured input and output data

$$D^N = [y(1), u(1), y(2), u(2), y(3), u(3), \ldots, y(N), u(N)] \qquad \text{(C.1)}$$

and $M(\theta)$ = the selected model containing the unknown parameter vector θ

The prediction error is defined as the difference between the measured output and the predicted output provided by the model $M(\theta)$ when $M(\theta)$ is subjected to the same measured input $u(t)$

$$e(t, \theta) = y(t) - y^*(t|\theta) \qquad \text{(C.2)}$$

where $y(t)$ = measured output

$y^*(t)$ = predicted output provided by $M(\theta)$

Obviously, when the data set D^N is known, the prediction errors can be calculated for $t = 1, 2, \ldots N$

The guiding principle for the parameter estimation can thus be summarized as follows: "Given D^N the prediction error $e(t, \theta)$ can be computed using equation (C.2). At time $t = N$, choose θ_N so that the prediction error $e(t, \theta_N)$, $t = 1, 2, \ldots N$, becomes as small as possible".

The problem becomes how to qualify what "small" should mean in the above statement. One of the well-known approach used in the Prediction Error method is to form a scalar-valued criterion function that measures the size of $e(t, \theta)$.

Let the prediction error sequence be filtered through a stable linear filter $L(q)$, where q is the forward shift operator

$$e_F(t, \theta) = L(q)\, e(t, \theta) \qquad \text{(C.3)}$$

then use the following criterion:

$$V_N(\theta, D^N) = \frac{1}{N}\sum_{t=1}^{N} l(e_F(t, \theta)) \qquad \text{(C.4)}$$

where $l(.)$ is a scalar-valued function

The function $V_N(\theta, D^N)$ is a well-defined scalar-valued function of the model parameter θ. The estimate θ^* of the model parameter θ can then be defined by minimization of the function $V_N(\theta, D^N)$

$$\theta^* = \min V_N(\theta, D^N) \qquad \text{(C.5)}$$

in other words, the vector θ^* in (C.5) is the set of minimizing arguments of the function $V_N(\theta, D^N)$

The next appropriate discussion is how to select the linear filter $L(q)$ and the criterion function $l(.)$ $L(q)$ is usually chosen to remove the effects of disturbances not essential to the modeling problem, i.e. high-frequency signals above the frequencies of interest and low-frequency signals such as offsets and drift. There are many choices for the norm $l(.)$. One of the standard choices which is convenient for both computation and analysis purposes is the quadratic norm

$$l(e) = \frac{1}{2}e^2$$

C2. Computational Aspects of the Prediction Error Methods

The following material is described in [35] (Ljung) and [61] (Soderstrom) as well as in many Optimization and Numerical Analysis textbooks. In this study we have been dealing with a scalar output system. We further assume a quadratic criterion function

$$V_N(\theta, D^N) = \frac{1}{N}\sum_{t=1}^{N}\frac{1}{2}e^2(t,\theta) \qquad \text{(C.6)}$$

The criterion function (C.6) has the gradient (derivative)

$$V_N'(\theta, D^N) = -\frac{1}{N}\sum_{t=1}^{N}\psi(t,\theta)e(t,\theta) \qquad \text{(C.7)}$$

where $\psi(t,\theta)$ is the d x p gradient matrix of the predicted output $y^*(t)$, with d the number of parameters to be estimated and p the dimension of the output $y(t)$

A general family of numerical search routines, which includes the commonly used method Newton-Ralphson algorithm, is then given by

$$\theta^{*(k+1)} = \theta^{*(k)} - \mu^k[R^k]^{-1}V_N'(\theta^{*(k)}, D^N) \qquad \text{(C.8)}$$

where $\theta^{*(k)}$ denotes the k^{th} iteration point in the search. The sequence of scalar μ^k is used to control the step size and to improve convergence of (C.8) and it is chosen so that

$$V_N(\theta^{*(k+1)}, D^N) < V_N(\theta^{*(k)}, D^N) \qquad \text{(C.9)}$$

R^k is a d x d matrix that modifies the search direction. It is usually chosen as the Hessian (2nd derivative) of $V_N(\theta, D^N)$

$$R^k = V_N''(\theta, D^N) = \frac{1}{N}\sum_{t=1}^{N}\psi(t,\theta)\psi^T(t,\theta) - \frac{1}{N}\sum_{t=1}^{N}\psi'(t,\theta)e(t,\theta) \qquad \text{(C.10)}$$

where $\psi'(t,\theta)$ is the d x d Hessian of the error $e(t)$. However, it may require significant effort to compute all the terms of $\psi'(t,\theta)$ in (C.10). A suitable choice for (C.10) is recommended by [35] (Ljung)

$$R^k = V_N''(\theta, D^N) = \frac{1}{N}\sum_{t=1}^{N}\psi(t,\theta)\psi^T(t,\theta) \qquad \text{(C.11)}$$

For the case $\mu^k = 1$, (C.8) and (C.11) are called the Gauss-Newton algorithm.

To use the formulas above, we need to determine the expressions for $\psi(t,\theta)$, the gradient of the prediction. The method to compute the gradient for an ARMAX model (5.2) is shown below

$$A(q^{-1})y(t) = B(q^{-1})u(t) + C(q^{-1})e(t)$$

ARMAX model:
$$A(q^{-1}) = 1 + a_1 q^{-1} + \ldots + a_{na} q^{-na}$$
$$B(q^{-1}) = b_1 q^{-1} + \ldots + b_{nb} q^{-nb}$$
$$C(q^{-1}) = 1 + c_1 q^{-1} + \ldots + c_{nc} q^{-nc}$$

The predictor is given by

$$C(q^{-1})y^*(t,\theta) = B(q^{-1})u(t) + [C(q^{-1}) - A(q^{-1})]y(t) \qquad \text{(C.12)}$$

First differentiate equation (C.12) with respect to a^k to get

$$C(q^{-1})\frac{\partial}{\partial a_k}y^*(t,\theta) = -q^{-k}y(t) \qquad \text{(C.13)}$$

Similarly, differentiate (C.12) with respect to b^k and c^k

$$C(q^{-1})\frac{\partial}{\partial b_k}y^*(t,\theta) = -q^{-k}u(t) \tag{C.14}$$

$$q^{-k}y^*(t,\theta) + C(q^{-1})\frac{\partial}{\partial c_k}y^*(t,\theta) = -q^{-k}u(t) \tag{C.15}$$

Define $\varphi(t,\theta)$ (called the regression vector) as

$$\varphi(t,\theta) = [-y(t-1)\ldots - y(t-n_a)u(t-1)\ldots u(t-n_b)e(t-1,\theta)\ldots e(t-n_c,\theta)]^T \tag{C.16}$$

where $e(t,\theta) = y(t) - y^*(t,\theta)$

From (C.13) through (C.16), the gradient $\psi(t,\theta)$ can be written in terms of the regression vector $\varphi(t,\theta)$

$$C(q^{-1})\psi(t,\theta) = \varphi(t,\theta) \tag{C.17}$$

The gradient $\psi(t,\theta)$ is thus obtained by filtering the regression vector $\varphi(t,\theta)$ through the filter $1/C(q^{-1})$. We now have all the terms for the equation (C.8).